AFRL-RX-TY-TR-2010-0085

VALIDATION AND DESIGN OF SHEET RETROFITS

Rhett Johnson and Hani A. Salim
Department of Civil and Environmental Engineering
University of Missouri
Columbia, MO 65211

John M. Hoemann
Applied Research Associates
P.O. Box 40128
Tyndall Air Force Base, FL 32403

Keith M. Nelson
Jacobs Technology, Advanced Systems Group
104 Research Road, Bldg 9742
Tyndall Air Force Base, FL 32403

Bryan T. Bewick and Michael I. Hammons
Air Force Research Laboratory
139 Barnes Drive, Suite 2
Tyndall Air Force Base, FL 32403-5323

Contract No. FA4819-07-D-0001

DECEMBER 2009

AIR FORCE RESEARCH LABORATORY
MATERIALS AND MANUFACTURING DIRECTORATE

■ **Air Force Materiel Command** ■ **United States Air Force** ■ **Tyndall Air Force Base, FL 32403-5323**

DISCLAIMER

Reference herein to any specific commercial product, process, or service by trade name, trademark, manufacturer, or otherwise does not constitute or imply its endorsement, recommendation, or approval by the United States Air Force. The views and opinions of authors expressed herein do not necessarily state or reflect those of the United States Air Force.

This report was prepared as an account of work sponsored by the United States Air Force. Neither the United States Air Force, nor any of its employees, makes any warranty, expressed or implied, or assumes any legal liability or responsibility for the accuracy, completeness, or usefulness of any information, apparatus, product, or process disclosed, or represents that its use would not infringe privately owned rights.

NOTICE AND SIGNATURE PAGE

Using Government drawings, specifications, or other data included in this document for any purpose other than Government procurement does not in any way obligate the U.S. Government. The fact that the Government formulated or supplied the drawings, specifications, or other data does not license the holder or any other person or corporation; or convey any rights or permission to manufacture, use, or sell any patented invention that may relate to them.

This report was cleared for public release by the Air Force Research Laboratory Airbase Technologies Division Public Affairs Office and is available to the general public, including foreign nationals. Copies may be obtained from the Defense Technical Information Center (DTIC) (http://www.dtic.mil).

AFRL-RX-TY-TR-2010-0085 HAS BEEN REVIEWED AND IS APPROVED FOR PUBLICATION IN ACCORDANCE WITH ASSIGNED DISTRIBUTION STATEMENT.

DENIS S. CLAYSON, 2nd Lt, USAF
Work Unit Manager

CHRISTOPHER L. GENELIN, Captain, USAF
Chief, Engineering Mechanics Section

ALBERT N. RHODES, PhD
Chief, Airbase Technologies Division

This report is published in the interest of scientific and technical information exchange, and its publication does not constitute the Government's approval or disapproval of its ideas or findings.

REPORT DOCUMENTATION PAGE

Form Approved
OMB No. 0704-0188

PLEASE DO NOT RETURN YOUR FORM TO THE ABOVE ADDRESS.

1. REPORT DATE *(DD-MM-YYYY)*	2. REPORT TYPE	3. DATES COVERED *(From - To)*
31-OCT-2010	Final Technical Report	01-OCT-2007 -- 31-DEC-2009

4. TITLE AND SUBTITLE

Validation and Design of Sheet Retrofits

5a. CONTRACT NUMBER

FA4819-07-D-0001

5b. GRANT NUMBER

5c. PROGRAM ELEMENT NUMBER

62102F

6. AUTHOR(S)

*Johnson, Rhett; *Salim, Hani A.; #Hoemann, John M.; ##Nelson, Keith M.; **Bewick, Bryan T., **Hammons, Michael I.

5d. PROJECT NUMBER

4915

5e. TASK NUMBER

F0

5f. WORK UNIT NUMBER

Q210FA72

7. PERFORMING ORGANIZATION NAME(S) AND ADDRESS(ES)

*Department of Civil and Environmental Engineering, University of Missouri, Columbia, MO 65211; #Applied Research Associates, Inc., P.O. Box 40128, Tyndall Air Force Base, FL 32403; ##Jacobs Technology, Advanced Systems Group, 104 Research Drive, Bldg 9742, Tyndall Air Force Base, FL 32403

8. PERFORMING ORGANIZATION REPORT NUMBER

9. SPONSORING/MONITORING AGENCY NAME(S) AND ADDRESS(ES)

**Air Force Research Laboratory
Materials and Manufacturing Directorate
Airbase Technologies Division
139 Barnes Drive, Suite 2
Tyndall Air Force Base, FL 32403-5323

10. SPONSOR/MONITOR'S ACRONYM(S)

AFRL/RXQEM

11. SPONSOR/MONITOR'S REPORT NUMBER(S)

AFRL-RX-TY-TR-2010-0085

12. DISTRIBUTION/AVAILABILITY STATEMENT

Distribution Statement A: Approved for public release; distribution unlimited.

13. SUPPLEMENTARY NOTES

Ref AFRL/RXQ Public Affairs Case #10-180. Document contains color images.

14. ABSTRACT

The objective of this research was to validate the analytical design model for determining the effectiveness and feasibility of a sheet retrofit. This report focuses on a polypropylene sheet as the retrofit material for validating the mechanics of the model and includes an informed and accurate design methodology for blast retrofit of CMU infill walls. The model was developed to be material independent, and the engineering level calculations can be completed, if the stress versus strain response of the material is known.

15. SUBJECT TERMS

adhesion connection, blast, mechanical connection, polypropylene sheet, retrofit, stress-strain relationship, structure

16. SECURITY CLASSIFICATION OF:			17. LIMITATION OF ABSTRACT	18. NUMBER OF PAGES	19a. NAME OF RESPONSIBLE PERSON
a. REPORT	b. ABSTRACT	c. THIS PAGE			Clayson, Denis S.
U	U	U	UU	103	19b. TELEPHONE NUMBER *(Include area code)*

Reset

Standard Form 298 (Rev. 8/98)
Prescribed by ANSI Std. Z39.18

TABLE OF CONTENTS

LIST OF FIGURES

LIST OF TABLES

1. SUMMARY

The retrofit of structures to resist external explosions is becoming increasingly necessary. The use of thin sheets on the tension face of a wall is one of the practicable methods for blast retrofitting concrete masonry infill walls. Properties of materials desirable for this application range from low stiffness and high ductility to high stiffness and low ductility. The research conducted by the Air Force Research Laboratory (AFRL), Tyndall Air Force Base, FL, and documented in this report used a polypropylene sheet that exhibited a balance of these properties, large ductility and high strength-to-weight ratio, for validation of the proposed modeling technique. To promote the widespread use of such sheets for blast retrofit, it was necessary to first develop an engineering design-and-analysis methodology for predicting the dynamic response of a concrete masonry unit (CMU) wall system. AFRL, therefore, developed the constitutive relationship of the material, the connection details, the static resistance function, and the dynamic model for the retrofit material and evaluated them in this report. AFRL developed and experimentally verified an analytical model for the static resistance function of the sheet retrofit–CMU wall system. A full-scale field test using bare explosives to provide the impulsive load verified the engineering method developed in this report. In this report, AFRL researchers developed a practical method for connecting the sheet retrofit to the floor/ceiling slabs of a building. The results include a comparison of the analytical static resistance function with full-scale component membrane laboratory data and a comparison of the dynamic predictions with the full-scale blast test response. Conclusions include a short discussion of failure limits, such as connection failure and material failure. This report also includes, but only briefly discusses, additional materials that could be used as alternatives for the retrofit.

2. INTRODUCTION

The rise of terrorist threats on military and government occupied structures in recent years has made blast-resistant design increasingly more common and necessary. These threatened structures are commonly constructed using CMU blocks to infill non-load bearing walls (Hammons, 1999). Many of these structures were built in a time period when their designers did not consider blast resistance. For this reason it is imperative that designers develop retrofitting techniques and design methods for these now-high-risk structures.

Typically, as blast pressures are exerted on an unreinforced CMU infill wall with no retrofit, the wall breaks apart, or fragments, into pieces that become projectiles that may become deadly to the occupants inside the structure. Unreinforced CMU walls behave in this fashion because they have very little energy absorption capabilities in pure flexure. For a wall system to withstand a given blast, it can be idealized in the purest form as a wall system where the potential energy of the system must be equal to or greater than the kinetic energy imparted from the impulsive load. Increasing the ductility in the wall system also increases the potential-energy capabilities. This may result in a wall system that absorbs greater amounts of energy from blasts and decreases the hazards inside the structure to people and property.

AFRL has been recently researching and developing ways of increasing the energy absorption of CMU wall systems. Several proposed materials have shown promise in this application. Salim's (2007) paper helped to bound the problem by showing that the use of different materials ranging from high stiffness and low ductility to low stiffness and high ductility could be used to achieve the desired response. Thin steel sheets (Kennedy, 2005) have proven to be a practicable option for CMU wall sheet retrofits and would be considered the upper bound. Polymer materials have also been extensively examined with varying application methods including either spray-on or trowel-on polymers (Beckman, 2004), polymer sheets (Fitzmaurice, 2006), and fiber-reinforced polymers (Davidson, 2005). The polymers hold the lower bound of the problem.

This report focuses on the increased energy absorption capabilities gained by the use of a sheet retrofit CMU wall system against impulsive loads. Figure 1 shows the basic concept of a retrofit system, either sheet or spray-on, for unreinforced CMU walls. The sheet retrofit is stretched along the backside of the wall. The thin sheet is then connected behind the CMU wall by means of a chemical or mechanical connection. The mechanical systems typically consist of a stiff plate clamped to the floor/ceiling with fasteners, either concrete anchors or nails, depending on the stiffness of the material. It is apparent that research needs to pay special attention to the connections as this report discusses later. This is due to the fact that the connections themselves tend to be weaker than the theoretical resistance of the sheet. Stress concentrations develop at the point of connection and reduce the global strength of the retrofit sheet. For this reason the optimization of the connections is of particular importance for an installation to develop the highest possible axial loads within the sheet.

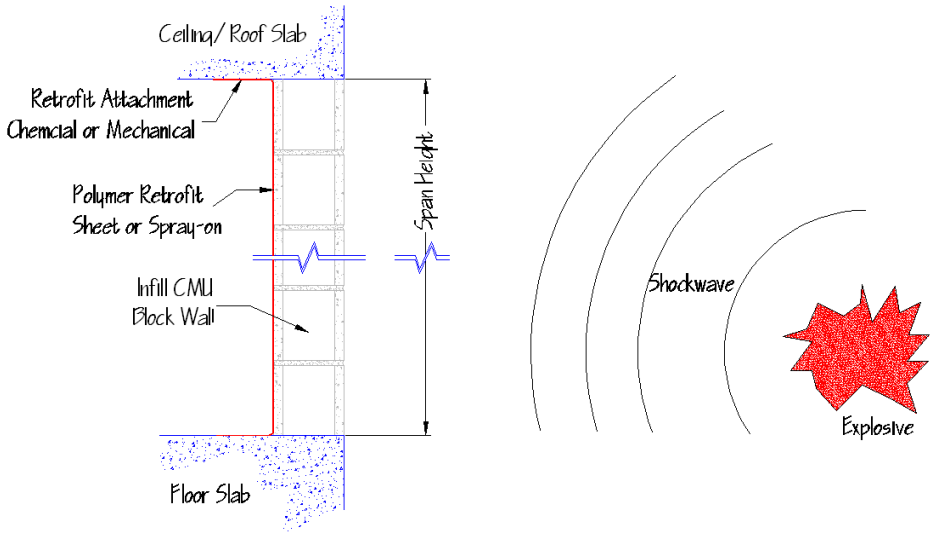

Figure 1. Infill Masonry Wall Retrofit Concept

2.1. Objective

The objective of the research documented in this report was to validate the analytical design model for determining the effectiveness and feasibility of a sheet retrofit. This report focuses on a polypropylene sheet, trade name CURV©, as the retrofit material for validating the mechanics of the model. It is important to note that the model was developed to be material independent and, if the stress versus strain response of the material is known, the engineering level calculations can be completed. See Appendix for other explored materials considered during this program. This process involved the steps that follow below:

1) Consider previous research on the topics. Closely study and document the research to aid in the achievement of the objectives listed.
2) Conduct preliminary coupon testing to develop the stress–strain relationships for the polypropylene composite material. Use this relationship in the determination of the analytical static resistance function.
3) Perform three sets of connection testing to find the optimum connection for the final design. Use steel angles with bolts and washers through the sheet for the first test, adhesive chemical bonders for the second test, and flat steel connection plates with bolts and washers through the sheet as means of connection from the floor slabs to the sheet retrofit for the third test.
4) Create a static resistance function to accurately model the behavior of the retrofit material. Mathematically develop the function using concepts from geometry, equilibrium equations, constitutive stress–strain relationships, and compatibility relationships. Use this static resistance function later to create the single-degree-of-freedom (SDOF) model.
5) Conduct quasi-static, component membrane tests using sheets of polypropylene loaded under a simulated uniform pressure by means of a loading tree. Use different connection configurations and sheet combinations. Verify the analytical static resistance function

and determine connection strength limitations. Also optimize the connection configuration and find the strength limitations of the connections themselves.

6) Create a SDOF model to predict the dynamic response of the entire wall system. Use the static resistance function created earlier and other research data pertaining to the strength of CMU walls. This model gives a deflection versus time plot for a given CMU infill wall system using a polypropylene sheet retrofit for a given blast loading function.
7) Validate SDOF model using test data from a live explosive test on a CMU infill wall system with a polypropylene sheet retrofit.
8) Draw conclusions from the models developed and the tests performed. Recommend feasible retrofit design procedures for the CMU infill wall system using varying materials.

The process outlined in this section allowed engineers to use an informed and accurate design methodology for blast retrofit of CMU infill walls.

3. LITERATURE REVIEW

Recently, it has become apparent that many structures throughout the world have a need for blast resistance. Designing for such blast loads is very different from designing for other common forces such as wind or seismic loads. Since builders designed many existing structures in a time when the threat from explosions was far less likely, the structures do not have adequate resistance to withstand the powerful effects of a blast loading. For this reason many researchers have investigated the area of blast design seeking to minimize the destruction and human life toll in the event of a blast situation. They have written numerous technical reports and publications evaluating structures exposed to blast loading and proposing systems for mitigating the damage. This section presents areview of the aforementioned literature.

3.1. Technical Background

A blast is most simply defined as a sudden release of energy. When a blast occurs, by way of a chemical or nuclear explosion, it heats the surrounding medium very rapidly. This results in very high local pressures radiating outward from the center of the blast in the form of a blast wave, which is very similar to a shockwave (Smith and Hetherington, 1994). Structures that are in the path of these high pressures are affected according to the distance from that blast, the angle of incidence, and the size of the explosive charge. Figure 2 depicts a blast wave pressure–time profile.

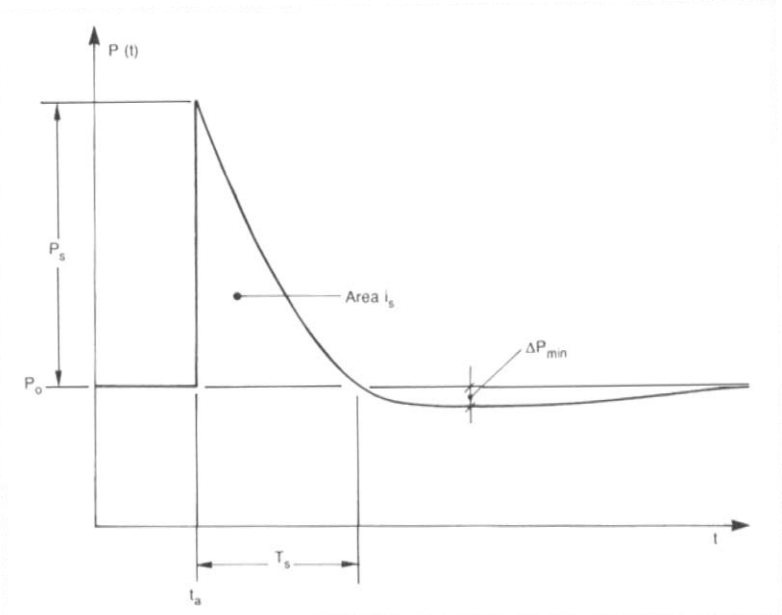

Figure 2. Idealized Blast Loading

Figure 2 illustrates that a large maximum pressure (P_s) follows a blast arrival time (t_a) at ambient pressure (P_o). A negative-phase duration follows the positive-phase duration (T_s), which can be advantageous to the design process, since this minimizes some of the damage caused by the blast. The positive-phase duration occurs in a very short period of time that is usually measured in milliseconds. This idealization necessitates an overly conservative blast wall design to absorb

the blast loading. This research considered the negative phase of the blast loading so that a more accurate blast design is produced.

As noted earlier, blast loads induce very high pressures on the structures that are targeted. Typical structures are not designed to withstand pressures of these magnitudes, since they are several orders of magnitude greater than a strong wind loading. Although the magnitude of the pressure is much higher, the duration of the loading event is much shorter. This is highly beneficial in the design of blast-resistant structures.

The area under the curve of the positive-phase duration is equal to the energy that is imparted to the structure during the blast event. The short duration of the positive phase limits the amount of energy that is transmitted to the structure. A structure subjected to a blast load must be able to absorb the energy that is released through its structural components. A blast event typically loads many components of the structure into the plastic loading range. It is effective to design the structural components to have a plastic response provided that the structure is not susceptible when progressive collapse is a consideration. The blast resistance of a structure may be characterized by its ability to stay within deflection tolerances while effectively absorbing the energy from a given blast loading (Dinan, 2005).

3.2. Blast Resistance Research

The term "blast retrofit" refers to modifying a structure already in service using parts or systems made available after the original construction of the structure. Many researchers have increasingly explored the blast retrofit topic in the past several years. Many structures that were built before blast-resistant design was more prominent are now at a higher risk for blast attacks. These structures are especially good candidates for blast retrofits. Researchers have explored many different designs and methods, but this section discusses only a few relevant cases. Research pertaining to concrete masonry unit walls are of particular interest due to their tendency to fracture and gain velocity under blast loadings.

P.A. Jones (1989) performed research for the purpose of creating a design methodology for CMU block walls. This research obtained analytical resistance functions for different types of CMU wall construction and entered this information into a software-based wall analysis code that engineers used for the purpose of designing CMU walls subjected to blast loading. This research showed that the blast resistance of the CMU wall itself greatly depends on the type of wall construction that is implemented.

Steel has also been used in the quest for more-blast-resistant walls. Dinan (2005) explored the advantages of steel stud walls for their blast resistance in retrofit or new construction, generated analytical models, and verified the models using test data from a field explosion test. This test retrofitted a full-scale CMU wall with steel studs and subjected it to a live explosive test. The test showed that properly anchored steel stud walls can be an effective solution due to their increase in strength and ductility to the wall system.

3.3. Masonry Retrofits

Sheet retrofits are another type of blast-resistant wall system, in which a "sheet" of a given material is applied to the interior of a wall subjected to a blast loading. The sheet is then responsible for an addition in strength and ductility of the wall system. The added strength and ductility allow the wall system to provide more energy absorption. Many researchers have evaluated this area of blast wall retrofits, and several pertinent studies are cited in this section.

For example, Kennedy (2005) evaluated steel sheets as a potential retrofit system. The research evaluated the resistance of different thicknesses of thin steel sheets to blast loads, then created a resistance function and incorporated it into a dynamic modeling system. This research also evaluated other parameters relating to the connections, such as welding versus bolting, bolt spacing, and connection plate thickness. This research demonstrated that steel sheet retrofits could sufficiently resist certain blast loads, and that dynamic modeling can predict the response of such a system (Kennedy, 2005). Salim (2007) later revised this research and added curvatures of connection plates to the matrix.

Silas Fitzmaurice (2006) conducted very similar research using polymer sheets. This research connected different thicknesses of polymer sheets, used varying bolt spacing and connection plate thicknesses, and tested the sheets for the purpose of evaluating their blast resistance. The test showed the polymer sheets had much less strength than steel sheets but found their ductility was much greater. This research also used dynamic modeling to predict the failure response of the polymer and concluded that if the sheets were allowed to develop their full energy absorption capabilities, they too would provide adequate resistance to blast loads (Fitzmaurice, 2006).

Davidson (2005) and Beckman (2005) also investigated spray-on polymer sheets. This research indicated that if a strong bond is achieved between the CMU wall and the spray-on polymer, concentrated strains can occur, which can lead to premature failure of the polymer. Moradi et. al. (2008) also discussed this concept. However, this retrofit system still allowed for the absorption of a considerable amount of blast energy. The mechanically connected thin sheet may have allowed for more energy absorption capabilities due to the fact that the stress in the sheet was applied over the entire sheet as opposed to several small crack lengths.

In both steel and polymer sheet retrofits, connections seem to be a vital part of the research process. An optimized connection was essential for providing the system with the strength and ductility that each material offered. If connections are not optimized, stress concentrations at the connection points are likely to fail the system before it reaches the maximum capacity for energy absorption. This report evaluates an advanced sheet retrofit and thus provides a brief description of the sheet material below.

3.4. Polymer Specifications

The material properties of these polypropylene sheet materials, which were originally designed for use in the automotive industry, make polypropylene desirable for many other applications such as blast retrofitting. The high strength-to-density ratio of polypropylene makes this product especially desirable for blast retrofit applications. Polypropylene, CURV©, has a tensile strength of 17.4 ksi and a density of 57.4 lbs/ft^3 (Propex Fabrics), which are very low compared to steel or

other high-strength materials. This indicates that 50% weight saving may be possible with the same mechanical stiffness if careful attention is paid to the connections. In addition, polypropylene has high impact strength, a strong resistance to abrasion, and out-performs conventional thermoplastics and fiber-reinforced composites (Propex Fabrics).

This polypropylene sheet is made by combining the technology of fiber-reinforced composites with 100% polypropylene thermoplastic. First, the polypropylene thermoplastic is drawn or stretched into a thin string called a "tape." By drawing the polypropylene into a thin tape, the molecules become highly ordered and create a large increase in strength and stiffness. Next, these tapes are woven into a polypropylene fabric, which allows the material properties to be the same at 0 and 90 deg. Finally, the fabric is fed into a machine called a "double belt press," in which the surface of each tape is slightly melted and pressed together with other sheets of polypropylene fabric. When cooled, the sheets are permanently adhered together, creating the final product (Propex Fabrics, n.d.).

Polypropylene is safe and easy to handle as a result of its smooth finish and non-toxic properties. Polypropylene causes none of the irritation that is associated with materials containing glass fibers. Also, polypropylene sheets do not need to be coated with any corrosion-resistant material in the field upon installation due to their high resistance to corrosion. Polypropylene sheets come in thicknesses ranging from 0.012 to 0.118 inches (0.3 to 3.0 mm) and widths of up to 53.5 inches (1.36 m). Polypropylene also is available in a wide range of colors, color effects, and surface types.

4. COMPONENT-LEVEL EVALUATION

When sheet retrofits are used for blast design, it is imperative to focus on connection details since the area around the connection of the sheet to the floor or ceiling slabs is always the weakest area of the sheet. Consequently, AFRL performed several different types of experimental tests to find the most efficient connection type. AFRL performed:

1) Coupon tests to obtain reliable data for the following tests,
2) Mechanical connection tests with a flat polypropylene sheet connected to a steel angle and backing plate by bolts of different sizes ,
3) Chemically adhered connection tests using two different types of adhesive chemical bonders, and
4) Another set of mechanical connection tests that bent the polypropylene sheet to an angle of 90 degrees and connected it to the supports by means of a flat connection plate with bolts, nuts, and washers.

AFRL also considered and explored the feasibility of field installation in the connection tests.

4.1. Coupon Testing

Acquiring accurate coupon data was critical to analyzing the following experimental tests using the same material and to creating a proper working analytical model. Quasi-static coupon tension tests provided the stress–strain relationship for the polypropylene sheet material. Since this report uses the material data throughout, it was essential that tests confirm the data supplied by the manufacturer.

4.1.1. Setup and Procedure

AFRL test personnel cut the coupons from a rolled sheet of 1-mm (0.039-inch) polypropylene and tested all coupons in accordance with the ASTM D412 Standard. They cut the coupons to the specified dimensions shown in Figure 3 with the thickness of each dumbbell sample approximately 0.04 inches.

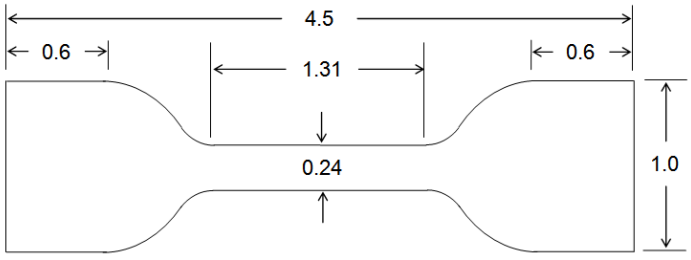

Figure 3. ASTM D412 Coupon

The tests used hydraulic grips to hold the end of each dumbbell sample and used an extensometer to measure the elongation of the middle portion of the sample. The extensometer began at a length of 1 inch at the beginning of each test with a maximum range of 2 inches. Figure 4 shows the extensometer fastened to a coupon sample. An MTS loading machine, shown in Figure 5, tested the coupons and applied tension until failure.

Figure 4. Coupon with Extensometer

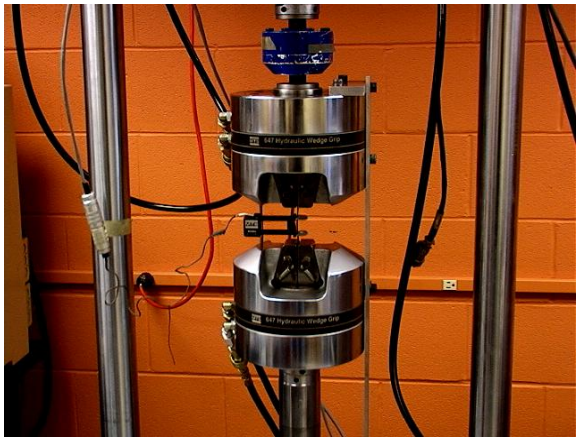

Figure 5. Coupon Experimental Setup

Using LabView Software, test personnel recorded the test data acquired via a 10,000-lb load cell and extensometer. All samples failed well within the 2-inch maximum deflection limit imposed by the extensometer. Test personnel analyzed the data from LabView and used it to create the stress–strain response plots shown in the next section. Figure 6 shows a photograph of the ten samples after testing.

Figure 6. Coupons (Post Test)

4.1.2. Results

Figure 7 shows stress–strain responses for eight of the ten coupons tested. The tests obtained bad data from the two coupons that were disregarded. The remaining eight coupons formed a representative sample, and AFRL compared this representative sample's average strain, yield stress, and ultimate stress with the other coupon samples. Figure 8 shows the data acquired from the representative sample. This plot shows engineering stress and true stress. The data acquired during the coupon test directly provided the engineering stress. After each test, using the procedure found in Section 4.1.1, AFRL test personnel calculated the true stress based on the attained engineering stress and used true stress and strain to analyze data for tests throughout the remainder of the report.

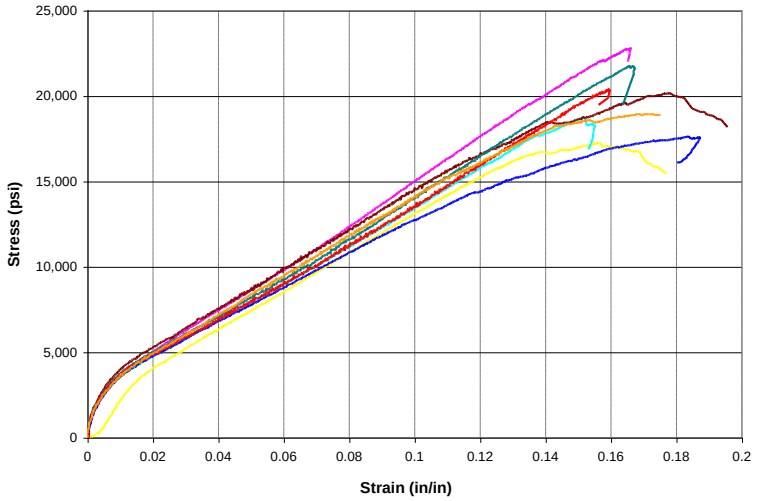

Figure 7. Stress vs. Stain Response of Polypropylene Coupons

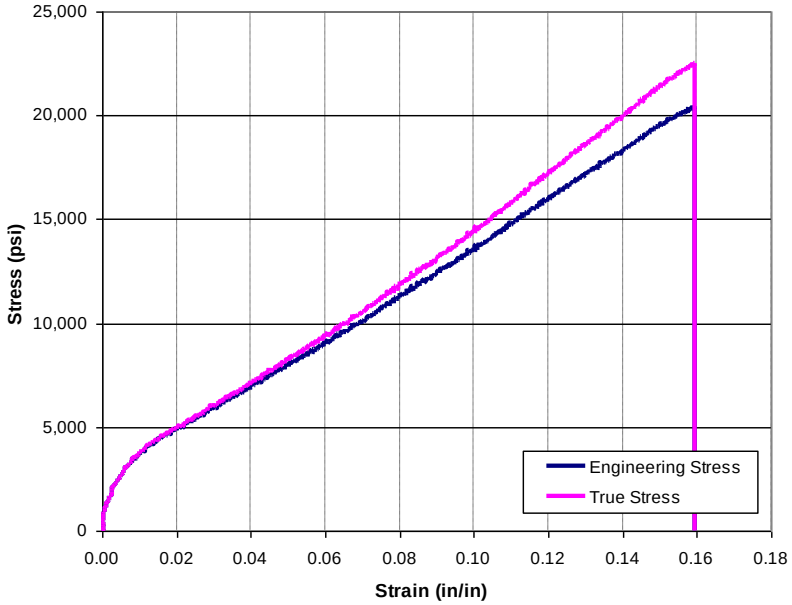

Figure 8. Typical Stress vs. Strain Response for Polypropylene Corrected for True Stress

4.2. Adhesion Connections

For the series of adhesion connection testing, test personnel used two different chemical bonding agents to create chemically adhered polypropylene sheet samples to be pulled in tension. In theory, if the chemical bonding was deemed to be effective, the polypropylene sheet could be chemically adhered to a pre-manufactured polypropylene angle that could be connected to the floor or ceiling slabs using concrete anchors and a steel connection plate (Figure 9a). Also, it would then be feasible to bond the polypropylene sheet directly to a steel angle that was anchored into the floor or ceiling slab (Figure 9b). These tests pulled chemically adhered strips of polypropylene in tension to find tensile loading capacity. AFRL completed these tests to determine if chemical bonding was a practicable option for polypropylene sheet retrofit connection design.

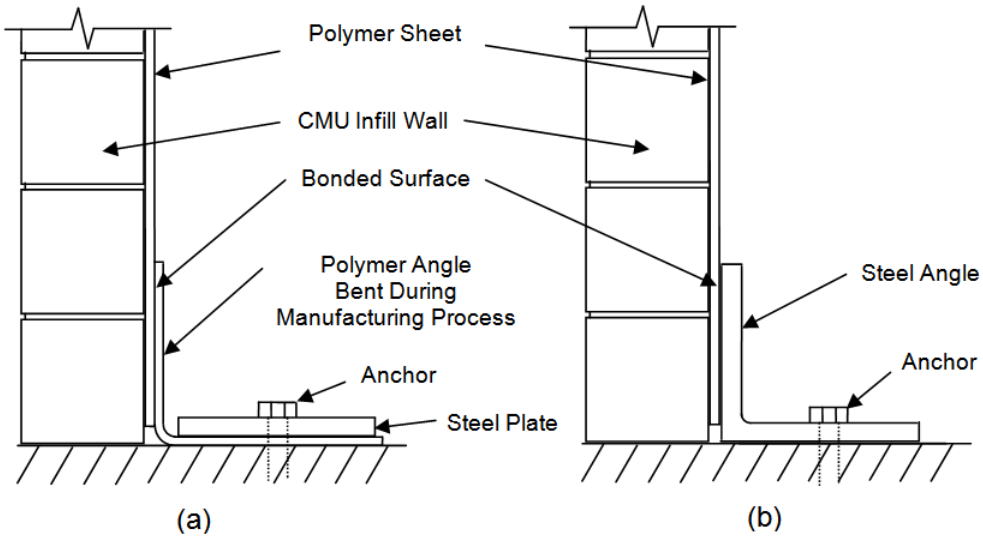

Figure 9. Schematic of Proposed Adhered Connection Setup

4.2.1. Setup and Procedure

For the chemically bonded testing, AFRL identified two adhesives, Loctite 3030 Polyolefin Bonder and 3M DP-8010 Polyolefin Bonder, which are made especially for the bonding of polypropylene. The packaging of Loctite 3030 and DP-8010 indicates that they have a worklife of 3 min. and 10 min., respectively. Both adhesives require minimal surface preparation—simply cleaning the intended contact surfaces.

AFRL test personnel cut six samples of 3-mm (0.118-inch) polypropylene sheet with a saw, prepared two strips 0.5 inches wide by 8 inches long for each sample, and roughened the strips with sandpaper on the 3-inch bonding surface. Test personnel then washed all samples with soap and water to ensure a clean bonding surface.

Test personnel bonded three samples with the Loctite 3030 Polyolefin Bonder by using the applicator nozzle on the cartridge and applying it to the 3-inch lap bonding surface. They prepared two samples with a smooth bonding surface and one with a roughened bonding surface.

The adhesion was accomplished within the specified 3-min worklife. They then used the same procedure to apply the DP-8010 to the remaining three samples. Again, they prepared two samples with a smooth bonding surface and one with a roughened bonding surface.
Table 1 lists the samples labeled 1 through 6. Figure 10 shows a photograph of the MTS test setup and the six samples before testing. Test personnel also prepared an extra sample without bonding, referred to as the "non-bonded control sample," to determine the maximum load that the 0.5-inch samples could withstand.

Figure 10. Adhesion Sample Test with Pretest View

Table 1. Adhered Connection Test Matrix

Sample Number	Adhesive Type	Bonding Surface Type
Control	N/A	N/A
1	Loctite	Smooth
2	Loctite	Smooth
3	Loctite	Roughened
4	3M	Smooth
5	3M	Smooth
6	3M	Roughened

4.2.2. Results

Only three of the six samples that the test subjected to axial tension withstood a substantial amount of load. The other three failed almost immediately after the test induced tension force and lacked sufficient bonding to allow them to acquire load. The failure mode of the three samples that took substantial load was facial shear. For each, the top layer of the polypropylene fiber matrix separated from the rest of the polypropylene sheet. The non-bonded control sample failed in tension across the middle of the sample and reached maximum load of 1,006 lbs, which was used to compare with the rest of the samples. Table 2 and Figure 11 show the test matrix with the maximum load resisted by each sample and the percent of load that each sample withstood with respect to the control sample.

Table 2. Adhesion Connection Test Results

Sample Number	Description	Max Load (lbs)	Percent of Non-Adhesion Sample
Control	Non-Bonded Control Sample	1,006	N/A
1	Loctite (Smooth Sample 1)	0 *	0
2	Loctite (Smooth Sample 2)	479	48%
3	Loctite (Rough Sample 1)	0 *	0
4	3M (Smooth Sample 1)	488	49%
5	3M (Smooth Sample 2)	0 *	0
6	3M (Rough Sample 1)	615	61%
* Insufficient bonding observed			

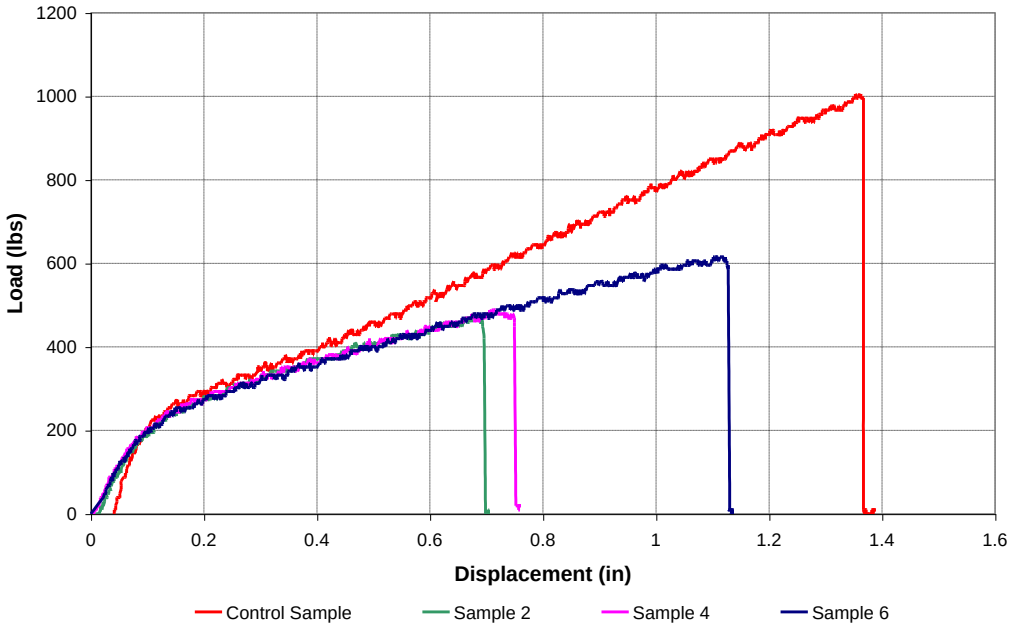

Figure 11. Adhesion Connection (Load vs. Deflection)

Sample 1 employed Loctite 3030 Polyolefin Bonder on a smooth bonding surface, Sample 3 employed Loctite 3030 Polyolefin Bonder on a roughened bonding surface, and Sample 5 employed 3M DP-8010 on a smooth bonding surface. These three samples all performed in the same manner and, at the start of the test, immediately pulled apart at the bonding surface. Table 2 presents the adhesion results matrix and identifies these samples as having an insufficient bond. An observation of the failed samples showed that the adhesive did not bond across the entire surface. This failure was partially due to the fact that the worklife of the adhesives was shorter than indicated by supplier, and test personnel had extreme difficulty applying the polyolefin bonder to the samples. Figure 12 shows the insufficient bonding that occurred to these three samples.

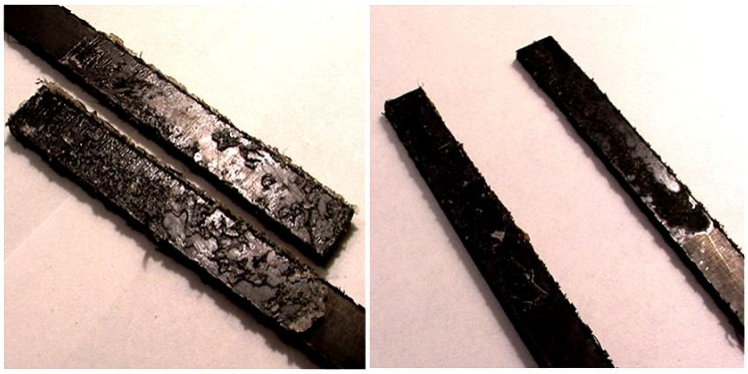

Figure 12. Typical Insufficient Bond

Figure 13 shows the corresponding load vs. displacement plot for these samples and illustrates that the displacement was essentially just noise in the system.

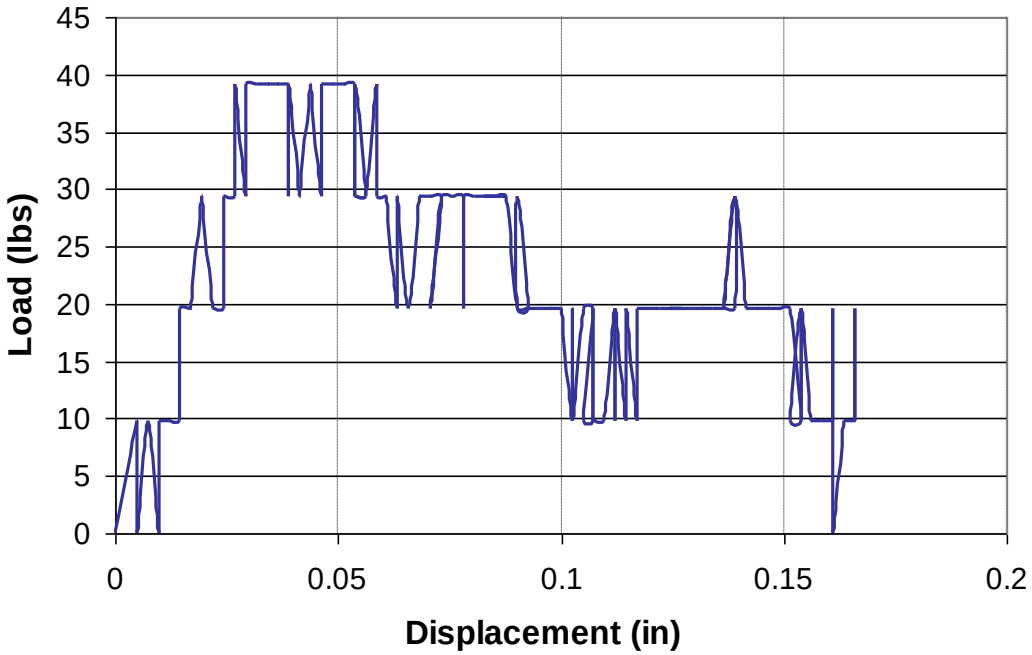

Figure 13. Insufficient Bond (Load vs. Deflection)

Figure 14–Figure 16 show photographs of the other three samples that obtained substantial load. These photos clearly show the facial shearing failure mode, which indicates the failure occurred in the material and not in the adhesion interface.

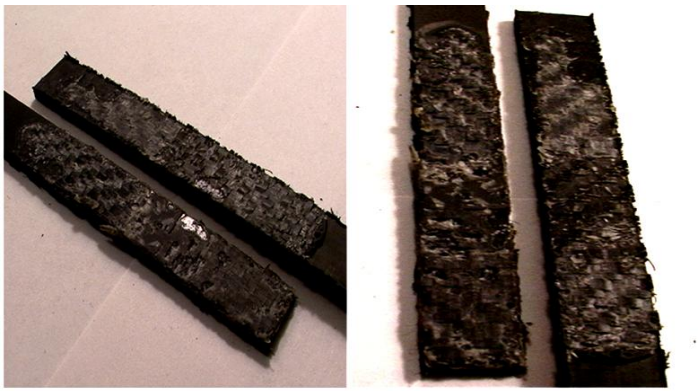

Figure 14. Adhesion Sample 2

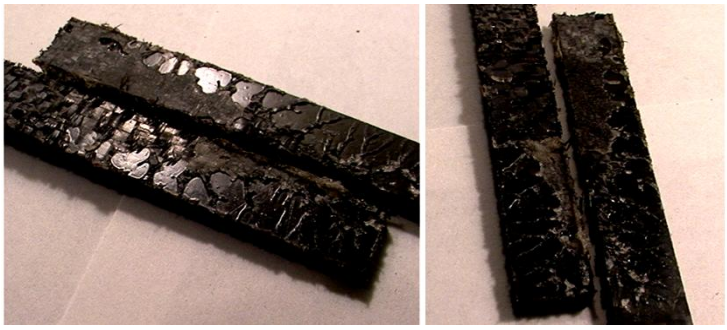

Figure 15. Adhesion Sample 4

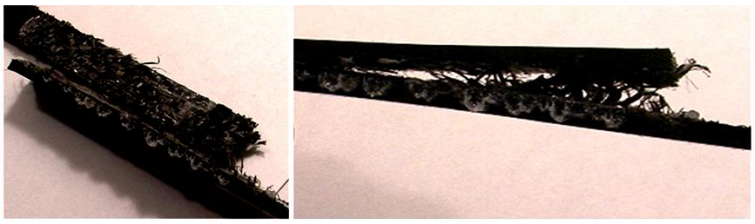

Figure 16. Adhesion Sample 6

4.2.3. Adhesion Conclusions

Sample 6 performed best during the chemical bond testing and utilized the 3M DP-8010 Polyolefin Bonder adhesive. This sample, roughened on the bonding surface with sandpaper, achieved a maximum load of 615 lbs, which corresponds to 61.1% of the non-bonded control sample's maximum load. This connection did not use the polypropylene to its optimum point. The weakness of this connection method was the fact that the top layer of polypropylene sheared away from the rest of the sample before the capacity of the actual chemical bond could be reached. Lengthening the lap length of the adhered area could possibly increase the bonding capacity. However, chemical bonding may not be a viable option for the connection of polypropylene composite due to the fact that this setup would be extremely difficult to prepare in the field. Since the worklife of the two adhesives is extremely short, working with much larger samples would take more than the amount of time available to get the adhesives and polypropylene sheets in place.

4.3. Mechanical Connections

AFRL performed mechanical connection testing to find the most efficient method to connect the polypropylene material to the floor and ceiling slabs. "Mechanical connections" are connections that use bolts, nuts and washers.

4.3.1. Mechanical Connections—Series A (Component)

In this set of tests, AFRL connected the polypropylene sheets to the supports of a tensile loading machine by using a steel angle, a backing plate, and nuts and bolts. This testing focused on finding the most efficient bolt spacing and the corresponding tensile load capacity, and evaluating the practicality of field installation of such a retrofit system.

4.3.1.1. Setup and Procedure

AFRL performed these tests using samples of 3-mm (0.118-inch) thick polypropylene cut to the dimensions of 24 by 34 inches. Test personnel cut the polypropylene sheets with a circular saw. This method worked well due to the fact that cutting the material slowly with the circular saw resulted in minimal fraying of the polypropylene fiber mesh. Once test personnel cut the samples, they drilled holes along the length of the sample for the bolt holes and employed bolt sizes of 0.25 and 0.5 inches along with bolt spacings of 2, 4, and 8 inches. Test personnel drilled three samples with hole diameters of 0.3125 inches for use with the 0.25-inch bolts and the other three samples with hole diameters of 0.5625 inches to be used with the 0.5-inch bolts. Figure 17 shows a typical sample sheet.

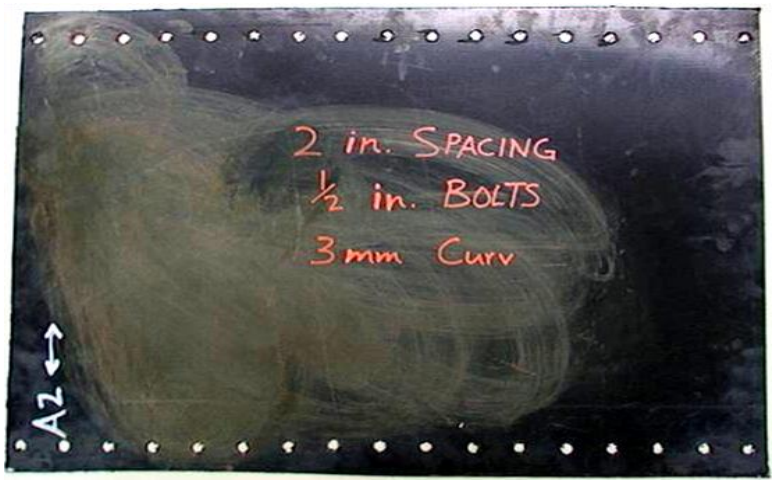

Figure 17. Mechanical Connection (Sample A2 – Pre-Test)

After cutting the samples, test personnel cut the connection plate and angle. They used an L3x3x1/2 steel angle along with a 0.75-inch thick steel plate and chose the plate and angle to be thick to prevent their bending and to ensure that the polypropylene sheet failed before the steel plate and angle. This testing focused on the optimum bolt spacing and response of the polypropylene composite, rather than the optimum angle and plate sizes. Test personnel drilled holes in the angle and plate every inch with alternating hole diameters of 0.3125 and 0.5625 inches, so they could use the same plates to test samples having either the 0.25- or 0.5-inch bolt diameter. Figure 18 shows the setup of the angle and the plate.

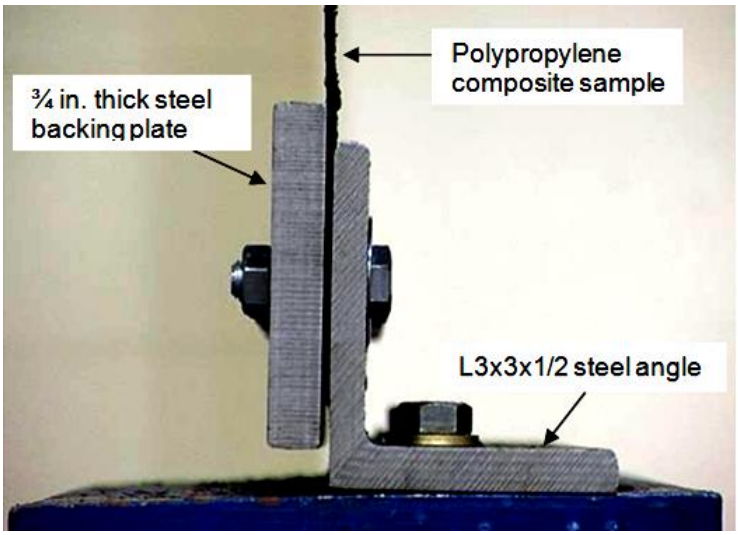

Figure 18. Mechanical Connection (Academic Slip-Critical Connection)

Test personnel then connected the steel angle and backing plate to rigid steel boxes that simulate the floor slabs inside a structure. These rigid steel boxes are painted blue in the following pictures. Nine 0.625-inch bolts with 1.25-inch outside-diameter washers, for load distribution, connected each of the steel angles to the rigid steel boxes. Test personnel then connected the rigid steel boxes to the supports of the MTS loading machine using large threaded steel rods and nuts. Once they positioned the supports and connection plates, they bolted the samples in place. For the connections, they used 0.625-inch washers for the samples with 0.25-inch bolts, 1.5-inch washers for the samples with 0.5-inch bolts, and an impact wrench to tighten all of the bolts of each size. For the 0.5-inch bolts, they used a torque wrench to apply 1200 in-lbs of torque for additional clamping friction. Figure 19 shows a depiction of the test setup and photographs of the test setup.

After AFRL test personnel positioned the supports, connections, and samples, they tested the samples in tension with the MTS loading machine at a rate of 1.5 inches per min. The test matrix in **Error! Reference source not found.** shows the details of each test.

Table 3. Mechanical Connection Testing Matrix (Series A)

Sample	Sample Length (in.)	Sample Width (in.)	Thickness of Material (in.)	Bolt Spacing (in.)	Bolt Diameter (in.)
A1	34	24	0.118	2	0.25
A2	34	24	0.118	2	0.5
A3	34	24	0.118	4	0.25
A4	34	24	0.118	4	0.5
A5	34	24	0.118	8	0.25
A6	34	24	0.118	8	0.5

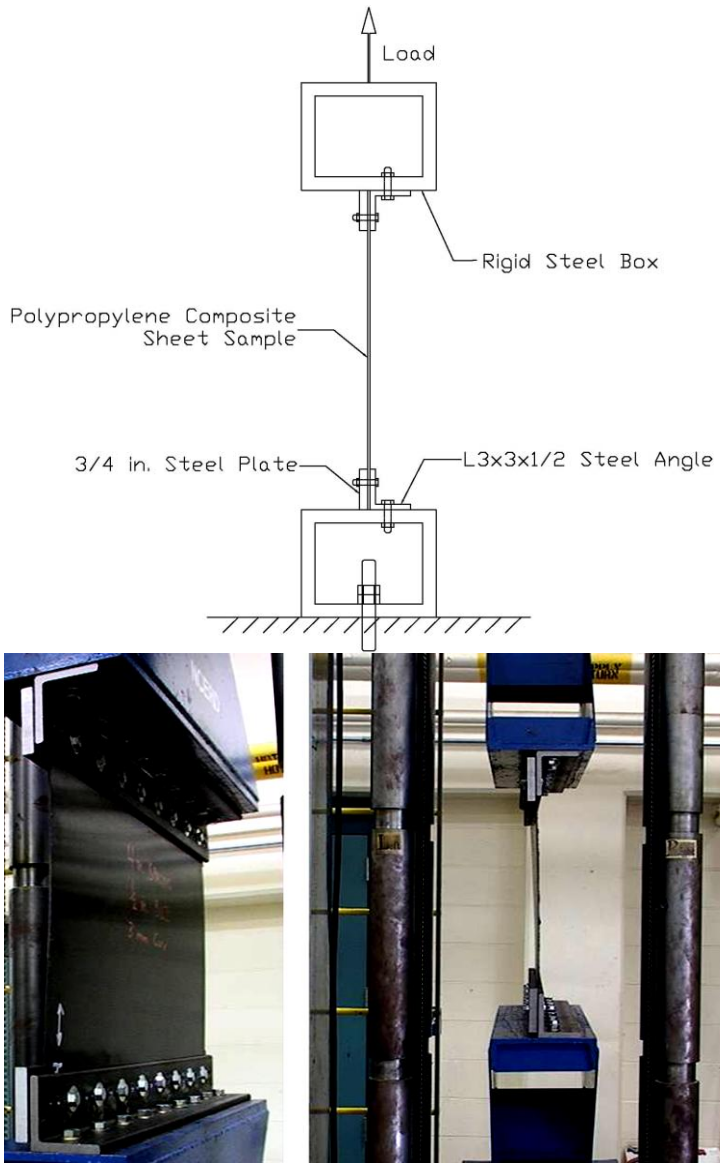

Figure 19. Mechanical Connection Setup

4.3.1.2. Results

Figure 20 shows the load–deflection response of Samples A1 through A6. Two different failure modes occurred during the six tests performed on the polypropylene sheet samples. The first was a tension failure whereby the sheet ripped across the bolt line. This failure was present when there was a higher clamping force due to larger bolt diameters (0.5 inches) or more bolts (2-inch spacing). Tension failure occurred in all three samples that used 0.5-inch bolts and also in the sample using 0.25-inch bolts with 2-inch bolt spacing. Figure 21 shows an example of this failure. The second failure type that occurred was shear failure where the bolt pulled through the edge of the polypropylene sheet sample. This type of failure occurred with the smaller-diameter bolt (0.25 inches) on the samples that used 4- and 8-inch spacing. Figure 23 shows an example of this failure.

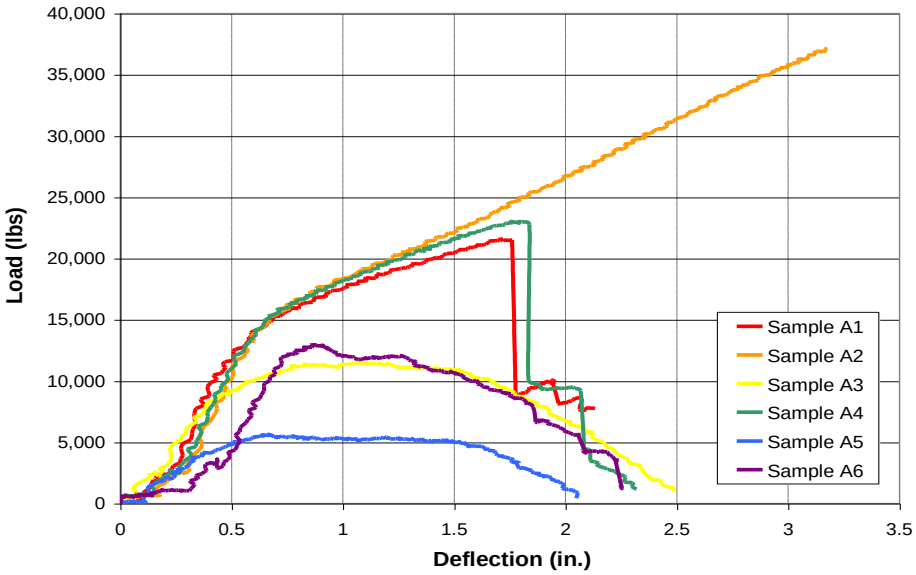

Figure 20. Mechanical Testing Results (Series A)

Using a representative stress–strain response found in Section 4.1, test personnel calculated a theoretical stress for the polypropylene composite sheet. They found that the theoretical maximum stress that they could apply to the middle cross section of the sheet was approximately 22,500 psi, which they compared to the maximum applied load in each test to show the efficiency of the connection that was used.

Table 4 presents the results of Samples A1 through A6. A detailed description of each sample and its response follow in this section.

Table 4. Mechanical Connection Testing Results (Series A)

Sample	Maximum Load (lbs)	Maximum Stress (psi)	Maximum Deflection	Percent of Theoretical Stress
A1	21,600	5,379	1.75	23.9%
A2	37,100	9,239	3.20	41.1%
A3	11,500	2,864	2.00	12.7%
A4	23,000	5,727	1.75	25.4%
A5	5,600	1,395	1.50	6.2%
A6	13,000	3,237	1.50	14.4%

Sample A1:
Sample A1 was a 3-mm (0.118-inch) polypropylene sheet using 0.25-inch bolts with 2-inch spacing. The sample began to fail in shear at the top section of the sample, but finally failed in tension (Figure 21) after reaching a maximum applied load of 21,600 lbs. This load corresponded to approximately 23.9% of the theoretical stress that the sheet could withstand.

Figure 21. Sample A1

Sample A2:
Sample A2 was a 3-mm (0.118-inch) polypropylene sheet using 0.5-inch bolts with 2-inch spacing and 1,200 in-lbs of torque applied to the bolts. The sample failed in tension (Figure 22) at the bottom section after reaching a maximum applied load of 37,100 lbs. This load corresponded to approximately 41.4% of the theoretical stress that the sheet could withstand.

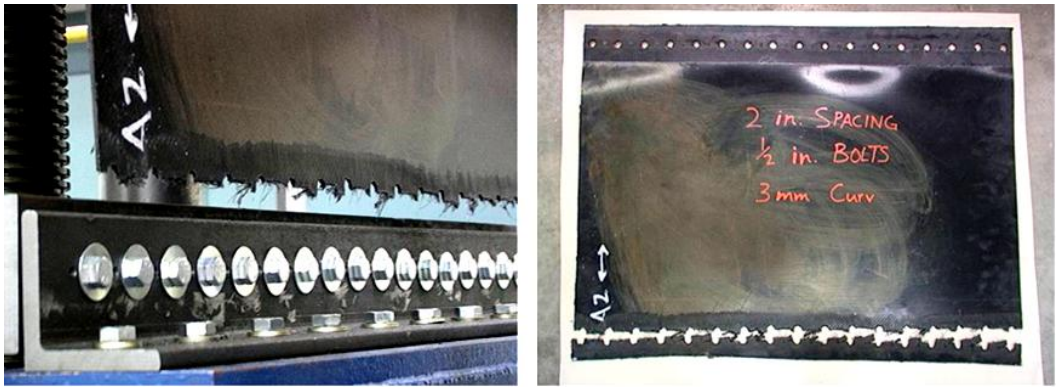

Figure 22. Sample A2

Sample A3:
Sample A3 was a 3-mm (0.118-inch) polypropylene sheet using 0.25-inch bolts with 4-inch spacing. The sample failed in shear (Figure 23) at the top section of the sample after reaching a maximum applied load of 11,500 lbs. This load corresponded to approximately 12.7% of the theoretical stress that the sheet could withstand.

Sample A4:
Sample A4 was a 3-mm (0.118-inch) polypropylene sheet using 0.5-inch bolts with 4-inch spacing and 1,200 in-lbs of torque applied to the bolts. The sample failed in tension (Figure 24) at the top section after reaching a maximum applied load of 23,000 lbs. This load corresponded to approximately 25.4% of the theoretical stress that the sheet could withstand.

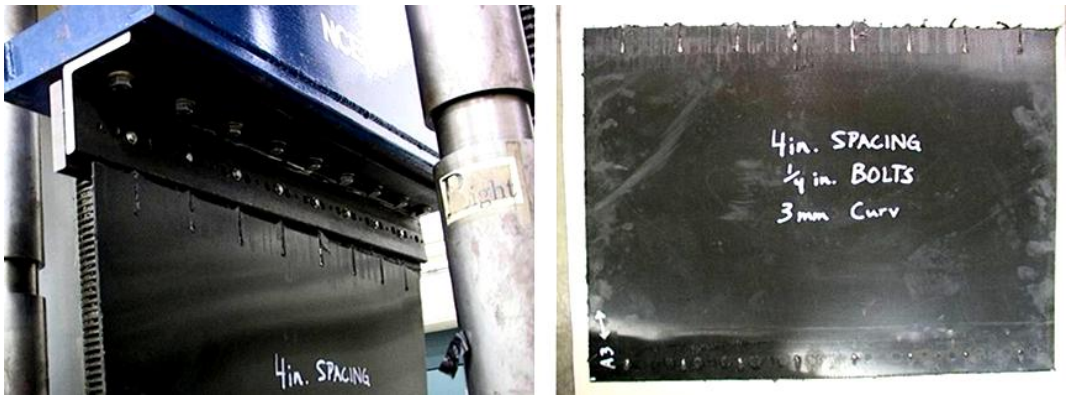

Figure 23. Sample A3

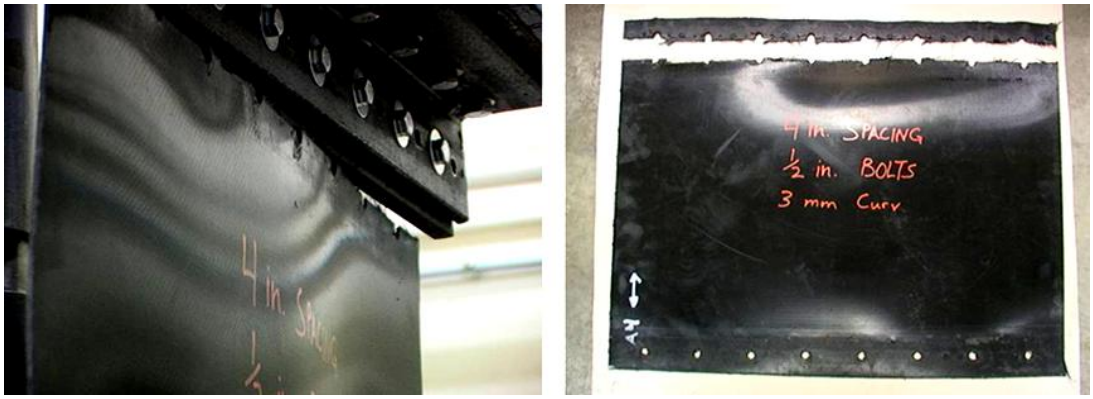

Figure 24. Sample A4

Sample A5:
Sample A5 was a 3-mm (0.118-inch) polypropylene sheet using 0.25-inch bolts with 8-inch spacing. The sample failed in shear (Figure 25) at the top section of the sample after reaching a maximum applied load of 5,600 lbs. This load corresponded to approximately 6.2% of the theoretical stress that the sheet could withstand.

Figure 25. Sample A5

Sample A6:
Sample A6 was a 3-mm (0.118-inch) polypropylene sheet using 0.5-inch bolts with 8-inch spacing and 1,200 in-lbs of torque applied to the bolts. The sample failed in tension (Figure 26) at the top section after reaching a maximum applied load of 13,000 lbs. This load corresponded to approximately 14.4% of the theoretical stress that the sheet could withstand.

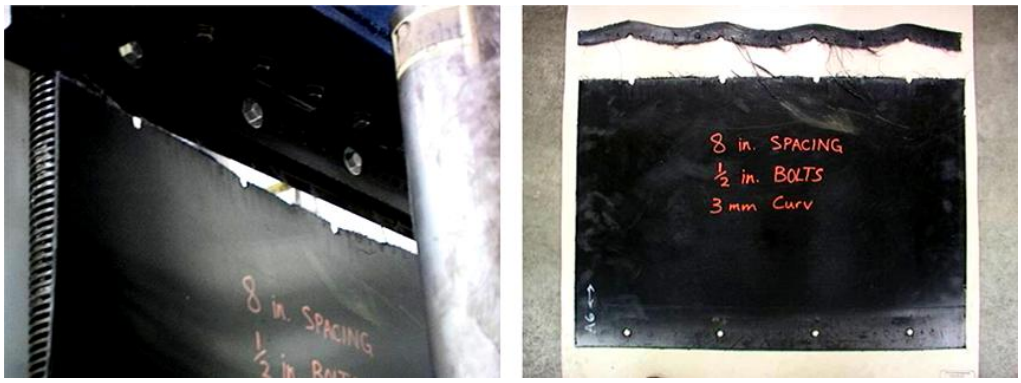

Figure 26. Sample A6

4.3.1.3. Conclusions—Series A (Component Level)

A review of the results from the first series of mechanical connection tests revealed that sample A2 performed best of all the samples. This sample employed a 2-inch bolt spacing with 0.5-inch bolt diameters for connection to the supports. This sample performed better than any of the other samples because it had the greatest clamping force subjected to the ends of the polypropylene composite section, due to the 1,200 in-lbs of torque applied to each bolt. This allowed the connection plates to "squeeze" the polypropylene sheet at the connections, which gave it the increased capacity due to the increase in friction between the sheet and the plate. The samples using 0.25-inch bolts could not get the same amount of clamping force; therefore, the resulting maximum loads for these tests were dramatically reduced. Sample A2 was able to achieve approximately 41% of the theoretical stress for the polypropylene, but this percentage was not near optimum for utilizing the entire strength of the polypropylene sheet. The amount of bolts used to provide the sample fixity may also be impractical for field installation due to the tedious nature of installing bolts every 2 inches.

4.3.2. Mechanical Connections—Series B (Full-Scale)

An evaluation of the first series of mechanical connection testing and chemically adhered connection testing revealed that finding a connection that used more of the polypropylene sheet's capacity and was more installation friendly would be beneficial. After AFRL researchers devoted considerable thought to this problem, they discovered that the 3-mm polypropylene sheets could be bent to a 90-degree angle if clamped in that position overnight. They also realized that it was much easier to bend the thinner sheets of polypropylene without even clamping them. These discoveries led to the second series of mechanical connection testing.

In this series, test personnel bent the polypropylene sheets to a 90-degree angle on the ends and connected the sheets and a long flat steel connection plate to the supports using bolts, nuts, and washers. They used a 16-point loading tree to test the samples, which was a slightly different

method than the previous two sets of connection testing. In this test, the 16-point loading tree simulated a uniform load applied perpendicular to the polypropylene sheet. The sheet then deflected into a parabolic deformed shape and transferred that loading to the supports through the tension in the sheet. AFRL performed this testing to determine the capacity of the polypropylene sheets when connected in this fashion and to evaluate the feasibility of this method of connection.

4.3.2.1. Setup and Procedure

For this series of mechanical connection testing, AFRL test personnel cut 3-mm (0.118-inch) thick sheets of polypropylene to a length of 136 inches long by 20 inches wide with a circular saw. They folded 6 inches on the end of each sample over a wooden 2x4 and clamped the fold overnight. This process allowed the polypropylene sheet to deform to approximately a 90-degree angle and made the installation much easier to accomplish. Figure 27 shows this process.

Figure 27. Bending of 3-mm Sheet

Once test personnel bent the sheets, they drilled 0.6875-inch holes 3 inches from each end at 8- or 12-inch spacing on center to be used in conjunction with 6-inch wide by 21-inch long steel connection plates with the same hole spacing. Test personnel then connected the polypropylene sheet and connection plates to the supports of the 16-point loading tree with 0.625-inch bolts and 1.75-inch washers. Since the connection plates were 6 inches wide, the sample length from plate to plate became approximately 123 inches after subtracting 12 inches due to the plates and approximately 1 inch for the curvature of the sample near the connection plate. Each test began with the sample already in a parabolic shape before loading. This initial deflection was approximately 8.5 inches for each sample. Figure 28 shows a close-up photograph of the connection plate setup, and Figure 29 shows the 16-point loading tree.

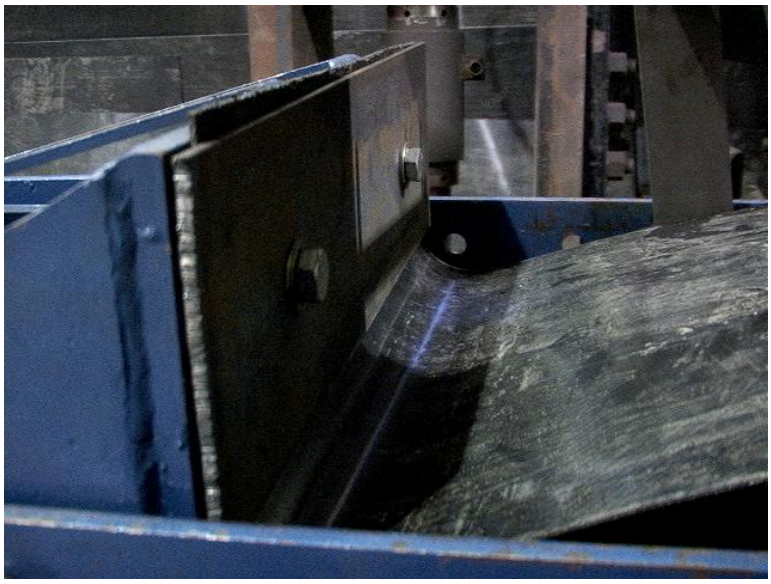

Figure 28. Connection Plate and Support

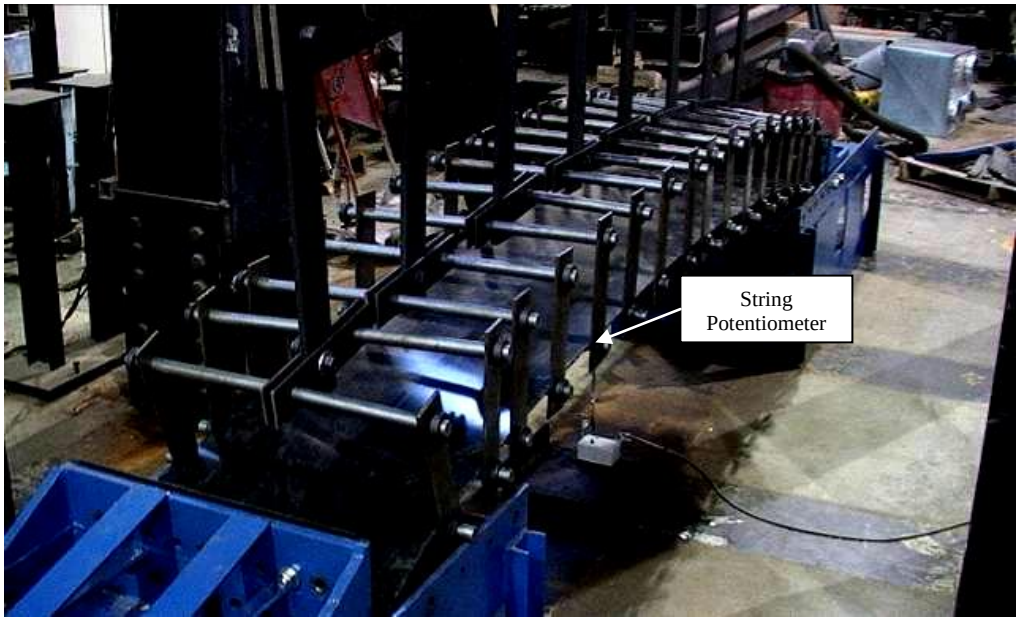

Figure 29. 16-Point Load Tree

AFRL acquired data from the tests with a 110-kip load cell attached to the top of the 16-point loading tree and one string potentiometer attached to the midpoint of the polypropylene sheet. Using LabView, test personnel recorded all load cell and string potentiometer data along with the RAM displacement of the loading tree cylinder and time. They used the data from the load cell and string potentiometer to create a pressure–deflection response and used the pressure–deflection response to find the internal tensile stress in the sheet. Section 4 thoroughly covers the process for finding the internal stress in the sheet. This series of experiments consisted of four tests. Table 5 shows the testing matrix.

Table 5. Mechanical Connection Testing Matrix (Series B)

Sample	Sample Length (in.)	Sample Width (in.)	Thickness of Material (in.)	Bolt Spacing (in.)	Plate Thickness (in.)
B1	123	20	0.118	8	0.125
B2	123	20	0.118	12	0.125
B3	123	20	0.118	8	0.25
B4	123	20	0.118	12	0.25

4.3.2.2. Results

One failure type happened during Series 2 of the mechanical connection testing. A bearing failure of the bolt on the connection plate occurred for Samples B1 and B2. In this failure, the bolt and washer ripped through the 0.125-inch steel connection plate and then through the 0.118-inch (3-mm) polypropylene sheet sample. Samples B3 and B4 did not have enough travel in the 16-point loading tree hydraulic cylinder to allow the sheet to fail. In these two cases, the connection plates bent approximately to a 45° angle before the tests concluded.

Table 6 shows the results of the Series 2 mechanical connection testing. The column "Percent of Theoretical Stress" refers to the maximum stress in the sheet divided by the ultimate stress for the sheet material, which was found to be 22,500 psi (Figure 8). The remainder of this section contains the detailed descriptions of each test.

Table 6. Mechanical Connection Testing Results (Series B)

Sample	Maximum Pressure on Sheet	Maximum Stress in Sheet	Maximum Deflection	Percent of Theoretical
B1	5.59	7,225	20.34	31.1%
B2	3.21	4,531	18.51	20.1%
B3	7.46	9,240	22.28	41.1%
B4	6.94	8,601	22.26	38.2%

Sample B1:

Sample B1 used a 3-mm (0.118-inch) thick sheet of polypropylene with a 0.125-inch thick connection plate and 8-inch bolt spacing. The sample failed due to a bearing connection of the bolts ripping through the connection plate and polypropylene sheet. The sample reached an internal stress of 7,225 psi before failing and a deflection of 20.34 inches (Figure 30). The failure mode alluded to the fact that a 0.125-inch steel connection plate was not strong enough to be used in conjunction with a 3-mm (0.118-inch) polypropylene sheet. This resulted in an inefficient connection.

Sample B2:

Sample B2 used a 0.118-inch (3-mm) thick sheet of polypropylene with a 0.125-inch thick connection plate and 12-inch bolt spacing. The sample failed due to a bearing connection of the bolts ripping through the connection plate and polypropylene sheet. The sample reached an

internal stress of 4,531 psi before failing and a deflection of 18.51 inches (Figure 31 andFigure 32).

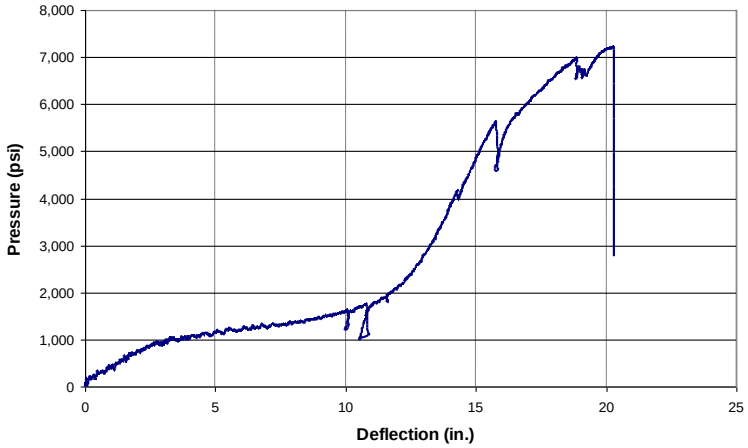

Figure 30. Sample B1 Results (Load vs. Deflection)

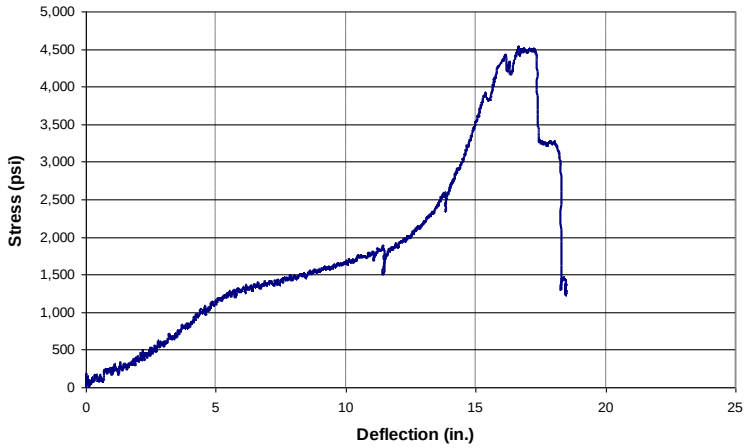

Figure 31. Sample B2 Results (Load vs. Deflection)

Figure 32. Sample B2 Results

This sample did not reach as high a stress as sample B1 due to the fact that it had less clamping force because of the longer bolt spacing. The failure mode could mean that a 0.125-inch steel connection plate was not strong enough to be used in conjunction with a 0.118-inch (3-mm) sheet of polypropylene. This resulted in an inefficient connection.

Sample B3:

Sample B3 used a 0.118-inch (3-mm) thick sheet of polypropylene with a 0.25-inch thick connection plate and 8-inch bolt spacing. The sample did not fail due to the hydraulic cylinder's running out of travel. The sample reached an internal stress of 9,240 psi and a deflection of 22.28 inches (Figure 33 and Figure 34) before the conclusion of the test. If the hydraulic cylinder had had more travel, the internal stress may have increased before the sample ultimately failed.

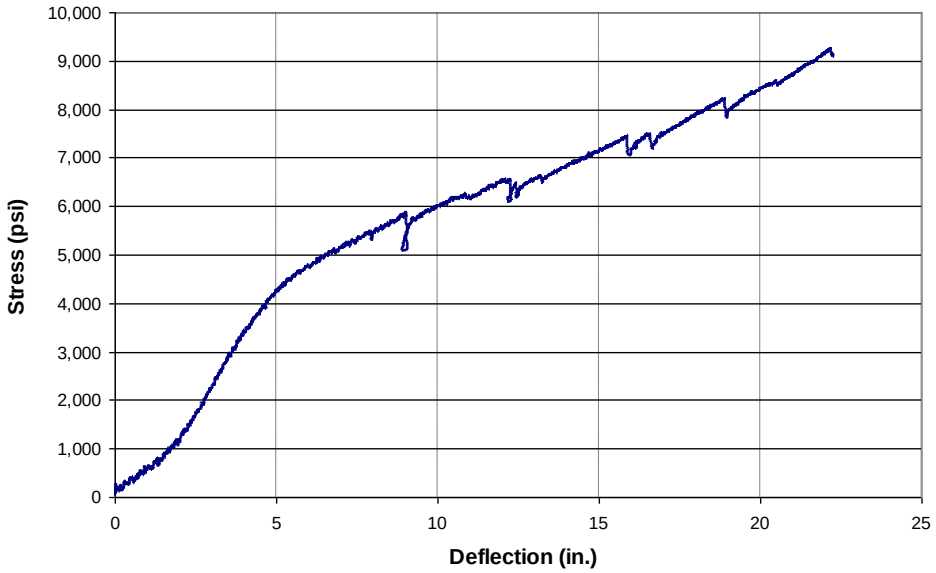

Figure 33. Sample B3 Results (Load vs. Deflection)

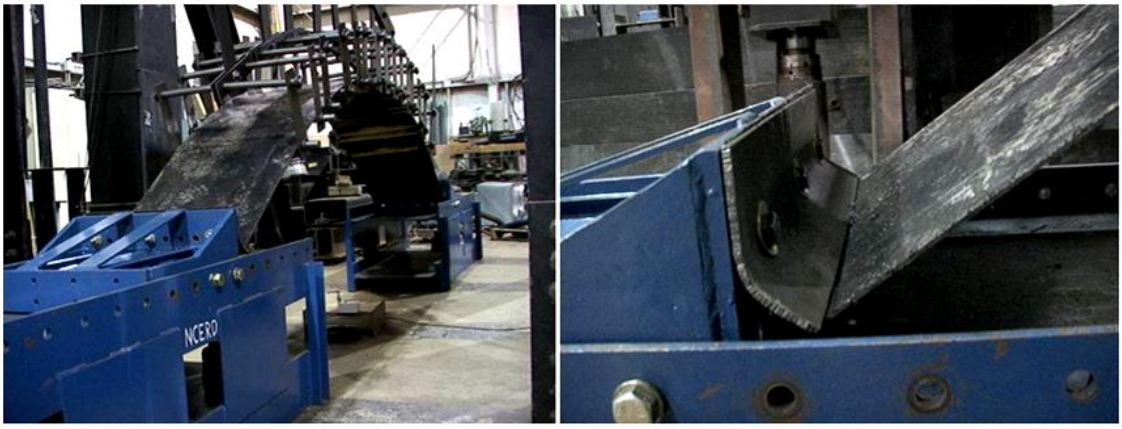

Figure 34. Sample B3 Results

Sample B4:
Sample B4 used a 0.118-inch (3-mm) thick sheet of polypropylene with a 0.25-inch thick connection plate and 12-inch bolt spacing. The sample did not fail due to the hydraulic cylinder running out of travel. The sample reached an internal stress of 8,601 psi and a deflection of 22.26 inches (Figure 35 and Figure 36) before the conclusion of the test. If the hydraulic cylinder had had more travel, the internal stress may have increased before the sample ultimately failed.

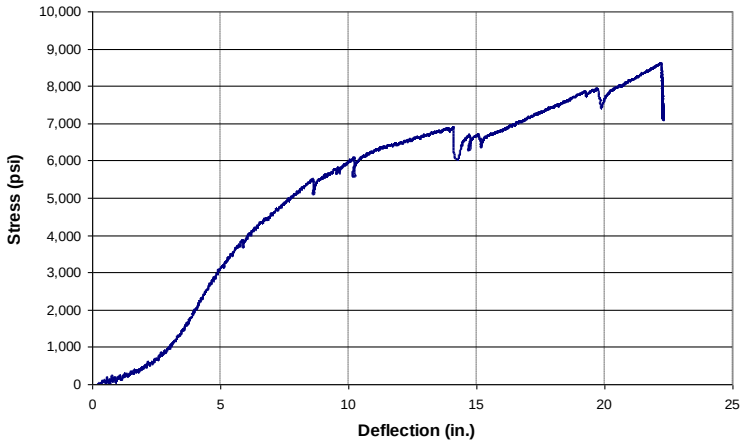

Figure 35. Sample B4 Results (Load vs. Deflection)

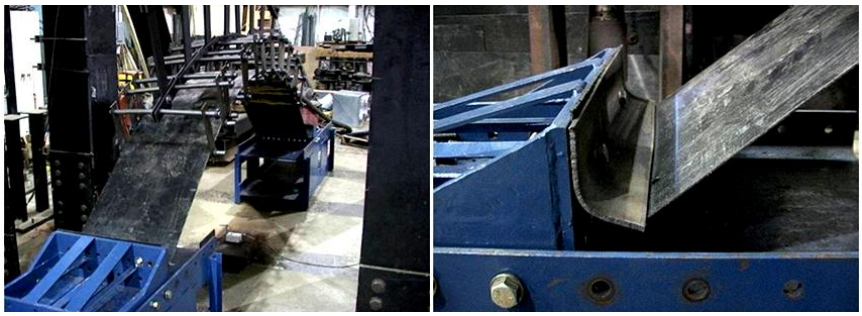

Figure 36. Sample B4 Results

4.3.2.3. Conclusions—Series B (Full-Scale)

A review of the second series of mechanical connection tests revealed that Sample B3 performed the best of all samples and achieved a maximum internal stress of 9,240 psi. This stress corresponded to approximately 41.1% of the theoretical stress that this polypropylene sheet was able to withstand. Also, the fact that the hydraulic cylinder ran out of travel before the failure of the sheet implied that there may have been more unused capacity in the sheet. Achieving 41.1% of theoretical stress in the highest performing sample was not near optimum, although at this point this method of connection appeared to be the most practical of all the methods that were investigated. The mechanical connections in the second series of tests were easier to install than the connections in the first series of tests, and these connections could feasibly be instituted in the field. Section 6 describes the tests that used this method of connection for the verification of the analytical model.

5. ANALYTICAL RESISTANCE FUNCTION

To develop an analytical model of the polypropylene sheet material used for blast resistant sheet retrofits, researchers must follow four basic steps based on a mechanics of materials approach.

1) Assume the deflected shape is parabolic and obtain the shape function.
2) Use equilibrium and a free body diagram of the sheet system under a uniform loading to relate the pressure exerted on the sheet and the tensile stress in the sheet.
3) Relate stress to strain by means of a stress–strain curve obtained for the material.
4) Correlate strain to the midspan deflection of the sheet using compatibility equations.

By means of these four steps researchers can plot a pressure versus deflection graph, which is also referred to as the static resistance function, for the material and can use the static resistance function as a model to predict the behavior of the polypropylene sheet under uniform loading.

To make a complete analytical model of the entire wall system, researchers must take the CMU wall into account within the analytical model. Government and military buildings such as embassies and barracks often use CMU. These walls have a large amount of mass, but not much ductility. Increasing the ductility in the system so that the energy is absorbed is an important part of making a structure blast resistant. To analyze these walls dynamically, researchers must first obtain the static resistance function. The following sections delve into more details about the methodology used to create polypropylene sheet and the CMU wall sections of the analytical model.

5.1. Theoretical Sheet Model

5.1.1. Deflected Shape

The first step in finding the analytical model is to assume a parabolic deflected shape for the retrofit sheet with an applied uniform load. Figure 37 below shows this shape.

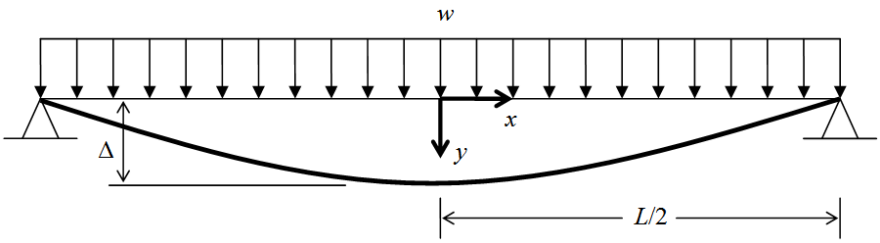

Figure 37. Assumed Deflected Shape

The general expression for a parabolic function, similar to the one shown in Figure 37, is as follows:

$$y(x) = Ax^2 + Bx + C \quad (1)$$

By using the general expression along with boundary conditions found from Figure 37, it is possible to solve for *A*, *B*, and *C* in Equation 1. To find the solution, the first derivative of Equation 1 must be established as shown below:

$$y'(x) = 2Ax + B \tag{2}$$

The first boundary condition may be written as:

$$y'(x) = 0 \text{ at } x = 0$$

When the first boundary condition is substituted into Equation 2, the result is:

$$B = 0$$

The second boundary condition is:

$$y(x) = \Delta \text{ at } x = 0$$

When the second boundary condition is substituted into Equation 1 and zero is substituted in for *B*, the following results:

$$C = \Delta$$

The third and final boundary condition is:

$$y(x) = 0 \text{ at } x = \frac{L}{2}$$

When the third boundary condition is substituted into Equation 1, zero is substituted in for *B*, and Δ is substituted in for *C*, the following results:

$$A = -\frac{4\Delta}{L^2}$$

At this point, *A*, *B*, and *C* may be substituted into Equations 1 and 2 to give the expressions for *y*(*x*) and *y'*(*x*) as shown below:

$$y(x) = -\frac{4\Delta}{L^2}x^2 + \Delta \quad or \quad y(x) = \Delta\left[1 - 4\left(\frac{x}{L}\right)^2\right] \tag{3}$$

$$y'(x) = -\frac{8\Delta}{L^2}x \tag{4}$$

5.1.2. Equilibrium and Free Body Diagram

At this point it is possible to find a relationship between the pressure being exerted on the sheet and tensile stress in the sheet. It is assumed that the tension throughout the sheet is uniform along its length. Although this may not be entirely accurate, as discovered by Kennedy (2005), for simplicity this methodology is used in this analysis.

Figure 38 shows a free body diagram of the retrofit sheet under loading. The distributed load, *w*, has been replaced by pressure, *p*, by the relationship *w* = *pb*. The unit width, *b*, is assumed to be equal to 1, resulting in *w* = *p*.

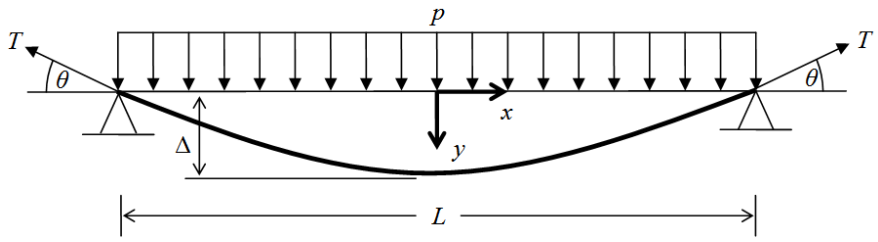

Figure 38. Free Body Diagram

By means of equilibrium it is possible to sum the forces in the *y*-direction of Figure 38 to obtain a relationship between *T* and *p* as shown below:

$$2T \sin\theta = pL \tag{5}$$

Since θ is equal to $y'(x)$ from Equation 4, Equation 5 can be replaced by the following:

$$2T \sin\left(\left|-\frac{8\Delta}{L^2}\right|\right) = pL \tag{6}$$

At this point it is possible to show that $T = \sigma A$ for a sheet in tension, and $A = bt$, where *b* is a unit width of 1 and *t* is the thickness of the sheet. Since θ is measured at the ends, $L/2$ can be substituted for *x*. Now Equation 6 may be written as:

$$2\sigma t \sin\left(\frac{8\Delta}{L^2}\frac{L}{2}\right) = pL \tag{7}$$

This finally reduces to:

$$p = \frac{2\sigma t}{L}\sin\left(\frac{4\Delta}{L}\right) \tag{8}$$

5.1.3. Constitutive Stress–Strain Relationship

Next, it is possible to use a typical stress–strain diagram for the polypropylene sheet material to show the constitutive relationship between stress and strain. Figure 8 shows a typical constitutive relationship. The curve labeled "engineering stress" is the average data that were taken from the coupon tests, and the curve labeled "true stress" is the corrected stress values that were obtained from the following equation:

$$\sigma_t = \frac{\sigma_e}{(1-\varepsilon\upsilon)^2} \tag{9}$$

It is important to calculate true stress because engineering stress does not take into account the fact that the coupon specimen is elongating and its cross-sectional area is decreasing. Engineering stress is directly proportional to the load, which results in less stress as the specimen elongates and the area gets smaller. True stress is directly proportional to the load, but also is inversely proportional to the area. This results in a higher stress as the specimen elongates (Beer, et al., 2002). An estimated value of 0.3 was entered for Poisson's ratio, υ, based on the approximate Poisson's ratio for polypropylene. The "true stress" plot may now be used to

correlate stress at any given point of strain. As an added note, this is only valid through the elastic portion of the curve; a transition from ν= 0.3 to an increasing value not to exceed 0.5 can be used in the plastic portion of the curve. But it is conservative to carry the 0.3 value throughout the design if a factor of safety will be used in the connection design.

5.1.4. Compatibility and Deflection

Finally, it is possible to find a relationship between deflection and strain using compatibility. This is done by using the initial equation:

$$\varepsilon = \frac{L' - L}{L} \tag{10}$$

This equation may be rewritten as:

$$L' = L(\varepsilon + 1) \tag{11}$$

Arc length, *L'*, may also be defined by the following equation:

$$Arc\ Length = L' = 2\int_0^{\frac{L}{2}} \sqrt{1 + \left(g'(x)\right)^2} \tag{12}$$

Equation 4 may be substituted for $g'(x)$ in this case. Using mathematics software to solve for *L'* gives the following equation:

$$L' = \frac{4\Delta}{L}\left[\sqrt{\frac{L^2}{4} + \frac{L^4}{64\Delta^2}} + \left(\frac{L^3}{32\Delta^2}\right)\ln\left(\frac{L}{2} + \sqrt{\frac{L^2}{4} + \frac{L^4}{64\Delta^2}}\right) - \left(\frac{L^3}{32\Delta^2}\right)\ln\left(\frac{L^2}{8\Delta}\right)\right] \tag{13}$$

5.1.5. Summary

Using the information and concepts from Sections 5.1.1 through 5.1.4, it is possible to plot a pressure versus deflection diagram, also known as static resistance function. The following list outlines the iterative process involved in generating the static resistance function:

1) Set Δ equal to zero, and then incrementally increase Δ by a small amount.
2) Use Equation 13 to find the new value for arc length, *L'*.
3) Use Equation 10 to find the strain corresponding to arc length.
4) Use Figure 8 to calculate the stress corresponding to strain.
5) Use Equation 8 to calculate the pressure related to stress.
6) Plot the calculated pressure against the incremented deflection.
7) Increment Δ and repeat Steps 2 through 6.

The steps shown above may be repeated until the predicted failure is reached in the polypropylene sheet. Figure 39 shows the resistance function of a theoretical polypropylene sheet retrofit sheet created by this procedure. This sheet has an arbitrary span length of 10 feet, width of 20 inches, and a thickness of 0.079 inches (2 mm). Figure 39 indicates that the sheet could deflect up to 30 inches, but this is before taking into account the fact that there is a failure

limit that would most likely occur before the deflection reaches this point. Section 6 includes a more thorough discussion of these topics.

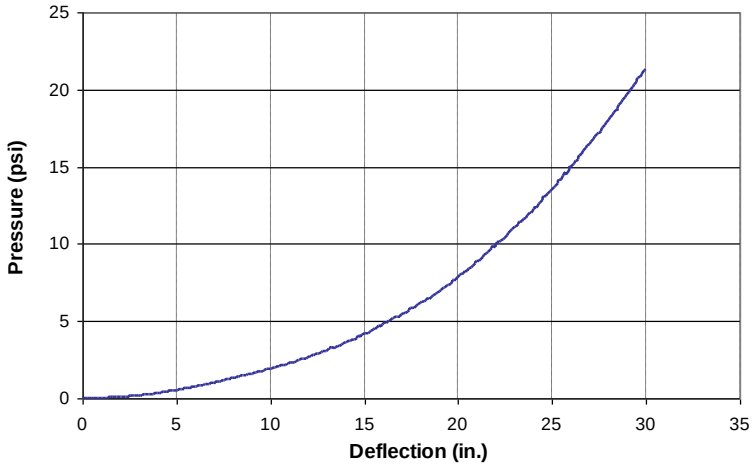

Figure 39. Static Resistance Function

5.1.6. Deflection Correction

The theoretical model described in the previous sections assumes that the polypropylene sheet has no initial deflection. In other words, that the entire retrofit sheet is initially in line with the connection to the supports. It may be necessary to obtain a static resistance function for a polypropylene sheet having an initial deflection. This is the case for the samples tested in Section 6. To obtain this initially deflected static resistance function, the procedure in the previous sections is slightly modified.

First, the initial deflection must be measured and a new L' must be obtained using Equation 13. L is equal to the length between the supports, and Δ is equal to the measured deflection. Next, the strain must be calculated using Equation 10, with the L' previously calculated being equal to L in Equation 10. This sets the strain at the initial position of loading to zero. At this point steps 4 through 7 in Section 5.1.5 can be followed.

If this method is not followed for finding the static resistance function for an initially deflected polypropylene sheet, there is strain present in the initial deflected position of the sheet being analyzed, when in reality there is none. Figure 40 compares the difference in the pressure–deflection curves of a polypropylene sheet with no initial deflection and a sheet with an initial deflection of 7 inches. Both sheets have an arbitrary span length of 10 ft, width of 20 inches, and a thickness of 0.079 inches (2 mm). It is seen that the sheet with an initial deflection gains in resistance pressure more quickly, but does not deflect as far before failure.

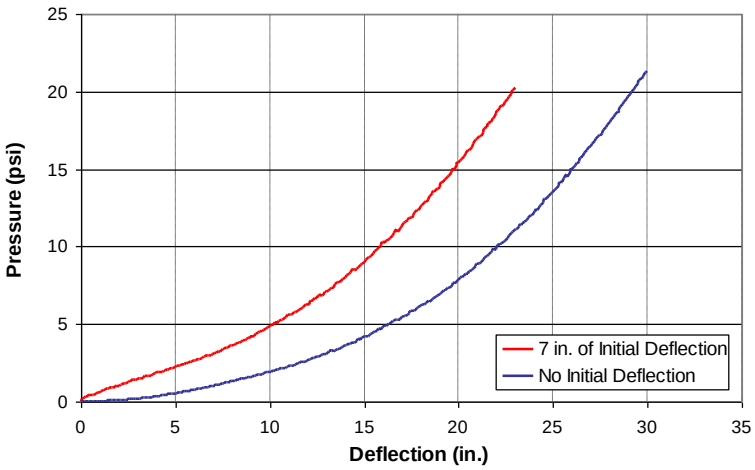

Figure 40. Static Resistance Functions with and without Initial Deflection

5.2. Theoretical Concrete Masonry Unit Wall Model

Various different boundary conditions can be used in securing CMU infill walls. For the sake of brevity only two types are discussed in this report. The first type of boundary condition consists of fixity, where the top and bottom sections of the wall are prevented from rotation until failure of the wall. With this boundary condition the wall experiences "arching," where a moment is developed at the top and bottom supports of the wall and an internal axial compressive force is developed in the CMU. In this case, construction of the wall allows for no gap between the top of the CMU wall and the floor slab above. This type of boundary condition creates load-bearing CMU walls. This type of wall construction is referred to as "arching walls."

The second type of boundary condition that is discussed in this report is a case where a gap is left between the top of the CMU wall and the floor slab above. This gap is large enough to allow for rotation of the top of the wall without development of an axial force. Obviously, these walls are not load bearing. This type of wall construction is referred to as "non-arching walls." It should be noted that no reinforcement is considered in either wall construction case. Also, both cases are essentially simply supported where the wall is supported on two sides, being the top and bottom, and not on either edge. The analytical models in this section are based on "WAC: An Analysis Program for Dynamic Loadings on Masonry and Reinforced Concrete Walls" (Jones, 1989).

5.2.1. Non-Arching Walls

The resistance functions for simply-supported one-way-action unreinforced masonry walls take place in two phases. First, there is an elastic phase in which the bending strength of the masonry dictates the resistance of the wall. Initial failure of the wall occurs when the modulus of rupture of the mortar is reached, at which point the second phase begins. in this phase, called the decaying phase, the resistance is dictated by the geometry of the wall and the magnitude of the overburden forces imposed on the wall. Figure 41 shows the assumed free body diagrams for the two resistance phases for simply-supported walls. In Figure 41, Q_1 and Q_2 are the maximum resistances of the elastic and decaying phases respectively, P_v is the axial load or overburden

from the floor above, *W* is the weight of the wall, *L* is the length of the wall, and *V* is the reaction at the support.

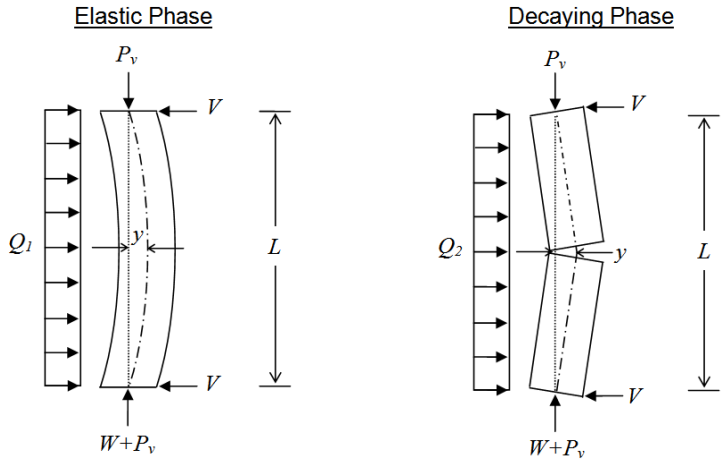

Figure 41. Resistance Phases of Simply-Supported Masonry Walls

From Jones (1989) the resistance function of the elastic phase can be given by:

$$Q_1 = \frac{4t_w}{3L}(f_r t_w + P_v) \tag{14}$$

where t_w is the thickness of the wall and f_r is the modulus of rupture of the mortar. The maximum elastic deflection, y_1, may be given by the following equation:

$$y_1 = \frac{5Q_1L^3}{384EI_g} \tag{15}$$

where E is the modulus of elasticity of the mortar and I_g is the gross moment of inertia. After the maximum elastic deflection is reached the resistance function drastically drops down to the resistance of the decaying phase, which is given by:

$$Q_2 = \frac{4}{L}(t_w - y_2)\left(P_v + \frac{W}{2}\right) \tag{16}$$

where y_2 is the deflection corresponding to Q_2.

The following Figure 42 shows the static resistance function of a one-way-action simply-supported unreinforced masonry wall without arching effects with the following properties:

- Wall thickness, t_w = 8 in
- Wall height, L = 120 in
- Axial load, P_v = 0 lbs
- Modulus of rupture of mortar, f_r = 65 psi
- Modulus of elasticity of mortar, E = 3.12 x 10^6 psi
- Gross moment of inertia, I_g = 35.5 in^4

- Weight of the wall, W = 33 lb/in

It can be observed from Figure 42 that this wall has a very small deflection before cracking occurs. The actual deflection when cracking occurs is 0.0094 inches, but this cannot be determined from this figure due to the lack of precision. Once cracking occurs, the resistance drops to an almost negligible value of 0.04 psi. It is obvious from this model that a simply-supported masonry wall without the effects of arching has essentially no resistance to a blast event.

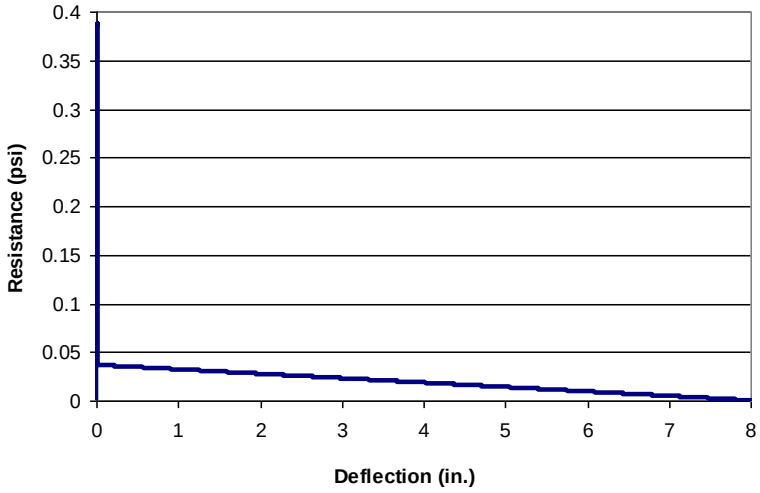

Figure 42. Static Resistance Function of Arbitrary Simply-Supported Masonry Wall

5.2.2. Arching Walls

The resistance functions for one-way-action unreinforced masonry walls experiencing the effects of arching also take place in two phases just as with the simply-supported walls. The effects of arching increase the strength of the walls due to the axial compressive forces imparted by the restraint of the in-plane movement of the wall. This analysis assumes rigid supports at the top and bottom of the wall to restrain the geometry of the wall during bending. Figure 43 shows the

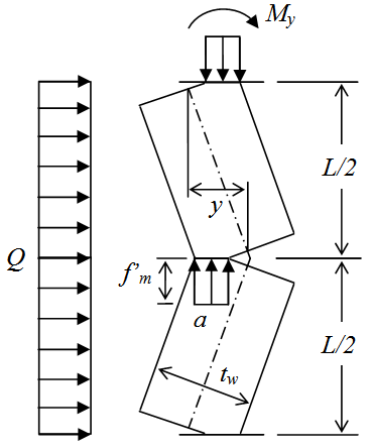

Figure 43. Resistance of Masonry Walls Experiencing Arching Effects

free body diagram of the wall experiencing arching after initial cracking has occurred. In the figure Q is the resistance of the cracked wall section, f'_m is the modulus of rupture of the masonry, M_y is the maximum moment, and a is the width of the Whitney stress block. It should be noted that the forces at the bottom half of the figure are not shown.

From Jones (1989) the deflection corresponding to the yield strain, y_y, can be expressed by:

$$y_y = \frac{t_w f'_m L_d}{E_m\left(L_d - \frac{L}{2}\right)} \tag{17}$$

where E_m is the modulus of elasticity of the masonry. L_d is given by:

$$L_d = \sqrt{\left(\frac{L}{2}\right)^2 + {t_w}^2} \tag{18}$$

The maximum resistance corresponding to the maximum yield strain, Q_y, is given by:

$$Q_y = \frac{2f'_m}{L}\left(t_w - y_y\right)^2 \tag{19}$$

When deflections become greater than y_y, the resistance function is governed by the decaying phase. This resistance is given by:

$$Q = \frac{2f'_m}{L}(t_w - y)^2 \tag{20}$$

When $y > y_y$.

Figure 44 shows the static resistance function of a one-way-action unreinforced masonry wall experiencing the effects of arching with the same properties as mentioned for the wall in Figure 44, with the addition of the following properties for masonry:

- Modulus of rupture of the masonry, f'_m = 3,000 psi
- Modulus of elasticity of masonry, E = 3.12 x 10^6 psi

It can be observed from Figure 44 that the same wall as in Figure 42 with the addition of arching effects increases the resistance of the wall by a very significant amount. The deflection before cracking is also significantly increased to approximately 1 inch. It is apparent from these models that the method of construction can affect the amount of blast resistance a wall exhibits.

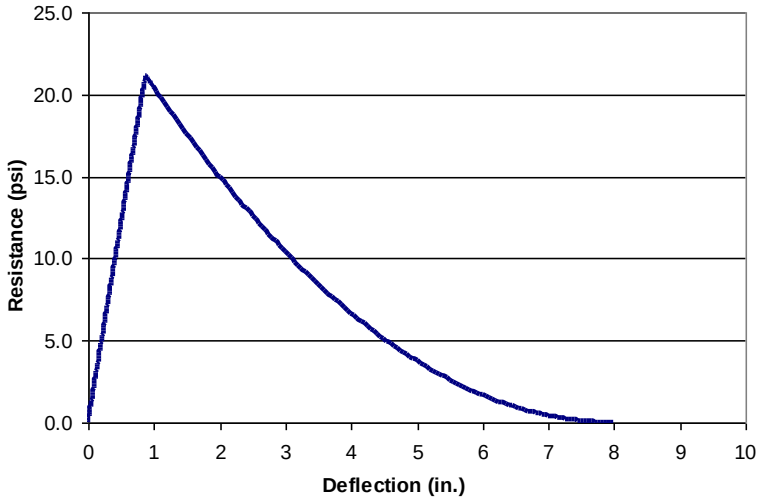

Figure 44. Static Resistance Function of an Arbitrary Masonry Wall with Arching Effects

5.3. CMU and Polypropylene Composite Sheet Wall System

The final static resistance function for the CMU wall with a polypropylene composite sheet retrofit consists of the resistance of the CMU wall itself in addition to the polypropylene sheet resistance. It can be seen from the models that the CMU wall has a relatively brittle failure, while the polypropylene sheet has a ductile failure. The polypropylene sheets provide added energy absorption, which is critical to the absorption of the blast pressures and the safety of the occupants inside the structure.

Since the polypropylene sheet is not bonded to the CMU wall, it is reasonable to assume that non-composite action between the sheet and the wall is present. Research done by Moradi et al. (2008) indicates that for a sheet retrofit that is adhered or fastened to a CMU wall, the length of the sheet that is affected by the cracking of the wall is far less than the length of the wall. Even though the sheet covers the entire backside of the wall, the tributary length of the sheet is dependent on the crack width and the strain development that extends past the edges of the crack. In this method of securing the retrofit sheet, the sheet may be strained much quicker with smaller deflections leading to rupture of the sheet due to the fact that the available resistance of the entire sheet is not being used.

For the CMU–polypropylene composite wall system, it is assumed that the friction between the CMU wall and the polypropylene sheet is negligible. These assumptions allow the resistance function for the system to be calculated by simply adding the values of the two component resistance functions already obtained at any given deflection. This method allows for the resistance of the entire retrofit sheet to be used. Figure 45 shows a resistance function for a one-way-action unreinforced masonry wall system experiencing the effects of arching with a polypropylene sheet retrofit. The properties for this wall system are the same as the properties given for the examples in Sections 5.1 and 5.2.2.

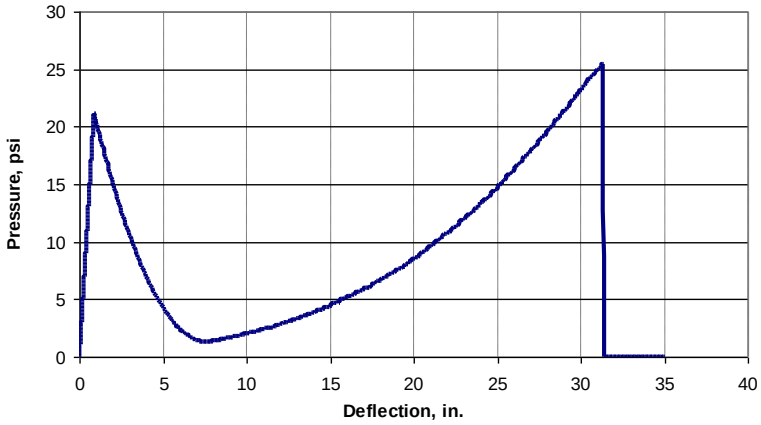

Figure 45. Static Resistance Function of an Arbitrary Wall System

Previous research on this topic (Fitzmaurice, 2006) has indicated that the resistance of the sheet should immediately increase to the point of resistance that the CMU wall is at when the masonry cracks. This is not correct due to the fact that the sheet retrofit is still relatively loose on the wall when compared to the tension that is required for the sheet resistance to increase to that point. Figure 46 shows an example of such behavior. The dotted vertical line in the figure shows the point at which the masonry cracks.

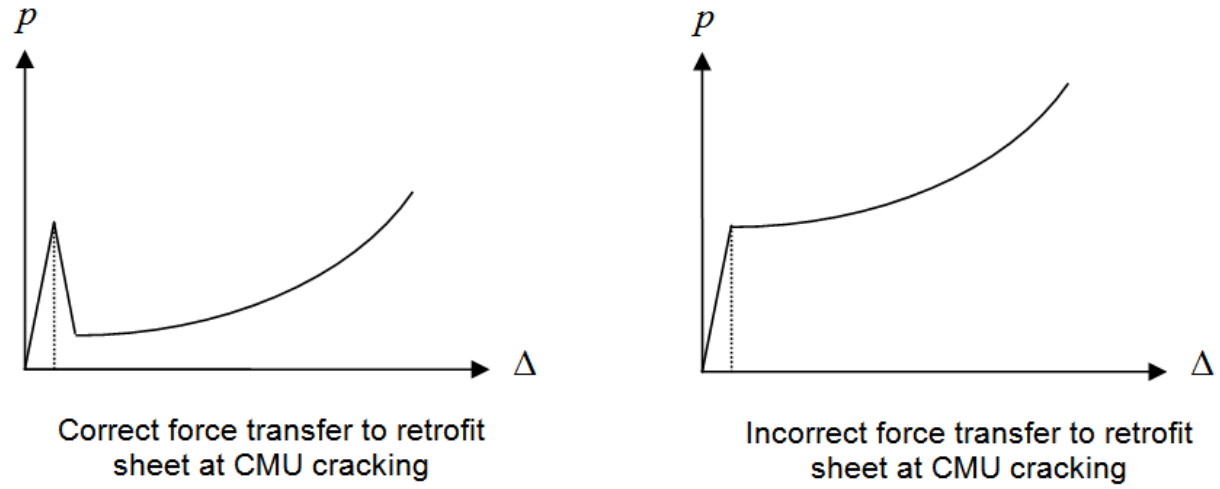

Figure 46. Difference in Retrofit Sheet Model Methodologies

A preliminary program has been developed for the use of analyzing CMU walls with polypropylene sheet retrofits. This program allows for the input of CMU wall and retrofit sheet properties and calculates the static resistance function for a given wall system. After the input parameters are entered the program runs through the steps outlined in Section 5.1 to create the static resistance function for the polypropylene sheet. During this process the program references the stress–strain response curve for the material automatically at each new deflection length. Also, the program uses the equations from Section 5.2 to create the static resistance function for the CMU wall. These two static resistance functions are then added together to form a graph of the static resistance function for the entire system similar to the one shown in Figure 45.

6. EXPERIMENTAL VERIFICATION OF STATIC RESISTANCE FUNCTION

After obtaining an analytical resistance function, AFRL validated the model with experimental data. In this set of tests, test personnel subjected component membranes to uniform static loading by means of a 16-point loading tree. From the tests, they obtained pressure–deflection curves and compared the curves to the analytical static resistance function. Also, they closely examined and evaluated connection optimization and field installation feasibility.

6.1. Setup and Procedure

For the component membrane tests AFRL cut polypropylene sheets 136 inches long by 20 inches wide with a circular saw and drilled 0.6875-inch holes in a line (using different spacing) 3 inches from each end. Test personnel then used a flat 6-inch wide by 21-inch long connection plate (with hole spacing corresponding to the sheet) to connect the sheet to the supports of the 16-point loading tree. For this connection they used 0.625-inch bolts in conjunction with 1.75-inch washers. Since the connection plates were 6 inches wide, the sample length from plate to plate became approximately 123 inches after subtracting the 12-inch depth of the connection plates and approximately 1 inch for the curvature of the sample near the connection plate. Each test began with the sample already in a parabolic shape before loading. This initial deflection was approximately 7 inches for each sample. Test personnel corrected the analytical model for this initial deflection following the procedure outlined in Section 4.3.2.

To optimize the performance of the polypropylene sheets test personnel changed three main variables during the course of testing. The modified variables were sheet thickness, connection plate thickness and bolt spacing.

In addition to changing these variables, test personnel conducted two tests (Samples 10 and 11) with a 6-inch × 6-inch polypropylene angle between the sample sheet being tested and the connection plate. They used double-sided adhesive tape to connect the polypropylene angle to the polypropylene sheet. In two different tests (Samples 31 and 32), they replaced the 6-inch wide by 21-inch long flat connection plate with three 4-inch wide by 7-inch long connection plates. Table 7 summarizes all samples tested.

6.2. Results

Test personnel obtained the results for each sample listed in Table 7 via the procedure described in Section 4.3.2. They recorded three main quantities from each test: the energy absorbed, the maximum deflection of the sheet, and the maximum pressure that was exerted on the sheet by the simulated uniform loading. The energy absorbed by the sheet is equivalent to the area under the pressure-deflection curve. Finding this area is a good way to evaluate the blast-energy absorbing capability that is present in the sheet. The maximum pressure and deflection are related to this energy absorbing capability because the more pressure or deflection that a sheet obtains, the

more energy it absorbs.

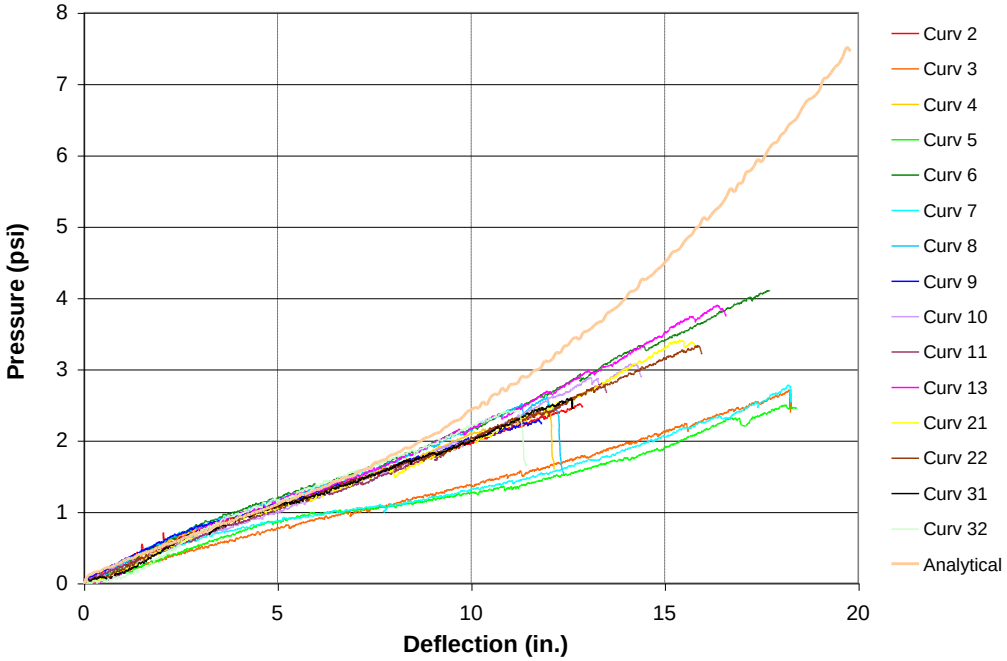

Figure 47. Response Summary of 1-mm Samples

Most pressure deflection curves from **Error! Reference source not found.** match well with the analytical resistance function up to a deflection of approximately 7 or 8 inches except for Samples 3, 5, and 7. These three samples were the only samples to use 0.125 inch connection plates. The remainder of this section includes an explanation of the results from each individual test.

shows a breakdown of the component membrane test results. In this table, researchers determined the analytical energy absorbed at the maximum deflection of the experimental sample to make a true comparison between the analytical and the experimental energy absorbed. The "Percent of Analytical" column shows the percent of energy absorbed that

the experimental sample obtained compared to that of the analytical resistance function. Refer to Table 7 to correlate the sample name in

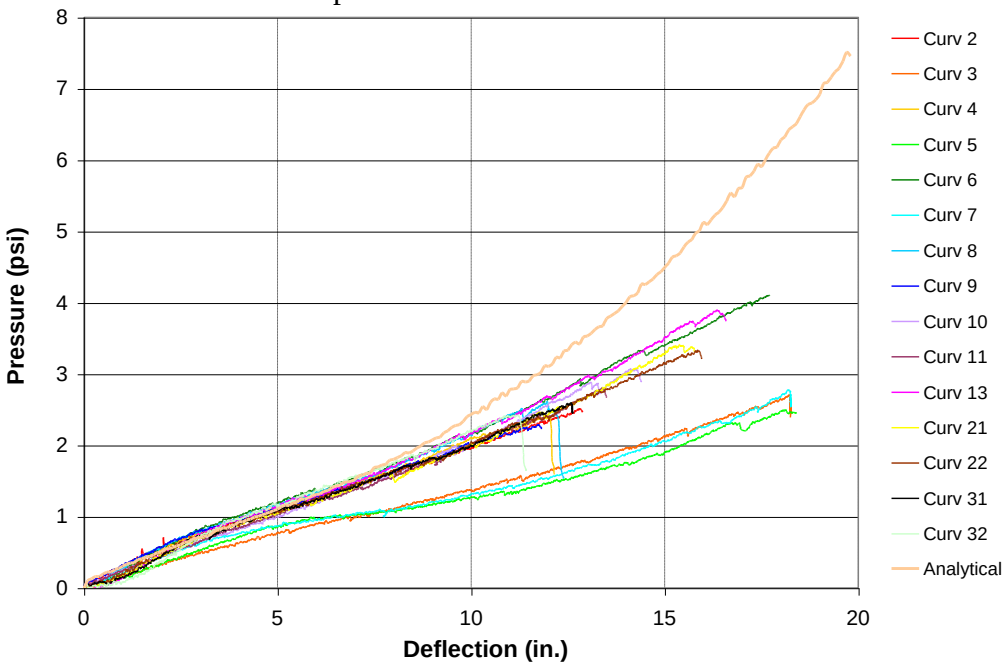

Figure 47. Response Summary of 1-mm Samples

Most pressure deflection curves from **Error! Reference source not found.** match well with the analytical resistance function up to a deflection of approximately 7 or 8 inches except for Samples 3, 5, and 7. These three samples were the only samples to use 0.125 inch connection plates. The remainder of this section includes an explanation of the results from each individual test.
with the testing variables.

Table 7. Component Membrane Testing Matrix

Sample Number	Material Thickness (mm)	Bolt Spacing (in)	Plate Thickness (in)
7	1	8	1/8
6 & 22	1	8	1/4
13 & 21	1	8	3/8
5	1	12	1/8
4	1	12	1/4
8	1	12	3/8
3	1	16	1/8
2	1	16	1/4
9	1	16	3/8
10*	1	12	3/8
11*	1	16	3/8
16	2	8	3/8
12 & 17	2	12	3/8
15	2	16	3/8
20	1 x 2	8	3/8
14 & 19	1 x 2	12	3/8
18	1 x 2	16	3/8
29	0.35	4	1/4
23 & 27	0.35	8	1/4
24	0.35	12	1/4
30	0.49	4	1/4
25 & 28	0.49	8	1/4
26	0.49	12	1/4
31** & 32**	1	8	1/4
*3-mm angles were used at the connections			
**Three 4-in x 7-in connection plates were used			

Table 8. Component Membrane Testing Results

Sample Number	Energy Absorbed			Deflection (in)	Pressure (psi)
	Experimental (psi-in)	Analytical (psi-in)	Percent of Analytical		
2	17.20	20.34	84.6	12.88	2.51
3	23.68	45.74	51.8	18.25	2.71
4	15.71	17.33	90.7	12.15	2.40
5	22.72	46.38	49.0	18.39	2.50
6	35.60	42.61	83.5	17.70	4.10
7	23.75	45.74	51.9	18.26	2.78
8	16.95	17.98	94.3	12.38	2.62
9	14.86	16.40	90.6	11.81	2.29
10	21.53	25.34	85.0	14.40	3.07
11	18.45	21.80	84.6	13.50	2.80
12	34.91*	39.91	87.5	12.51	4.51
13	30.84	35.75	86.3	16.58	3.90
14	24.17	28.18	85.8	11.39	3.86
15	24.42	36.61	66.7	12.44	3.88
16	47.43	62.34	76.1	15.62	2.21
17	29.10	37.95	76.7	12.72	4.59
18	21.09	28.18	74.8	12.00	2.90
19	24.80	29.86	83.1	12.44	3.35
20	43.11	54.09	79.7	14.71	5.98
21	25.80	31.66	81.5	15.78	3.41
22	26.38	32.65	80.8	15.96	3.33
23	10.78	13.09	82.4	16.85	1.40
24	3.70	4.55	81.3	10.95	0.61
25	13.80	16.75	82.4	16.62	1.82
26	6.62	9.30	71.2	12.81	0.95
27	8.03	9.93	80.9	15.08	1.19
28	11.34	13.90	81.6	15.04	1.62
29	11.69	13.68	85.5	17.20	1.41
30	15.48	18.59	83.3	16.93	1.98
31	16.39	18.97	86.4	12.62	2.60
32	14.23	14.93	95.3	11.42	2.42
*= Actual experimental energy absorbed is expected to be higher than shown, load cell went out of range on this experiment.					

6.2.1. 1-mm Thick Sheets

AFRL tested 15 single 0.039-inch (1-mm) polypropylene sheets as a part of the component membrane testing. **Error! Reference source not found.** shows a summary of the pressure–deflection curves compared to the static resistance function for a 0.039-inch (1-mm) polypropylene sheet.

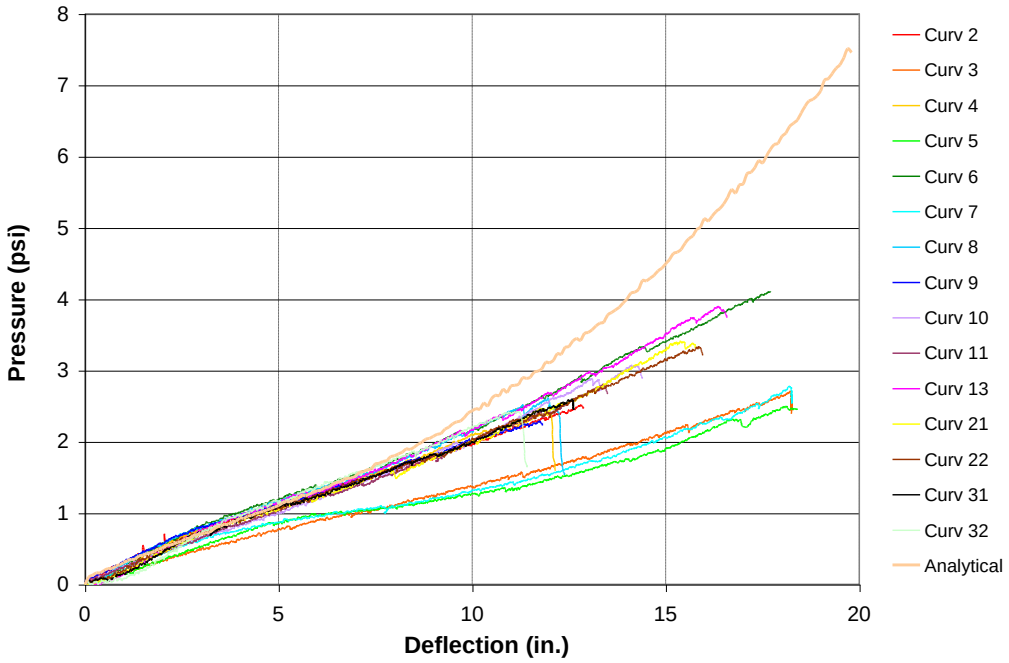

Figure 47. Response Summary of 1-mm Samples

Most pressure deflection curves from **Error! Reference source not found.** match well with the analytical resistance function up to a deflection of approximately 7 or 8 inches except for Samples 3, 5, and 7. These three samples were the only samples to use 0.125 inch connection plates. The remainder of this section includes an explanation of the results from each individual test.

Sample 2:

Sample 2 was a sheet 0.039 inch (1 mm) thick, 20 inches wide and 123 inches long. It used 16-inch bolt spacing and 0.25-inch thick steel connection plates to connect to the supports, and it obtained a maximum pressure of 2.51 psi and maximum deflection of 12.88 inches before failure occurred in tension along the edge of the plate, which caused a tear to propagate along the edge of the plate. Figure 48 shows the damage to Sample 2. Also, the tension in the sample bent the connection plates approximately 10 degrees. Figure 49 shows a comparison of the experimental results from this test with the theoretical static resistance function prediction for this sample.

Figure 48. Sample 2 (Failure/Post-Test Damage)

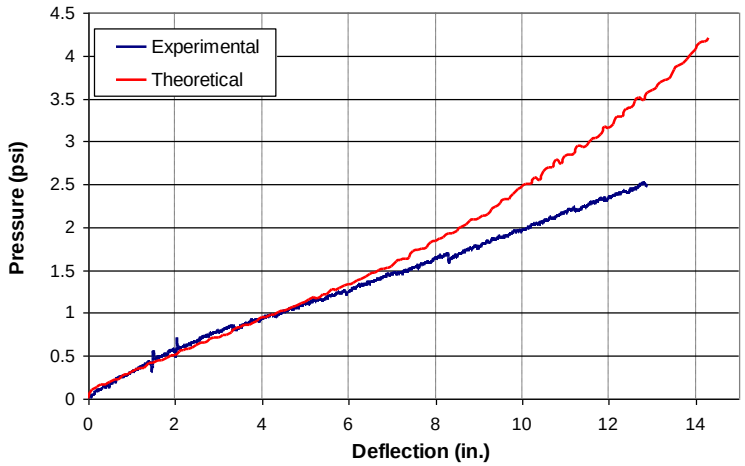

Figure 49. Sample 2 (Results/Comparison)

Sample 3:
Sample 3 had the same dimensions as Sample 2. This sample used 16-inch bolt spacing and 0.125-inch thick steel connection plates for the connection to the supports. This sample obtained a maximum pressure of 2.71 psi and maximum deflection of 18.25 inches before the conclusion of the test. Test personnel heard tearing of the polypropylene fibers around the bolt holes, but the sample did not fail before the hydraulic cylinder ran out of travel. Figure 50 shows the damage to Sample 3 and the 80-degree bend in the connection plates with a bulge in the center that testers observed at the conclusion of the test. Figure 51 shows a comparison of the experimental results from this test with the theoretical static resistance function prediction for this sample.

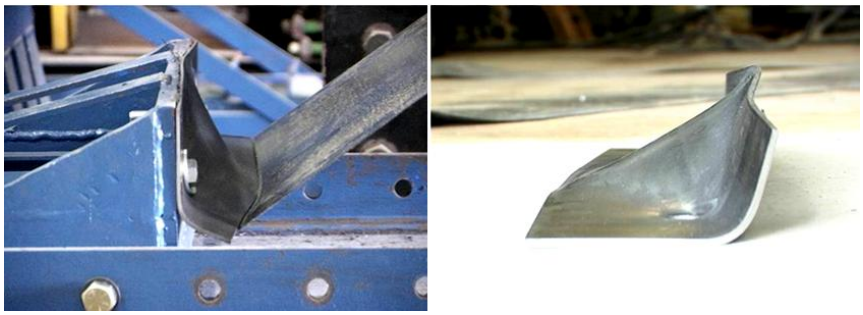

Figure 50. Sample 3 (Failure/Post-Test Damage)

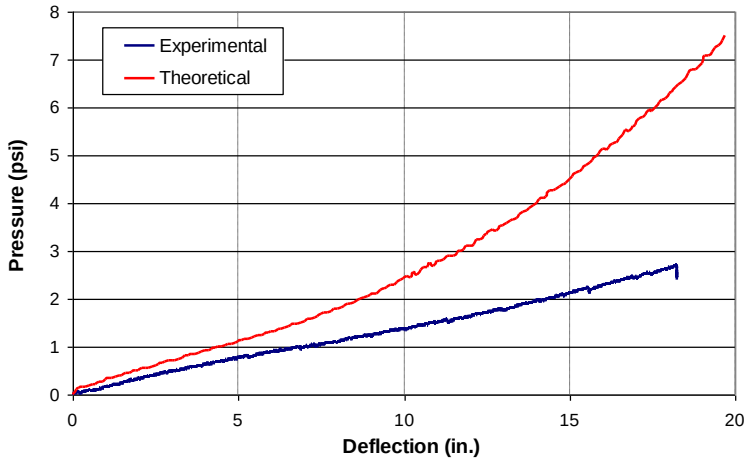

Figure 51. Sample 3 (Results/Comparison)

Sample 4:
Sample 4 had the same dimensions as Sample 2. This sample used 12-inch bolt spacing and 0.25-inch thick steel connection plates for the connection to the supports. This sample obtained a maximum pressure of 2.40 psi and maximum deflection of 12.15 inches before tension failure around the bolt holes occurred, which caused a tear to propagate along the bolt line. Figure 52 shows the damage to Sample 4 and a very slight bend in the connection plates. Figure 53 shows a comparison of the experimental results from this test with the theoretical static resistance function prediction for this sample.

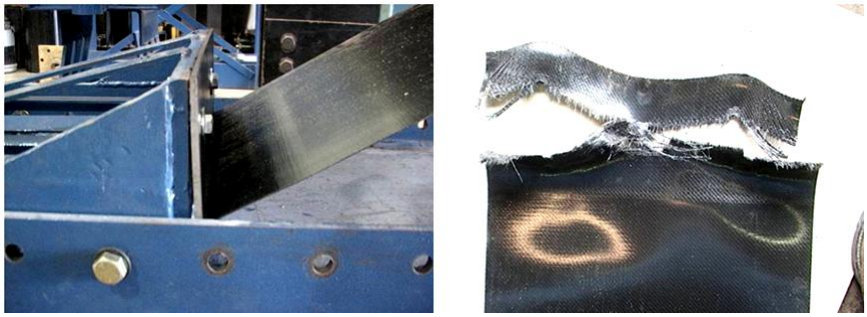

Figure 52. Sample 4 (Failure/Post-Test Damage)

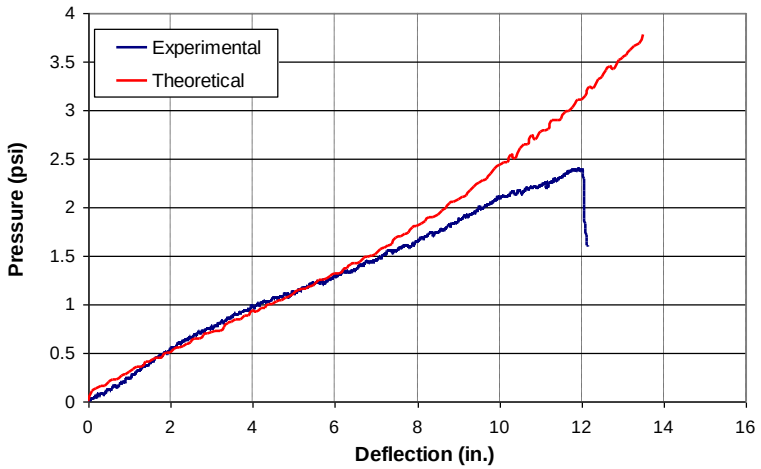

Figure 53. Sample 4 (Results/Comparison)

Sample 5:

Sample 5 had the same dimensions as Sample 2. This sample used 12-inch bolt spacing and 0.125-inch thick steel connection plates for the connection to the supports. This sample obtained a maximum pressure of 2.50 psi and maximum deflection of 18.39 inches before tension failure around the bolt holes occurred, which caused a tear to propagate along the bolt line. Figure 54 shows the damage to Sample 5 and an 80-degree bend in the connection plates that testers observed along with severe bending of the flat washers and bolt heads. Figure 55 shows a comparison of the experimental results from this test with the theoretical static resistance function prediction for this sample.

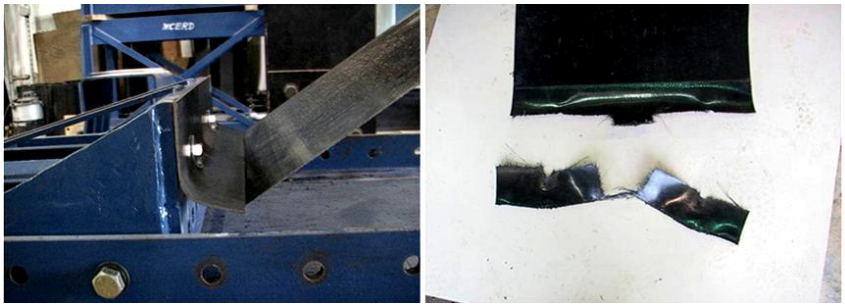

Figure 54. Sample 5 (Failure/Post-Test Damage)

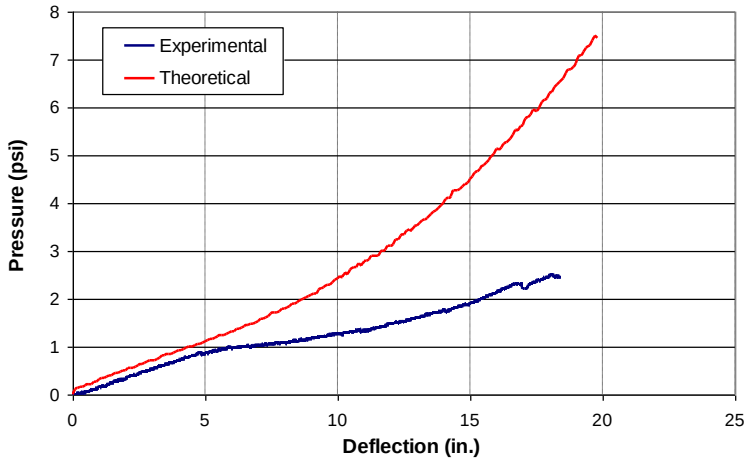

Figure 55. Sample 5 (Results/Comparison)

Sample 6:
Sample 6 had the same dimensions as Sample 2. This sample used 8-inch bolt spacing and 0.25-inch thick steel connection plates for the connection to the supports. This sample obtained a maximum pressure of 4.10 psi and maximum deflection of 17.70 inches before tension failure around the bolt holes occurred, which caused a tear to propagate along the bolt line. This enabled the sheet to become eccentric and produced a tear along the edge of the plate. Figure 56 shows the damage to Sample 6 and a bending of approximately 10 degrees in the connection plates. Figure 57 shows a comparison of the experimental results from this test with the theoretical static resistance function prediction for this sample.

Figure 56. Sample 6 (Failure/Post-Test Damage)

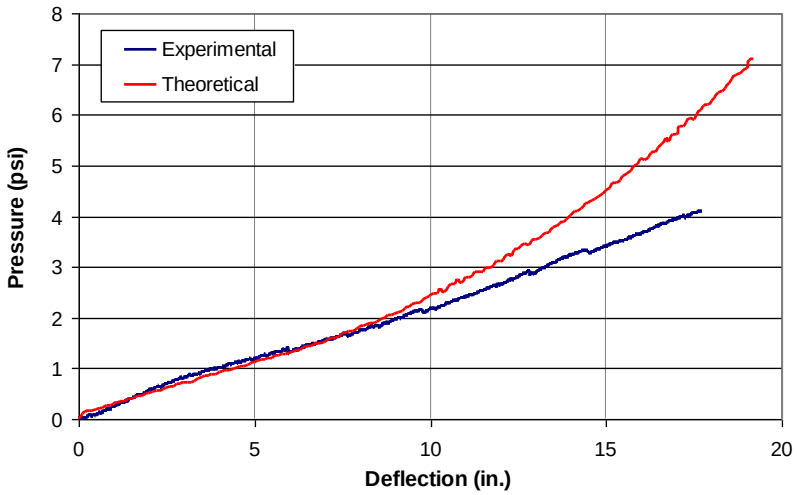

Figure 57. Sample 6 (Results/Comparison)

Sample 7:

Sample 7 had the same dimensions as Sample 2. This sample used 8 inch bolt spacing and 0.125 inch thick steel connection plates for the connection to the supports. This sample obtained a maximum pressure of 2.78 psi and a maximum deflection of 18.26 inches before the completion of the test. Test personnel heard a tearing of the polypropylene fibers around the connection, but the sample did not ultimately fail. Figure 58 shows the 90 degree bend in the connection plates along with bending of the flat washers that testers observed. Figure 59 shows a comparison of the experimental results from this test with the theoretical static resistance function prediction for this sample.

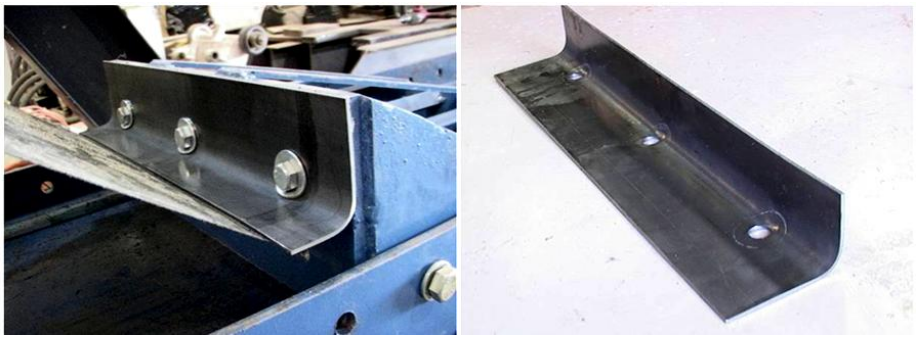

Figure 58. Sample 7 (Failure/Post-Test Damage)

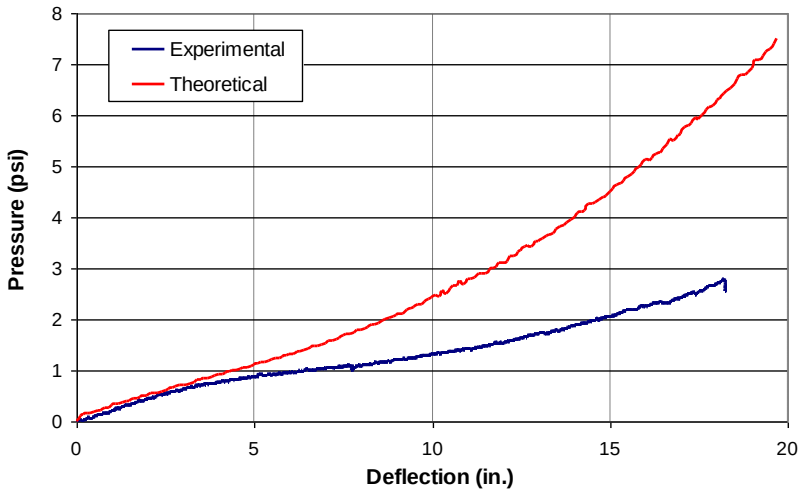

Figure 59. Sample 7 (Results/Comparison)

Sample 8:
Sample 8 had the same dimensions as Sample 2. This sample used 12-inch bolt spacing and 0.375-inch thick steel connection plates for the connection to the supports. This sample obtained a maximum pressure of 2.62 psi and maximum deflection of 12.38 inches before tension failure around the bolt holes occurred, which caused a tear to propagate along the bolt line. This enabled the sheet to become eccentric and produced a tear along the edge of the plate. Figure 60 shows the damage to Sample 8. The connection plates were undamaged. Figure 61 shows a comparison of the experimental results from this test with the theoretical static resistance function prediction for this sample.

Figure 60. Sample 8 (Failure/Post-Test Damage)

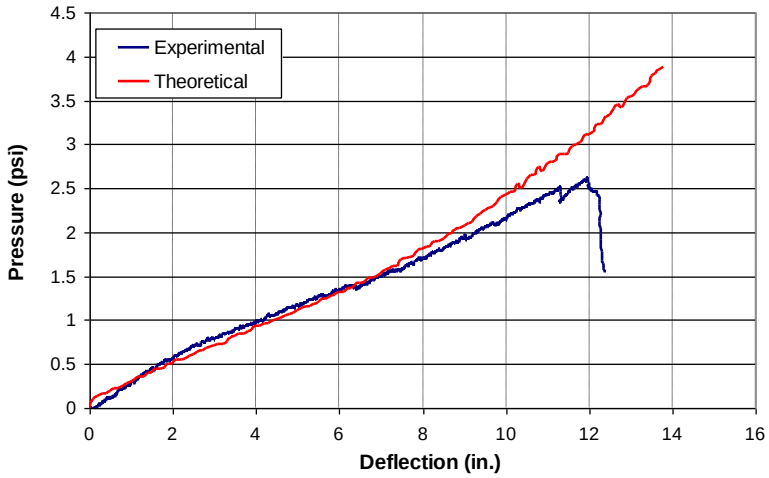

Figure 61. Sample 8 (Results/Comparison)

Sample 9:

Sample 9 had the same dimensions as Sample 2. It used 16-inch bolt spacing and 0.375-inch thick steel connection plates for the connection to the supports. This sample obtained a maximum pressure of 2.29 psi and maximum deflection of 11.8 inches before tension failure around the bolt holes occurred, which caused a tear to propagate along the bolt line. This enabled the sheet to become eccentric and produced a tear along the edge of the plate. Figure 62 shows the damage to Sample 9. The connection plates were undamaged. Figure 63 shows a comparison of the experimental results from this test with the theoretical static resistance function prediction for this sample.

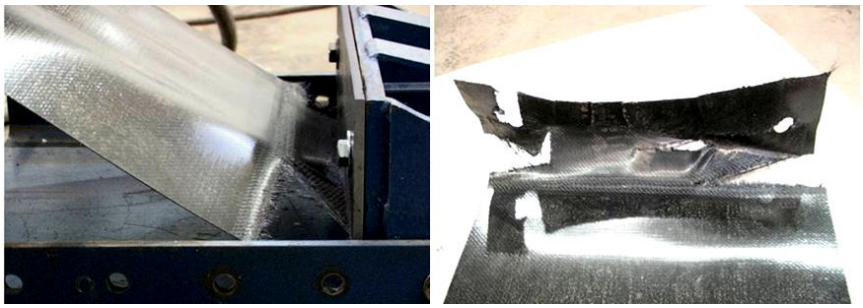

Figure 62. Sample 9 (Failure/Post-Test Damage)

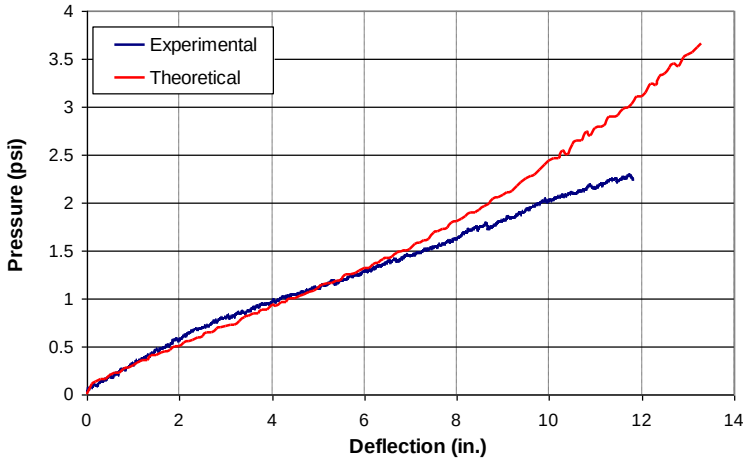

Figure 63. Sample 9 (Results/Comparison)

Sample 10:

Sample 10 had the same dimensions as Sample 2. This sample used 12-inch bolt spacing and 0.375-inch thick steel connection plates for the connection to the supports. Also, test personnel applied a 3-mm (0.118-inch) thick polypropylene angle between the sheet and the connection plate using double-sided tape. This sample obtained a maximum pressure of 3.07 psi and maximum deflection of 14.40 inches before tension failure around the bolt holes occurred, which caused a tear to propagate along the bolt line. Figure 64 shows the damage to Sample 10. The connection plates and polypropylene angle were undamaged. The tape did not bond well to the sheet and polypropylene angle; therefore, test personnel observed no benefit after inspecting the data. Figure 65 shows a comparison of the experimental results from this test with the theoretical static resistance function prediction for this sample.

Figure 64. Sample 10 (Failure/Post-Test Damage)

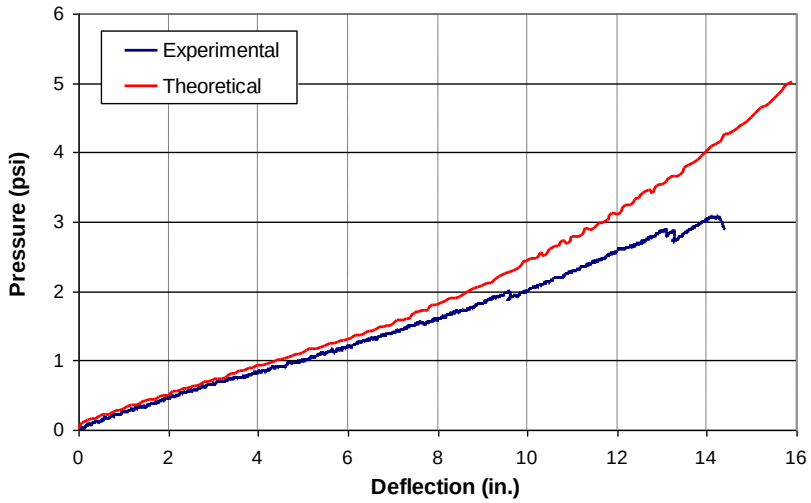

Figure 65. Sample 10 (Results/Comparison)

Sample 11:
Sample 11 had the same dimensions as Sample 2. This sample used 16-inch bolt spacing and 0.375-inch thick steel connection plates for the connection to the supports. Also, test personnel applied a 3-mm (0.118-inch) thick polypropylene angle between the sheet and the connection plate using double-sided tape. This sample obtained a maximum pressure of 2.80 psi and a maximum deflection of 13.50 inches before tension failure around the bolt holes occurred, which caused a tear to propagate along the bolt line. This enabled the sheet to become eccentric and produced a tear along the edge of the plate. Figure 66 shows the damage to Sample 11. The connection plates and polypropylene angle were undamaged. The tape did not bond well to the sheet and polypropylene angle; therefore, test personnel observed no benefit after inspecting the data. Figure 67 shows a comparison of the experimental results from this test with the theoretical static resistance function prediction for this sample.

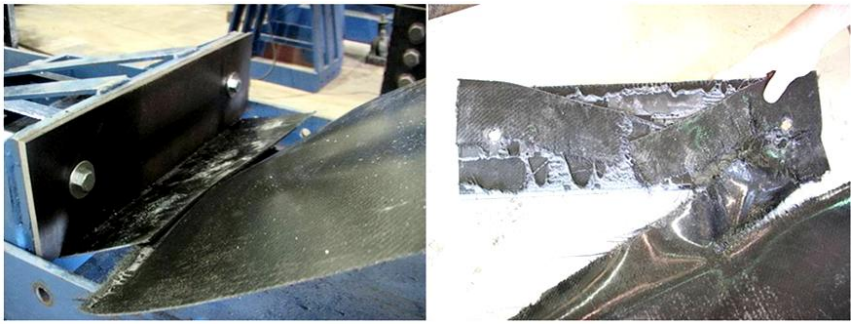

Figure 66. Sample 11 (Failure/Post-Test Damage)

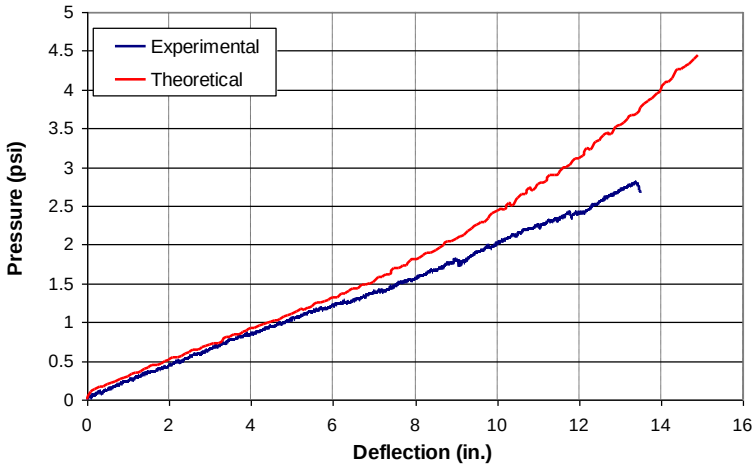

Figure 67. Sample 11 (Results/Comparison)

Sample 13:

Sample 13 had the same dimensions as Sample 2. This sample used 8-inch bolt spacing and 0.375-inch thick steel connection plates for the connection to the supports. It obtained a maximum pressure of 3.90 psi and a maximum deflection of 16.58 inches before failure of the sample occurred in tension around one bolt hole. The tear propagated along the line of the bolt hole, and the sample then became eccentrically loaded and began to tear along the edge of the plate on one side and along the bolt line on the other side. Figure 68 shows the damage to Sample 13. The connection plates were undamaged. Figure 69 shows a comparison of the experimental results from this test with the theoretical static resistance function prediction for this sample.

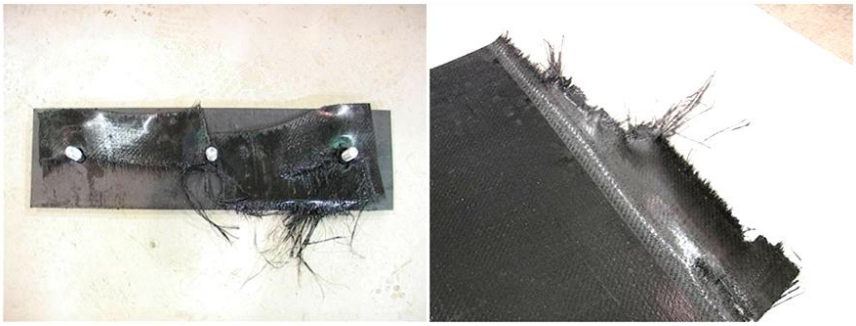

Figure 68. Sample 13 (Failure/Post-Test Damage)

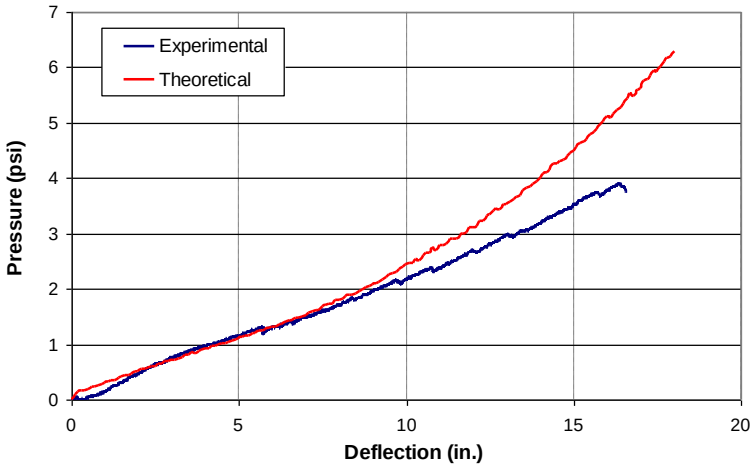

Figure 69. Sample 13 (Results/Comparison)

Sample 21:

Sample 21 was a retest of Sample 13. This sample obtained a maximum pressure of 3.41 psi and a maximum deflection of 15.78 inches before failure of the sample occurred in tension around one bolt hole. The tear propagated along the line of the bolt hole and then eccentrically loaded the sample, which began to tear along the edge of the plate on one side and along the bolt line on the other side. Figure 70 shows the damage to Sample 21. The connection plates were undamaged. Figure 71 shows a comparison of the experimental results from this test with the theoretical static resistance function prediction for this sample.

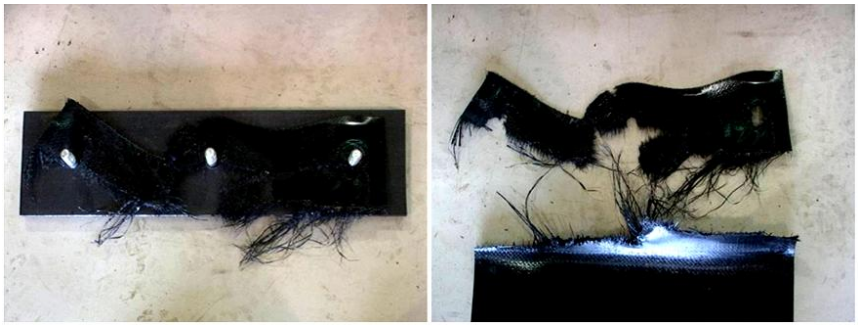

Figure 70. Sample 21 (Failure/Post-Test Damage)

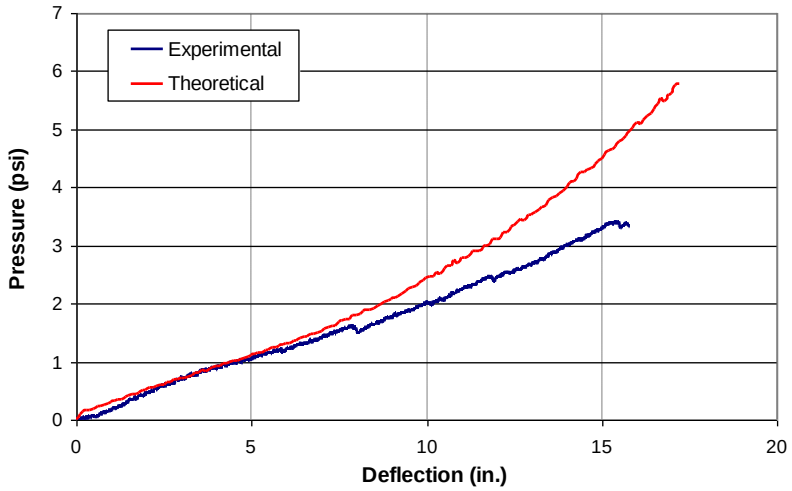

Figure 71. Sample 21 (Results/Comparison)

Sample 22:

Sample 22 was a retest of Sample 6. This sample had a sheet thickness of 0.039 inches (1 mm), a width of 20 inches, and a length of 123 inches. This sample used 8-inch bolt spacing and 0.25-inch thick steel connection plates for the connection to the supports. This sample obtained a maximum pressure of 3.33 psi and maximum deflection of 15.96 inches before tension failure around the bolt holes occurred. This caused a tear to propagate along the edge of the plate. Figure 72 shows the damage to Sample 22. Test personnel observed a bending of approximately 10 degrees in the connection plates. This sample was too tight in the tree and had load on it before the test started. Figure 73 shows a comparison of the experimental results from this test with the theoretical static resistance function prediction for this sample.

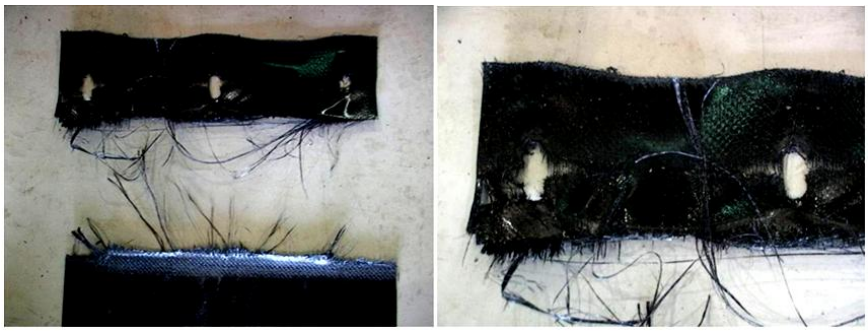

Figure 72. Sample 22 (Failure/Post-Test Damage)

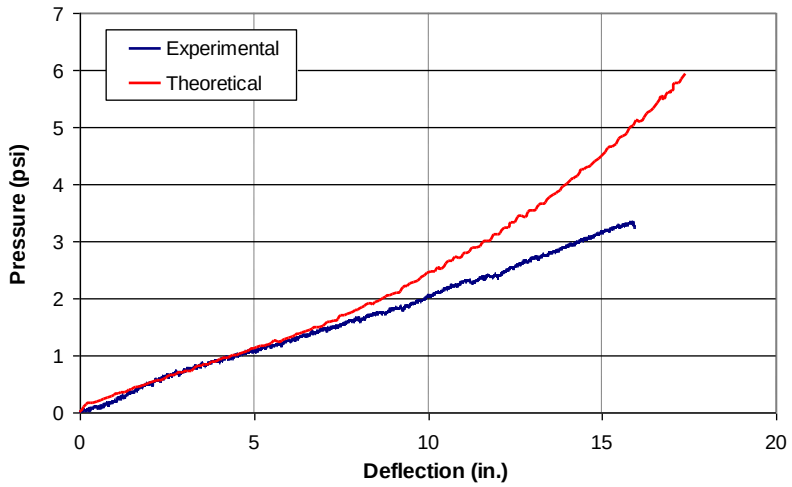

Figure 73. Sample 22 (Results/Comparison)

Sample 31:
Sample 31 had the same dimensions as Sample 2. This sample used 8-inch bolt spacing in conjunction with three 7-inch long by 4-inch wide steel connection plates that were 0.25 inches thick. It obtained a maximum pressure of 2.60 psi and maximum deflection of 12.62 inches before the completion of the test. The sample did not ultimately fail because the hydraulic cylinder of the loading tree ran out of travel, as shown in Figure 74. The connection plates were undamaged. Figure 75 shows a comparison of the experimental results from this test with the theoretical static resistance function prediction for this sample.

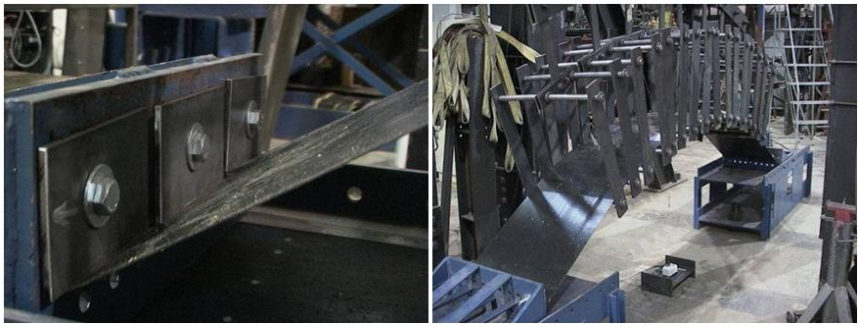

Figure 74. Sample 31 (Failure/Post-Test Damage)

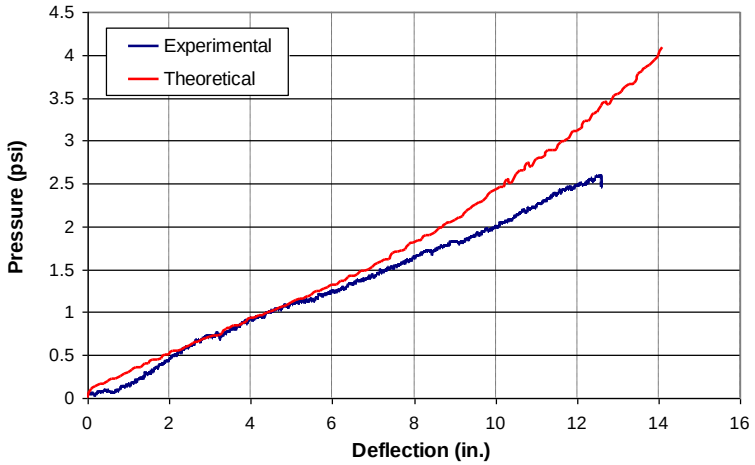

Figure 75. Sample 31 (Results/Comparison)

Sample 32:

Sample 32 was a retest of sample 31 where test personnel raised the tree height to get more travel from the cylinder. It obtained a maximum pressure of 2.42 psi and maximum deflection of 11.42 inches before failure. The sheet first failed in tension along the bolt line and then ripped along the edge of the plates. Figure 76 shows the damage to Sample 32. The multiple connection plates may have aided in the puncturing of the sample due to the exposed squared corners. The connection plates were undamaged, although the two on the ends turned slightly. Figure 77 shows a comparison of the experimental results from this test with the theoretical static resistance function prediction for this sample.

Figure 76. Sample 32 (Failure/Post-Test Damage)

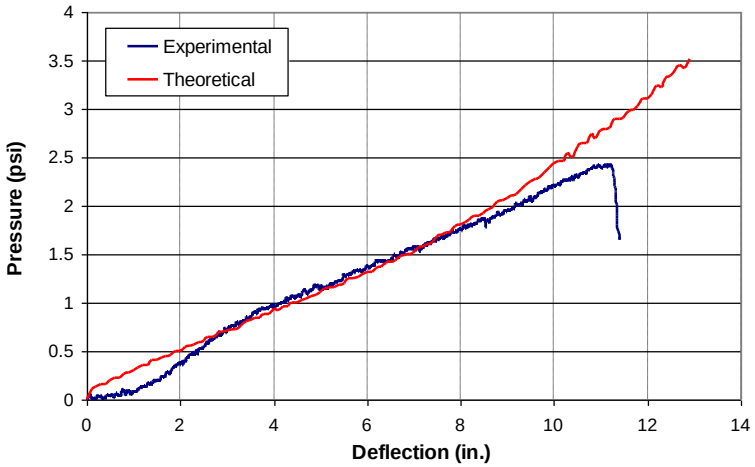

Figure 77. Sample 32 (Results/Comparison)

6.2.2. 2-mm Thick Sheets and Doubled 1-mm Thick Sheets

AFRL tested four 2-mm (0.079-inch) polypropylene sheets and four doubled 1-mm (0.039-inch) polypropylene sheets as a part of the component membrane testing. Figure 78 shows a summary of the pressure–deflection curves compared to the static resistance function for a 2-mm (0.079-inch) polypropylene sheet.

Most pressure deflection curves in Figure 78 match well with the analytical resistance function, but in general they do not match as well as the 1-mm (0.039-inch) sheets in the previous section. The pressures obtained from these tests are substantially higher for the 2-mm (0.079-inch) sheets than for the 1-mm (0.039-inch) sheets. The remainder of this section includes an explanation of the results from each individual test.

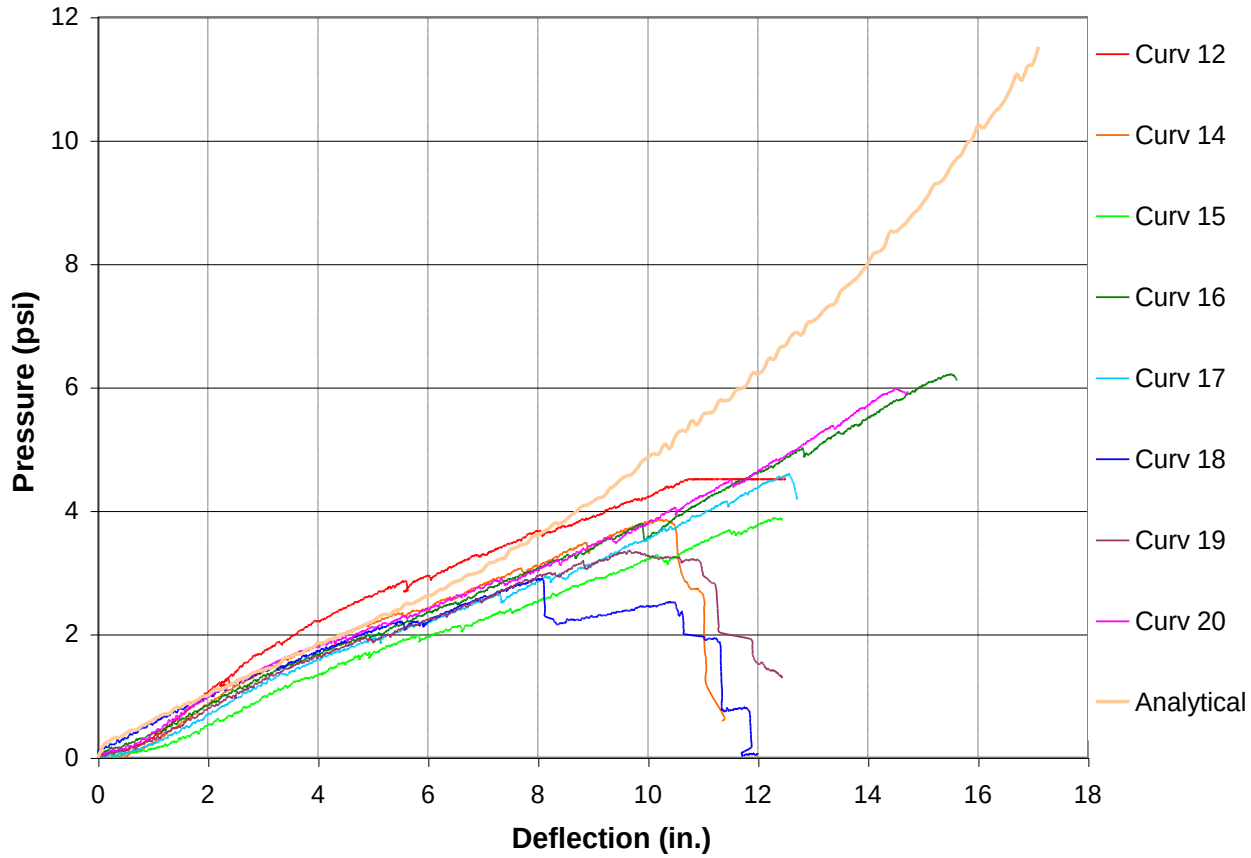

Figure 78. Response of 2-mm Samples

Sample 12:
Sample 12 had a sheet thickness of 2 mm (0.079 inches), a width of 20 inches, and a length of 120.25 inches. This sample used 12-inch bolt spacing and 0.375-inch thick steel connection plates to connect to the supports. This sample obtained a maximum deflection of 12.51 inches and a maximum pressure most likely from approximately 5 to 5.5 psi before failure. The data card reading the voltage from the load cell reached its maximum voltage reading before the failure of the sample occurred and caused the uncertainty in the maximum pressure. Because the data card reached its maximum reading, the load seemed to level off at approximately 4.5 psi when in actuality the load continued to increase. The failure of this sample occurred in bearing around the bolt holes and then in tension along the edge of the plate. Figure 79 shows the damage to Sample 12. The connection plates were undamaged. The use of an incorrect loading card for this test caused the load cell to go out of range and limited the total load to 11,000 lbs. Figure 80 shows a comparison of the experimental results from this test with the theoretical static resistance function prediction for this sample.

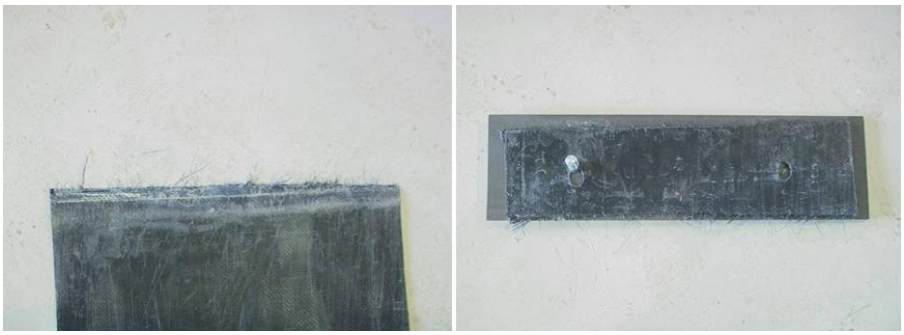

Figure 79. Sample 12 (Failure/Post-Test Damage)

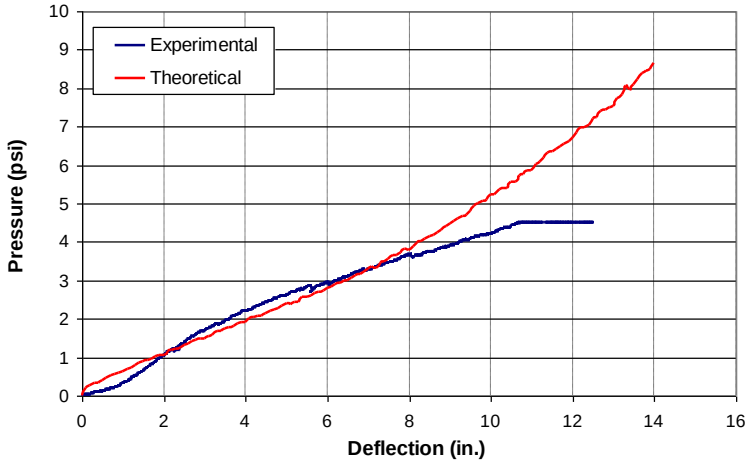

Figure 80. Sample 12 (Results/Comparison)

Sample 14:

Sample 14 used two sheets, each with the same dimensions as Sample 2. This sample used 12-inch bolt spacing and 0.375-inch thick steel connection plates for the connection to the supports. This sample obtained a maximum pressure of 3.86 psi and maximum deflection of 11.39 inches before failure. The failure of the sample occurred first due to the exterior sheet catastrophically failing along the bolt line. Then, the interior sheet tore along the bolt line, the sheet became eccentrically loaded, and the sample ripped at the edge of the plate. Figure 81 shows the damage to Sample 14. This was due to the fact that after the first sheet failed there was no clamping force left on the remaining sheet. The connection plates were undamaged. Figure 82 shows a comparison of the experimental results from this test with the theoretical static resistance function prediction for this sample.

Figure 81. Sample 14 (Failure/Post-Test Damage)

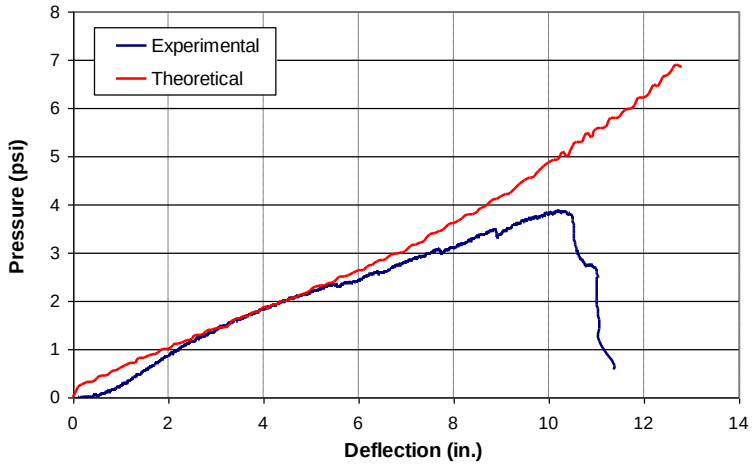

Figure 82. Sample 14 (Results/Comparison)

Sample 15:
Sample 15 had a sheet thickness of 2 mm (0.079 inches), a width of 20 inches, and a length of 123 inches. This sample used 16-inch bolt spacing and 0.375-inch thick steel connection plates to connect to the supports. It obtained a maximum pressure of 3.88 psi and maximum deflection of 12.44 inches before failure. The failure of this sample occurred because one side of the sheet ripped from the bolt hole to the outside edge, the sheet became eccentrically loaded, and the sheet ripped along the edge of the plate from the other side of the sample. Figure 83 shows the damage to Sample 15. The connection plates were slightly bent. Figure 85 shows a comparison of the experimental results from this test with the theoretical static resistance function prediction for this sample.

Figure 83. Sample 15 (Failure/Post-Test Damage)

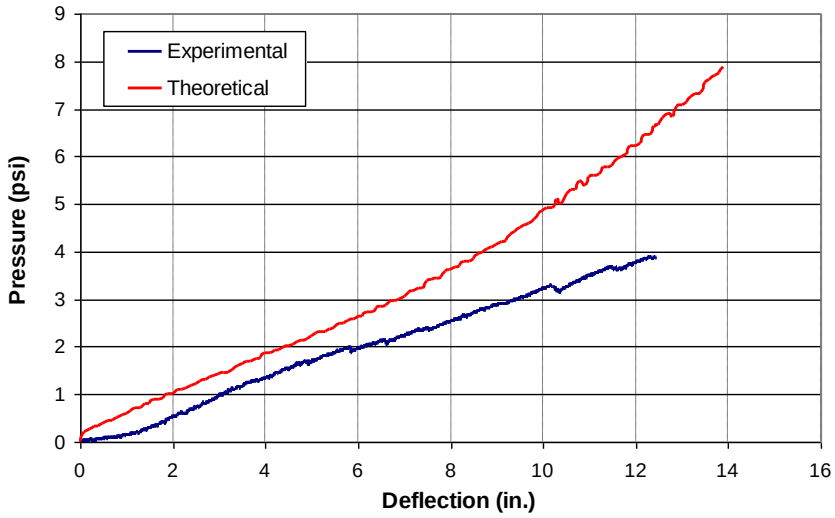

Figure 84. Sample 15 (Results/Comparison)

Sample 16:
Sample 16 had the same dimensions as Sample 15. This sample used 8-inch bolt spacing and 0.375-inch thick steel connection plates for the connection to the supports. It obtained a maximum pressure of 6.21 psi and maximum deflection of 15.62 inches before failure. Failure occurred as the bolt holes began to fail in shear toward the end of the sample. Then one side of the sheet ripped from the bolt hole to the outside edge, the sheet became eccentrically loaded, and the sheet ripped along the edge of the plate from the other side of the sample. Figure 85 shows the damage to Sample 16. The connection plates were slightly bent. Figure 86 shows a comparison of the experimental results from this test with the theoretical static resistance function prediction for this sample.

Figure 85. Sample 16 (Failure/Post-Test Damage)

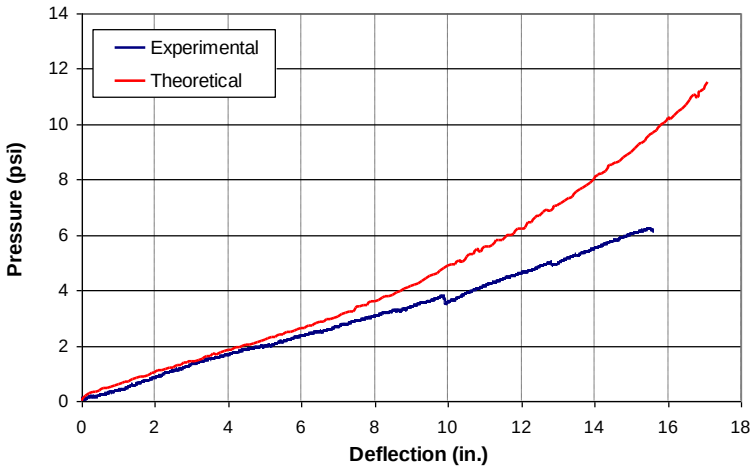

Figure 86. Sample 16 (Results/Comparison)

Sample 17:

Sample 17 was a retest of sample 12. This sample had the same dimensions as Sample 15 and used 12-inch bolt spacing and 0.375-inch thick steel connection plates for the connection to the supports. This sample obtained a maximum pressure of 4.59 psi and maximum deflection of 12.72 inches before failure. The failure of this sample occurred in tension along the bolt line. The sample became eccentrically loaded and ripped along the edge of the plate. Figure 87 shows the damage to Sample 17. The connection plates were undamaged. Figure 88 compares the experimental results from this test with the theoretical static resistance function prediction for this sample.

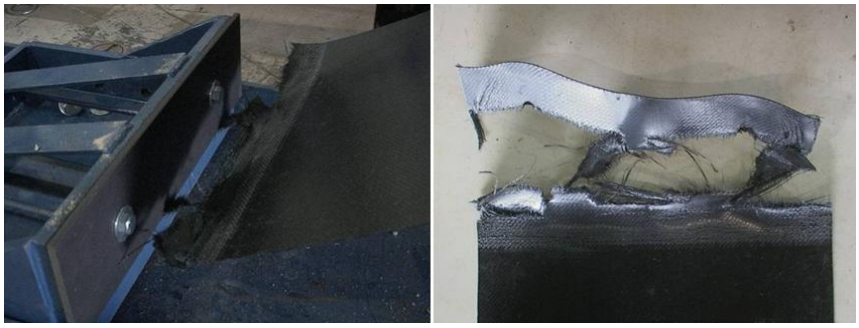

Figure 87. Sample 17 (Failure/Post-Test Damage)

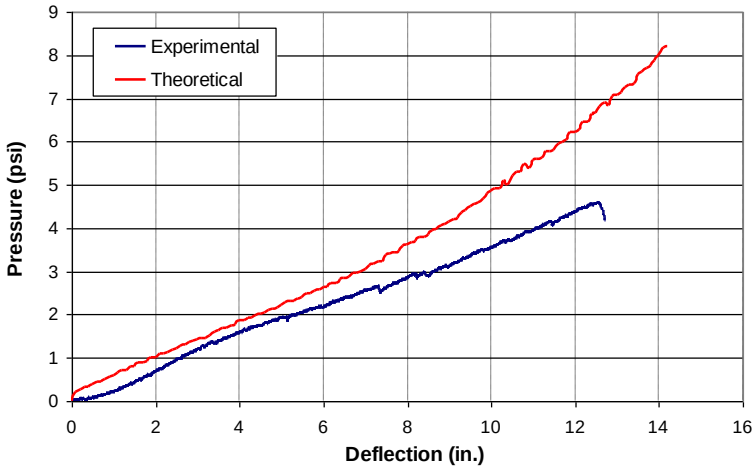

Figure 88. Sample 17 (Results/Comparison)

Sample 18:

Sample 18 used two sheets with the same dimensions as Sample 2. This sample used 12 inch bolt spacing and 0.375 inch thick steel connection plates for the connection to the supports. This sample obtained a maximum pressure of 2.90 psi and a maximum deflection of 12.00 inches before failure. The bottom sheet failed first in tension along the bolt line. Next, the top sheet experienced a partial tension failure along the bolt holes, and the sample became eccentrically loaded and tore along the edge of the plate. Figure 89 shows the damage to Sample 18. The connection plates were undamaged. Figure 90 shows a comparison of the experimental results from this test with the theoretical static resistance function prediction for this sample.

Figure 89. Sample 18 (Failure/Post-Test Damage)

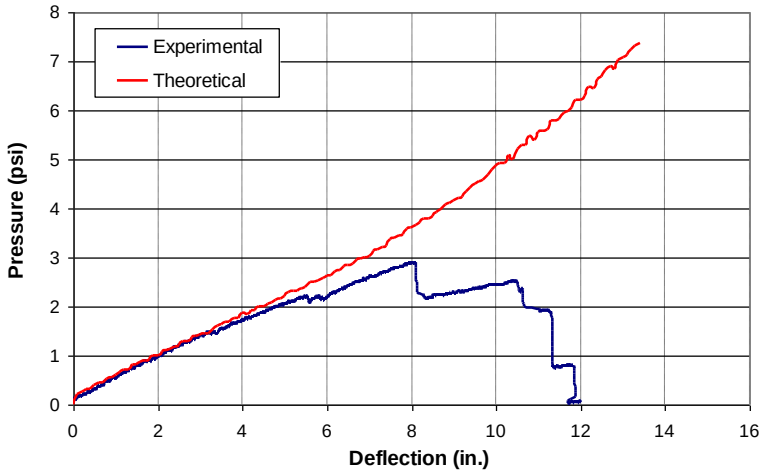

Figure 90. Sample 18 (Results/Comparison)

Sample 19:

Sample 19 was a retest of Sample 14. This sample obtained a maximum pressure of 3.35 psi and maximum deflection of 12.44 inches before failure. The sample was prestressed in the loading tree prior to the start of the test and had an initial load of approximately 2,500 lbs. The bottom sheet failed first in tension along the bolt line. Next, the top sheet experienced a partial tension failure along the bolt holes, and the sample became eccentrically loaded and tore along the edge of the plate. Figure 91 shows the damage to Sample 19. The connection plates were undamaged. Figure 92 shows a comparison of the experimental results from this test with the theoretical static resistance function prediction for this sample.

Figure 91. Sample 19 (Failure/Post-Test Damage)

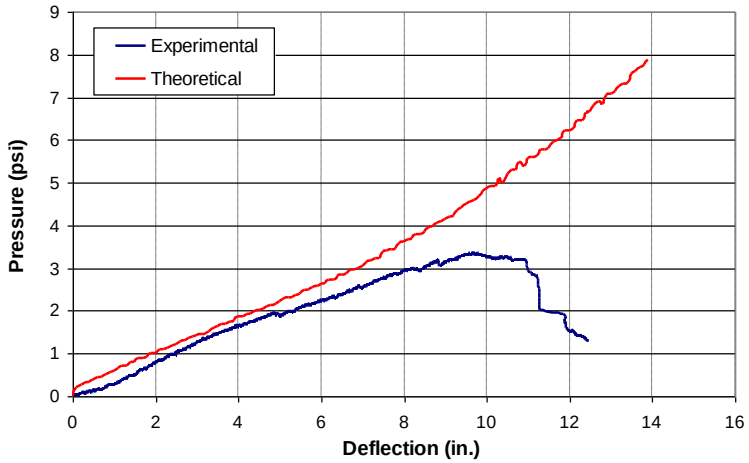

Figure 92. Sample 19 (Results/Comparison)

Sample 20:

Sample 20 used two sheets with the same dimensions as Sample 15. This sample used 8 inch bolt spacing and 0.375 inch thick steel connection plates for the connection to the supports. This sample obtained a maximum pressure of 5.98 psi and a maximum deflection of 14.71 inches before failure occurred. The bottom sheet failed in tension along the bolt line, and the top sheet then tore along the edge of the plate. Figure 93 shows the damage to Sample 20. The connection plates were undamaged. Figure 94 shows a comparison of the experimental results from this test with the theoretical static resistance function prediction for this sample.

Figure 93. Sample 20 (Failure/Post-Test Damage)

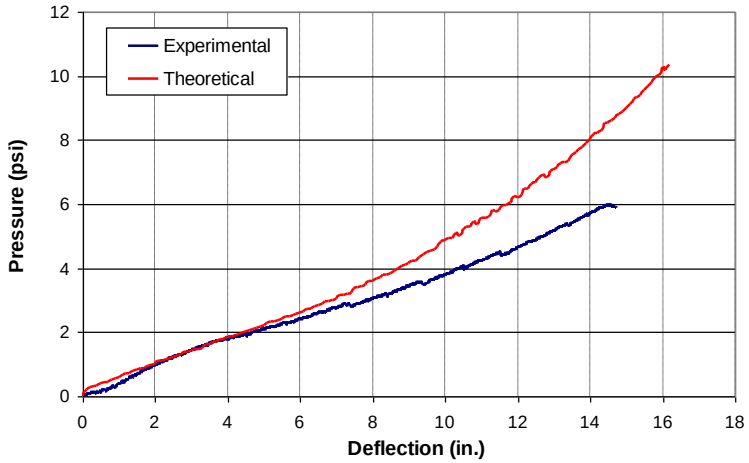

Figure 94. Sample 20 (Results/Comparison)

6.2.3. Thin Sheets—0.35 and 0.49-mm

AFRL tested four 0.35-mm (0.014-inch) polypropylene sheets and four 0.49-mm (0.019-inch) polypropylene sheets as a part of the component membrane testing. Figure 95 and Figure 96 compare the pressure–deflection curves to the static resistance functions for a 0.35-mm (0.014-inch) polypropylene sheet and a 0.49-mm (0.019-inch) polypropylene sheet, respectively.

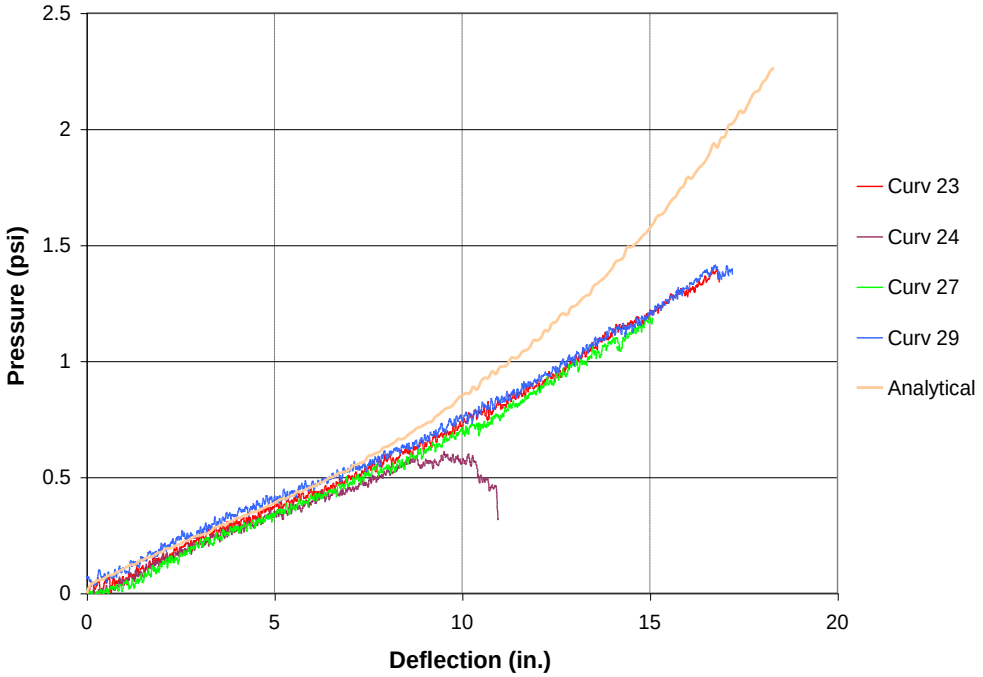

Figure 95. Pressure–Deflection Response Summary of 0.35-mm Samples

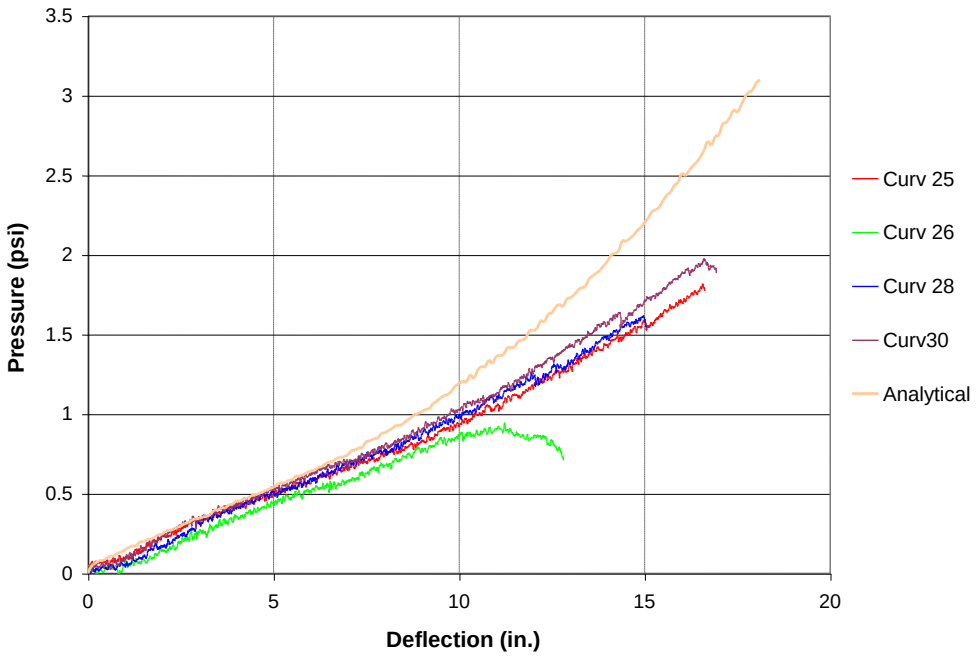

Figure 96. Pressure–Deflection Response Summary of 0.49-mm Samples

For these tests, the experimental data appear to match the analytical static resistance functions very well up to a deflection of approximately 7 to 8 inches. The remainder of this section includes an explanation of the results from each individual test.

Sample 23:
Sample 23 had a sheet thickness of 0.35 mm (0.014 inches), a width of 20 inches, and a length of 123 inches. This sample used 8-inch bolt spacing and 0.25-inch thick steel connection plates to connect to the supports. This sample obtained a maximum pressure of 1.40 psi and maximum deflection of 16.85 inches before failure. Shear failure around the bolt holes occurred first, and the sheet then failed due to tension failure along the bolt line. Figure 97 shows the damage to Sample 23. The connection plates were undamaged. Figure 98 compares the experimental results from this test with the theoretical static resistance function prediction for this sample.

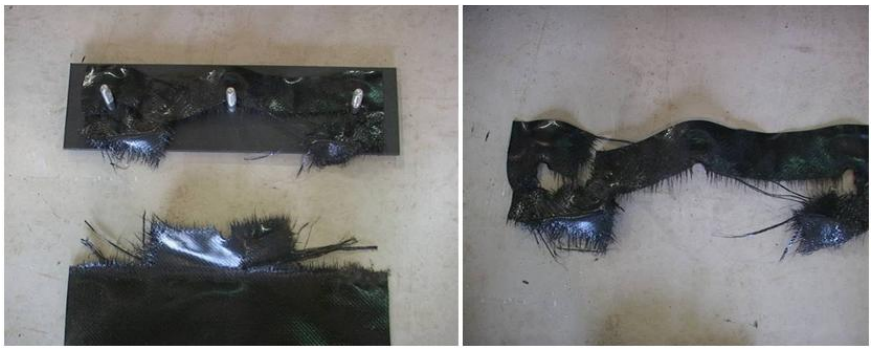

Figure 97. Sample 23 (Failure/Post-Test Damage)

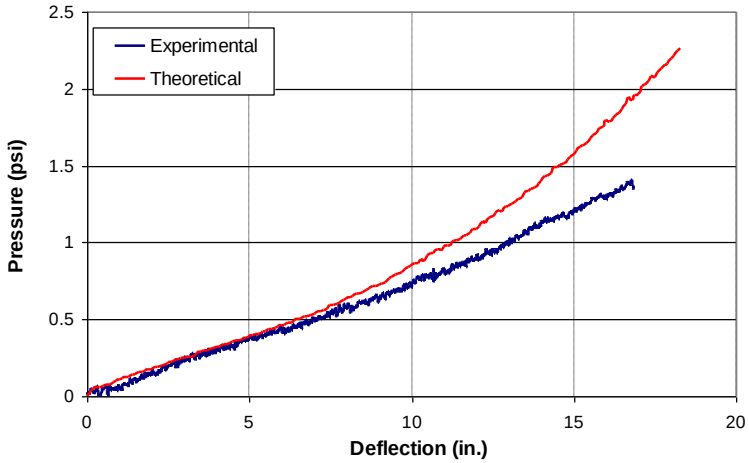

Figure 98. Sample 23 (Results/Comparison)

Sample 24:
Sample 24 had the same dimensions as Sample 23 and used 12-inch bolt spacing and 0.25-inch thick steel connection plates to connect to the supports. This sample obtained a maximum pressure of 0.61 psi and maximum deflection of 10.95 inches before failure of the sheet occurred due to a tension failure along the bolt line. Figure 99 shows the damage to Sample 24.

Figure 99. Sample 24 (Failure/Post-Test Damage)

The connection plates were undamaged. Figure 100 shows a comparison of the experimental results from this test with the theoretical static resistance function prediction for this sample.

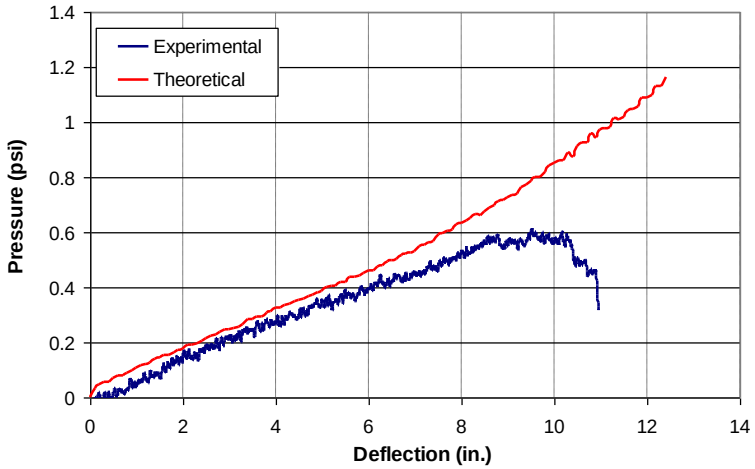

Figure 100. Sample 24 (Results/Comparison)

Sample 25:

Sample 25 had a sheet thickness of 0.49 mm (0.019 inches), a width of 20 inches, and a length of 123 inches. It used 8-inch bolt spacing and 0.25-inch thick steel connection plates to connect to the supports. This sample obtained a maximum pressure of 1.82 psi and maximum deflection of 16.62 inches before tension failure occurred along the bolt line. The sheet became eccentric and then ripped along the edge of the plate. Figure 101 shows the damage to Sample 25. The connection plates were undamaged. Figure 102 shows a comparison of the experimental results from this test with the theoretical static resistance function prediction for this sample.

Figure 101. Sample 25 (Failure/Post-Test Damage)

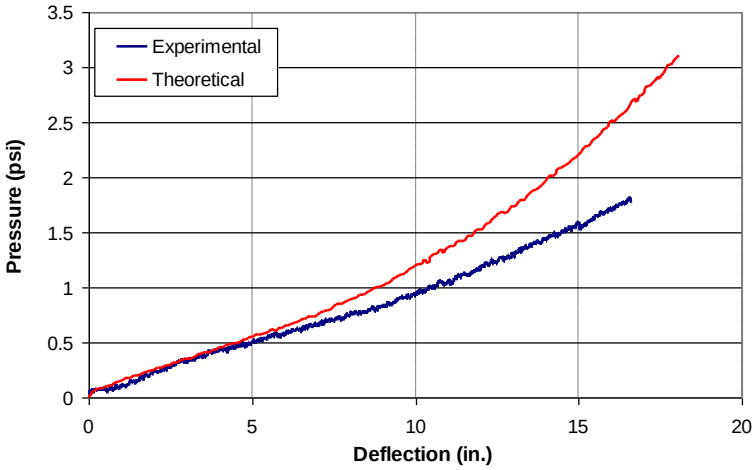

Figure 102. Sample 25 (Results/Comparison)

Sample 26:

Sample 26 had the same dimensions as Sample 25, and used 12-inch bolt spacing and 0.25-inch thick steel connection plates to connect to the supports. This sample obtained a maximum pressure of 0.95 psi and maximum deflection of 12.81 inches before failure. Shear failure around the bolt holes occurred first, and the sheet then failed due to tension failure along the bolt line. Figure 103 shows the damage to Sample 26. The connection plates were undamaged. Figure 104 compares the experimental results from this test with the theoretical static resistance function prediction for this sample.

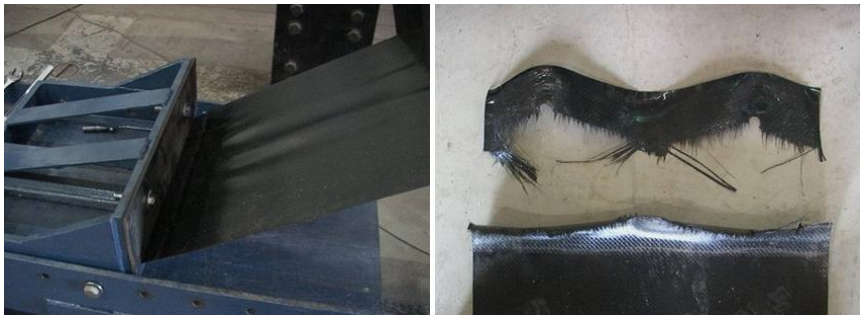

Figure 103. Sample 26 (Failure/Post-Test Damage)

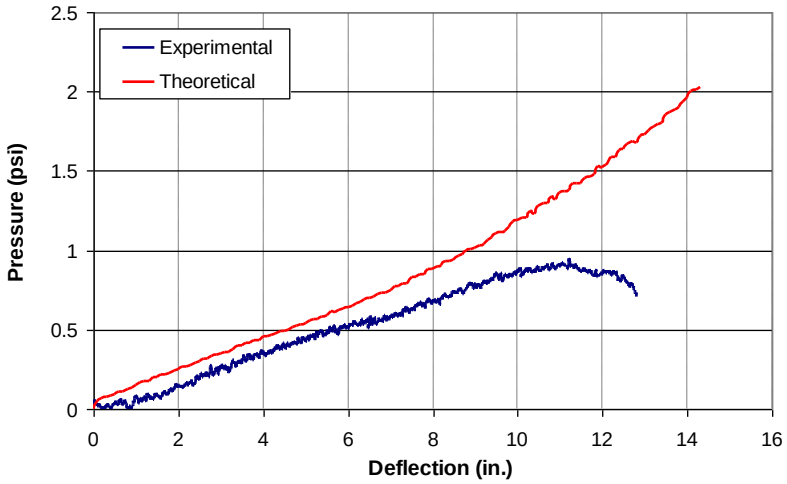

Figure 104. Sample 26 (Results/Comparison)

Sample 27:

Sample 27 was a retest of sample 23. It obtained a maximum pressure of 1.19 psi and maximum deflection of 15.08 inches before tension failure occurred along the bolt line. The sheet became eccentric and then ripped along the edge of the plate. Figure 105 shows the damage to Sample 27. The connection plates were undamaged. Figure 106 compares the experimental results from this test with the theoretical static resistance function prediction for this sample.

Figure 105. Sample 27 (Failure/Post-Test Damage)

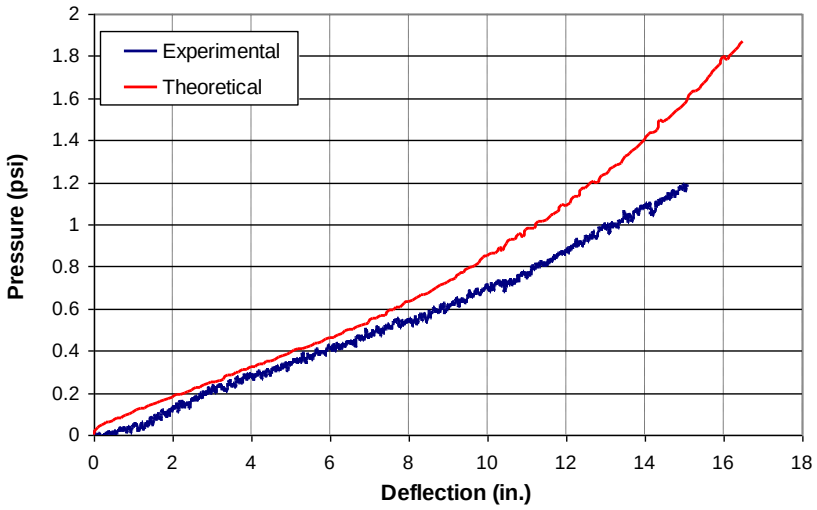

Figure 106. Sample 27 (Results/Comparison)

Sample 28:

Sample 28 was a retest of Sample 25. It obtained a maximum pressure of 1.62 psi and maximum deflection of 15.04 inches before tension failure occurred along the bolt line. The sheet became eccentric and then ripped along the edge of the plate. Figure 107 shows the damage to Sample 28. The connection plates were undamaged. Figure 108 compares the experimental results from this test with the theoretical static resistance function prediction for this sample.

Figure 107. Sample 28 (Failure/Post-Test Damage)

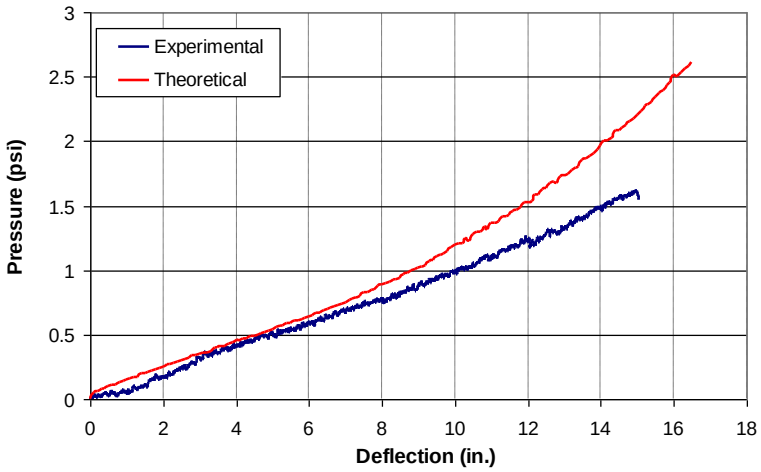

Figure 108. Sample 28 (Results/Comparison)

Sample 29:

Sample 29 had the same dimensions as Sample 23. This sample used 4-inch bolt spacing and 0.25-inch thick steel connection plates for the connection to the supports. This sample obtained a maximum pressure of 1.41 psi and maximum deflection of 17.20 inches before failure of the sheet occurred due to a tension failure along the bolt line. Figure 109 shows the damage to Sample 29. The connection plates were undamaged. Figure 110 compares the experimental results from this test with the theoretical static resistance function prediction for this sample.

Figure 109. Sample 29 (Failure/Post-Test Damage)

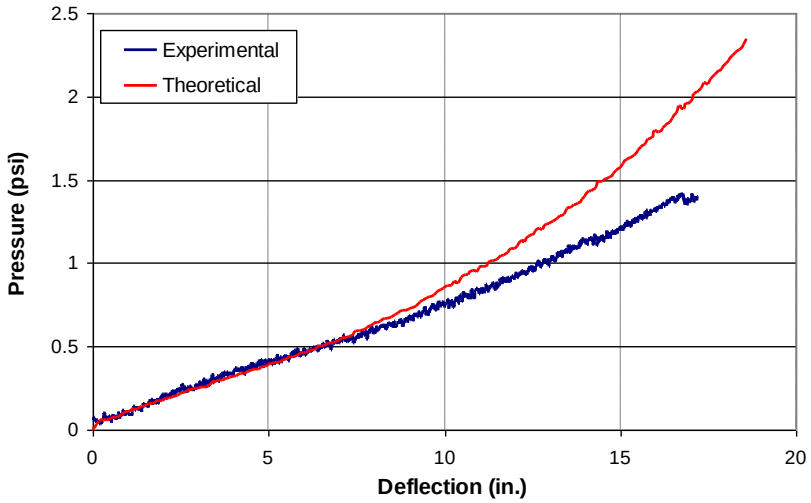

Figure 110. Sample 29 (Results/Comparison)

Sample 30:

Sample 30 had the same dimensions as Sample 25 and used 4-inch bolt spacing and 0.25-inch thick steel connection plates for the connection to the supports. This sample obtained a maximum pressure of 1.98 psi and maximum deflection of 16.93 inches before failure of the sheet occurred due to a tension failure along the bolt line. Figure 111 shows the damage to Sample 30. The connection plates were undamaged. Figure 112 compares the experimental results from this test with the theoretical static resistance function prediction for this sample.

Figure 111. Sample 30 (Failure/Post-Test Damage)

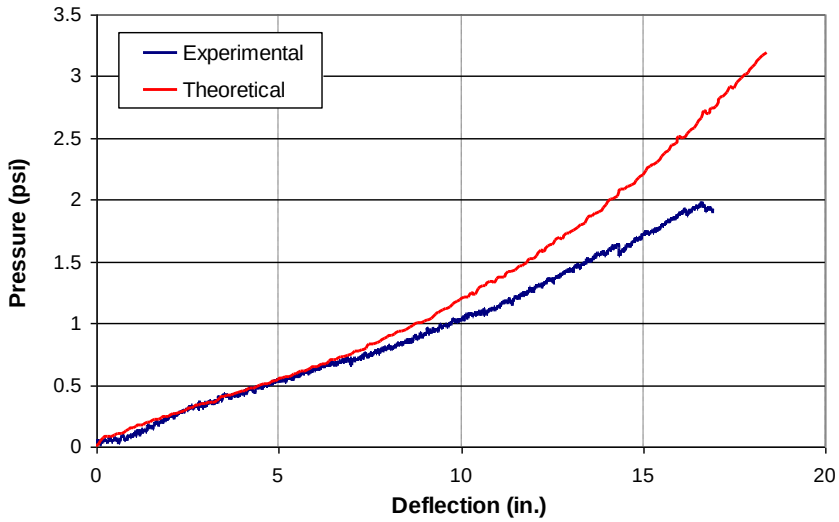

Figure 112. Sample 30 (Results/Comparison)

6.3. Conclusions

For the experimental verification of the static resistance function, AFRL tested 31 component membranes by applying a simulated uniform load perpendicular to the polypropylene sheet. Test personnel measured the maximum pressure, maximum deflection, energy absorbed, and failure type and compared the measurements to the analytical static resistance function. In these tests, AFRL considered three major variables: sheet thickness, connection plate thickness, and bolt spacing.

AFRL tested five configurations of sheet thickness: 1 mm (0.039 inches), 2 mm (0.079 inches), doubled 1 mm (0.039 inches), 0.35 mm (0.014 inches), and 0.49 mm (0.019 inches). In general, the pressure–deflection curves from the 1-mm (0.039-inch) sheets tended to match the closest with the static resistance function. The 0.35-mm (0.014-inch) and 0.49-mm (0.019-inch) sheets seemed to perform very similarly with the 0.49-mm (0.019-inch) sheets and obtained higher pressures. The 2-mm (0.079-inch) and doubled 1-mm (0.039-inch) sheets appeared, in general, to deviate the most from their respective static resistance functions, but they still performed very closely to the predicted values. There was no significant difference in the pressure–deflection curves of the 2-mm (0.079-inch) sheets and the doubled 1-mm (0.039-inch) sheets. This makes sense since the analytical static resistance function used the total thickness in the pressure calculations for both types. The 2-mm (0.079-inch) sheets seemed to be significantly harder to work with as far as flexibility and ease of installation is concerned. For this reason, AFRL suggests that, if higher blast resistance is desired, it is better to stack 1-mm (0.039-inch) sheets than to install sheets that are 2 mm (0.079 inches) or thicker.

AFRL tested three configurations of connection plate thickness: 0.125 inches, 0.25 inches, and 0.375 inches. The 0.125-inch plates showed a significant decrease in maximum resistance pressures. This was due to the fact that the 0.125-inch plates bent during loading. The maximum deflections obtained from the tests employing 0.125-inch connection plates were higher than all other tests with thicker connection plates because bending of the plate alone allowed for higher

deflections of the sheet. Overall, the 0.125-inch plates performed less desirably because they acquired less absorbed energy, which was a key aspect in evaluating the sheet retrofit setup. The most important factor of the steel connection plate thickness was whether or not the plates were allowed to bend under loading applied to the sheet. The 0.25-inch and the 0.375-inch plates performed very similarly because the 0.375-inch plates did not bend at all and the 0.25-inch plates bent only slightly.

AFRL tested four configurations of bolt spacing: 16 inches, 12 inches, 8 inches, and 4 inches. In general, the 16-inch and 12-inch bolt spacings performed similarly and had similar failure modes. The sheets that employed 8-inch spacings performed significantly better than the samples with 12-inch or 16-inch spacings. On the same note, the 4-inch spacings used in conjunction with the thin sheets performed even better. This was because the clamping force applied to the sheet from the plate was stronger when more bolts applied the force. Although the samples using 4-inch spacings performed slightly better than the samples using 8-inch spacings with the thin sheets, it may be too labor intensive to institute a bolt spacing pattern less than 8 inches. Also, the process of pre-drilling steel connection plates that are the length of an entire wall may be inefficient due to the degree of difficulty in lining up holes in the plate with the anchors that are secured to the floor slabs. For this reason, Samples 31 and 32 were tested to evaluate the efficiency of multiple connection plates. These two tests showed that the multiple connection plates were not as effective as the single connection plate used in the previous tests. Consequently, test personnel must pay careful attention to the drilling of the steel connection plates to make the holes and anchors line up correctly.

The main apparent inconsistency between the analytical static resistance functions and their respective experimental tests was that the analytical static resistance function curves tended to increase more quickly than the experimental curves around the deflection of approximately 7 or 8 inches. This was due to the fact that the uniform loading on the sheet was actually affecting a smaller area when the deflections were larger. The setup of the loading tree forced the bars that were bearing on the sheet to move toward the center of the sheet as the test progressed. In an ideal test setup, the uniform loading would be applied to the sheet throughout the entirety of the test. Unfortunately, in this case the testing setup did not allow for uniform loading. Figure 113 shows a test under large deformations, and Figure 114 shows a depiction of this concept. AFRL believes that if the same sheets were tested in a system that provided a more accurate uniform loading, the static resistance function and the experimental data would coincide more closely.

Overall, the static resistance functions and the experimental data agreed well. The three main variables that were tested (sheet thickness, connection plate thickness, and bolt spacing) worked well in determining an optimum design for the polypropylene sheet retrofit. As mentioned before, the testing process had some minor flaws. Researchers may need to test other types of material in the same manner to verify the initial deflection correction procedure, but in general the analytical model matched closely with the experimental data.

Figure 113. Load Points Sliding to Midspan

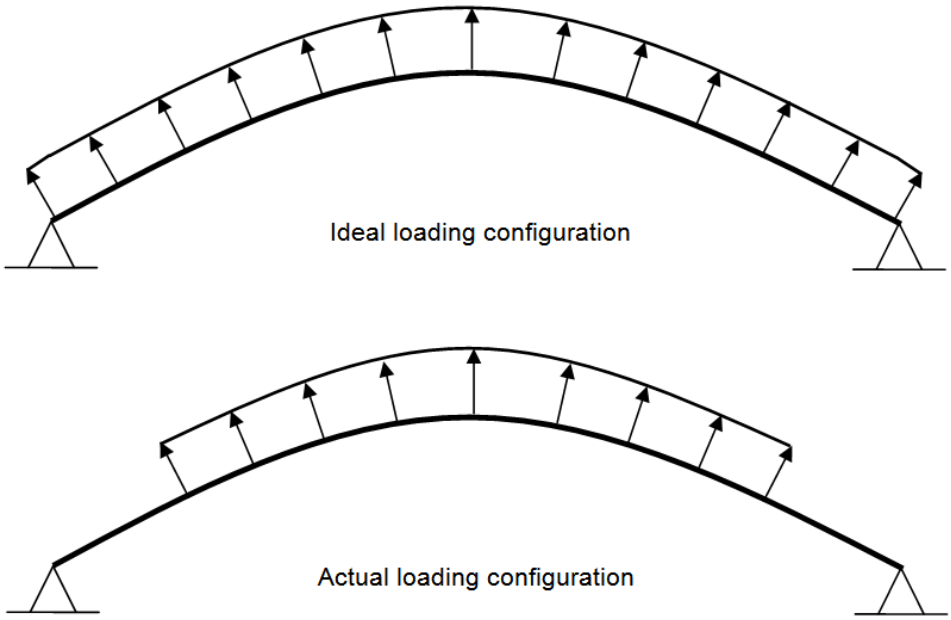

Figure 114. Illustration of Load Distribution at Large Deflection

7. FIELD VERIFICATION OF DYNAMIC MODEL

The dynamic analysis of polypropylene sheets was the final step in predicting the response of the CMU–polypropylene sheet wall retrofit system for blast loading. AFRL incorporated the ideas and information from the previous sections and combined them with dynamic modeling techniques discussed in *Introduction to Structural Dynamics* by John M. Biggs (1964).

Two types of dynamic analysis, exact or rigorous and approximate, are available for analyzing a structural system. It is shown in Biggs (1964) that exact or rigorous dynamic analysis is generally applicable only for simple structures. For this reason, it was necessary to employ approximate design techniques for this research. These techniques provide reasonably accurate dynamic analysis of complex structures with much less involvement. Problems in structural dynamics often have a considerable amount of uncertainty, in which situations complex analysis of the system is unjustified. It is unnecessary to use a method of analysis with a greater amount of precision than that of the input (Biggs, 1964).

AFRL applied the static resistance models developed in this report to Biggs' methods and designed and constructed a system to verify predictions for the polypropylene sheet with experimental data. The following sections present the test setup and results.

7.1. Experimental Setup

AFRL performed a full-scale live explosive field test to validate the static resistance function with the dynamic procedure. The wall tested had a height of 110.2 inches (280 cm) with 50% mortar joints between CMU blocks. The CMU blocks (Figure 115) weighed approximately 49 lbs, had a depth of 7.87 inches (200 mm), and a length of 15.76 inches (400 mm). The CMU blocks also had four hollow cores with 0.79-inch (20-mm) thick webs in the center, a 1.18-inch (30-mm) thick outside shell along the long edges, and a 0.98-inch (25-mm) thick outside shell along the short edges. The mortar used in conjunction with the CMU blocks had a tensile bond strength of approximately 50 psi (estimated from extensive experience). Test personnel created 50% mortar joints to be representative of poor construction to create a conservative test article.

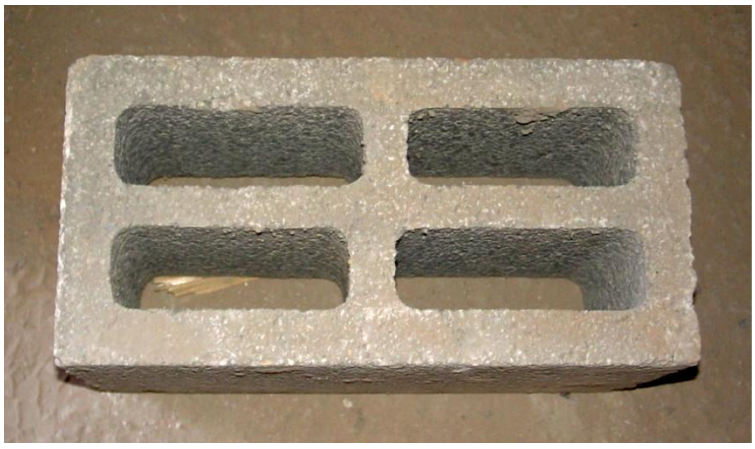

Figure 115. Israeli Normal Weight CMU Block

The sheet retrofit on the interior of the wall was a single polypropylene sheet with a thickness of 0.039 inches (1 mm) and vertical seams that overlapped 4 inches (102 mm). Test personnel pulled the sheet taut upon installation. The steel connection plate dimensions were 0.25 inches (6 mm) thick and 6 inches (150 mm) wide. Test personnel placed the edge of the plate 1.5 inches (40 mm) from the edge of the CMU wall and connected through the centerline of the plate with Hilti HSA M16x190-75 anchors spaced at 8 inches (200 mm) on centers with a minimum embedment of 3.2 inches (80 mm). In conjunction with the anchors and connection plate, they used 1.5-inch (38-mm) washers that had a thickness of 0.25 inches (6 mm).

For data acquisition during the test, AFRL used one deflection gauge and two pressure gauges. The deflection gauge was placed on the inside of the structure approximately 26.3 inches (67 cm) away from the backside of the wall as shown in Figure 116. One pressure gauge was placed next to the deflection gauge on the inside of the structure and the other on the front side of the structure directly exposed to the blast pressure. Figure 117 shows the exterior (front side) of the structure. Since the reaction structure was open on the back side away from the blast, blast pressure was able come back around and load the wall.

Figure 116. Pre-Test Photo (Interior)

Figure 117. Pre-Test Photo (Exterior)

7.2. Comparison of Test Results

Figure 118 shows the post-test damage to the wall with only the bottom course of blocks remaining. No debris passed the polypropylene sheet retrofit. Due to the reaction structure's being open on the back side of the wall, pressure inside the structure was greater than pressure outside the structure. Figure 119 shows the results from the internal and external gauges. It is important to note the "Internal Pressure" was applied opposite the "External Pressure." By subtracting the two pressures, AFRL achieved the "Net Pressure" that was applied to the wall. After AFRL executed the dynamic model for the given loading and system parameters, they obtained a time–deflection curve that bounded the arching and non-arching scenarios and compared this time–deflection curve to the data obtained from the deflection gauge used in the live blast test. Figure 120 shows the comparison of these curves.

Figure 118. Post-Test Photo

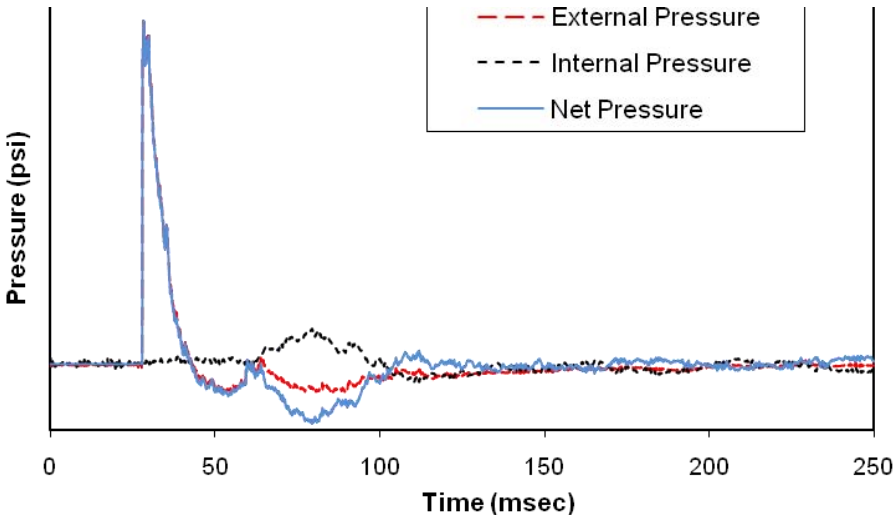

Figure 119. Measured Pressures

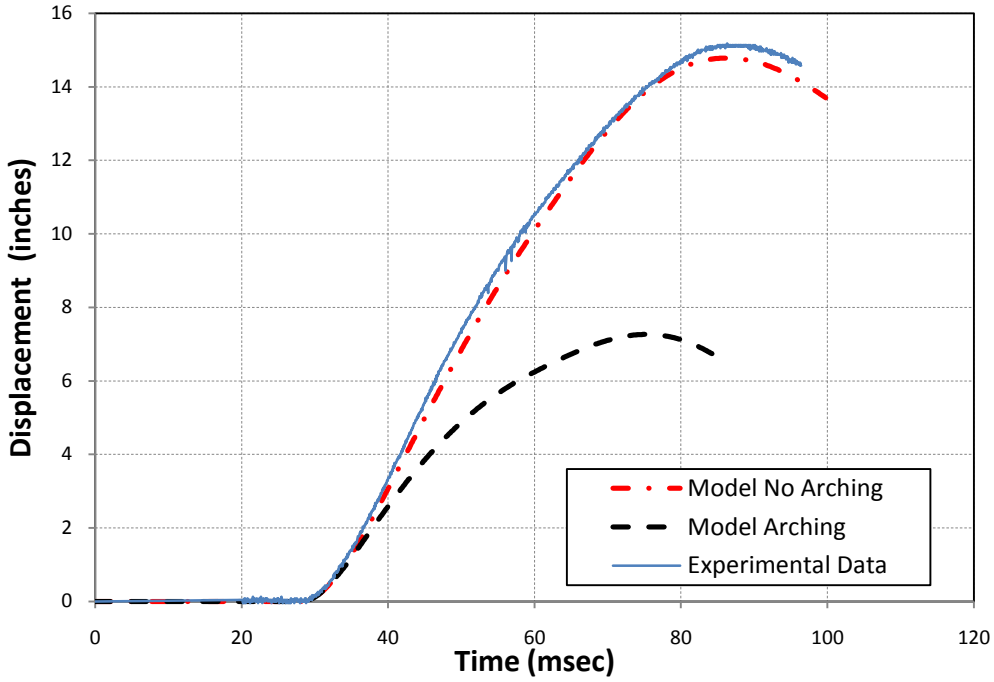

Figure 120. Dynamic Response of Polypropylene Sheet Retrofit

The results from Figure 120 indicate that the actual wall deflection from the blast test closely matched the case for a non-arching CMU wall system with a polypropylene sheet retrofit. The data suggested an approximate 2% error between the no arching and experimental results. This was due to constructing the experimental masonry to a poor but conservative condition. Note that the dynamic model assumed the polypropylene sheet was yielded at 1% strain making the tabulated values for KLM from Biggs (1964), simple supported uniformly distributed load condition, change from 0.78 to 0.66. This switch in KLM happened between 7 to 8 inches of system displacement.

8. CONCLUSIONS AND RECOMMENDATIONS

In this project AFRL researchers developed and validated a predictive method for determining the resistance of an unbonded sheet retrofit. During the process, they demonstrated the effectiveness and feasibility of using a polypropylene sheet as a candidate for blast retrofitting CMU walls by performing preliminary coupon and connection testing to characterize the performance of the material. In addition, AFRL compared measured physical properties with those provided by the manufacturers' theoretical sheet properties and assisted in the development of an optimal connection design. The coupon tests showed that the polypropylene composite was able to beneficially absorb energy if allowed to reach its ultimate tensile capacity. From this information, AFRL developed a static resistance function from which to predict the response of a polypropylene sheet under static loading. The connection tests showed that the connection design controlled the capacity of the sheet retrofit instead of the theoretical capacity of the polypropylene itself.

AFRL then verified the static resistance function by means of full-scale component membrane tests. These tests showed that the static resistance function developed was accurate for the design of polypropylene sheet blast retrofits for CMU infill walls and demonstrated that the polypropylene sheet tended to rip along the bolt line or the edge of the plate during the tests. These tests also verified the fact that a thicker polypropylene sheet with closer bolt spacing and thicker connection plates allowed the sheet retrofit to reach higher capacities before the connection failed.

Researchers from AFRL used analytical modeling techniques from Biggs (1964) to verify the dynamic prediction. The results showed that the polypropylene composite retrofit was sufficient to withstand the effects of the given blast load and that the SDOF model had a close correlation with the actual deflection data from the blast test.

While polypropylene sheets are a viable option for CMU infill wall blast retrofits, AFRL needs to conduct additional research before it can construct a standardized design procedure. Connection design appears to be the area most lacking in understanding. Researchers have not developed any models to predict the behavior of different connection combinations. Currently, researchers have applied only observational techniques to obtain greater resistance from the retrofit system. To achieve understanding of the entire retrofit system, AFRL recommends additional research pertaining to connection design capacities, and covering anchor sizing, anchor spacing, anchor embedment, and thickness of the steel connection plate. A model using these parameters would be helpful in the optimization of connections and ultimately the entire sheet retrofit.

9. REFERENCES

ASTM Standard D412 "Standard Test Method for Vulcanized Rubber and thermoplastic Elastomers—Tension," ASTM International, West Conshohocken, PA, 2006

ASTM Standard D638 "Standard Test Method for Tensile Properties of Plastics," ASTM International, West Conshohocken, PA, 2008

Beer, F.P., Johnston, E.R., and Dewolf, J.T. (2002). *Mechanics of Materials*, 3rd Edition, McGraw–Hill, Inc., New York.

Beckham, S. (2005). "Evaluation of Polymer Retrofit of CMU Walls for Blast Protection." Honors Thesis, University of Missouri, Department of Civil Engineering, Columbia, MO 65211-2200

Biggs, J.M. (1964). *Introduction to Structural Dynamics*, McGraw–Hill, Inc., New York.

Davidson, J. (2005). "Failure Mechanisms of Polymer-Reinforced Concrete Masonry Walls Subjected to Blast." *Journal of Structural Engineering.* American Society of Civil Engineers. Vol. 131, Number 8, pp 1194–1205. Reston, VA.

Dinan, R. (2005). "Blast Resistant Steel Stud Wall Design." Doctoral Dissertation, University of Missouri, Department of Civil Engineering, Columbia, MO 65211-2200.

Fitzmaurice, S. (2006). "Blast Retrofit Design of CMU Walls Using Polymer Sheets." Interim Report, Air Force Research Laboratory AFRL-ML-TY-TR-2006-4540

Hammons, M. (1999). "Baseline Study of Typical Construction Types for High-Occupancy Facilities on Military Installations" Final Report Prepared by Air Force Research Laboratory, Submitted to Air Force Civil Engineer Support Agency.

Jones, P.A.S. (1989). "WAC: An Analysis Program for Dynamic Loadings on Masonry and Reinforced Concrete Walls." Masters Thesis, Mississippi State University, Department of Civil Engineering, Mississippi State, MS 39762

Kennedy, J. (2005). "Analytical and Experimental Evaluation of Steel Sheets for Blast Retrofit Design." Masters Thesis, University of Missouri, Department of Civil Engineering, Columbia, MO 65211-2200

Kiger, S. and Salim, H. (1998). "Use and Misuse of Structural Damping in Blast Response Calculations," Concrete and Blast Effects, *ACI Special Publication SP-175*, pp.121–130.

Moradi, L.G., Davidson, J.S. and Dinan, R.J. (2008). "Resistance of Membrane Retrofit Concrete Masonry Walls to Lateral Pressure." *ASCE Journal of Constructed Facilities*. Vol. 22, Number 3, pp.131–142

Propex Fabrics. (n.d.). Curv advantage and technical analysis. Retrieved October 20, 2007, from the World Wide Web: http://www.curvonline.com/

Salim, H., Dinan, R. and Hoemann, J. (2007). "Blast-Retrofit of Gravity Infill Walls using Ductile Thin Sheets." International Symposium on Interaction of the Effects of Munitions with Structures, ISIEMS 12.1 Conference Proceedings

Smith, P.D. and Hetherington, J.G. (1994). *Blast and Ballistic Loading of Structures*, Butterworth–Heinemann, Ltd., Oxford.

APPENDIX

This appendix summarizes exploratory work done at AFRL for evaluating cheaper alternatives to commercial blast retrofits. Researchers at AFRL gathered materials that they could purchase at local hardware stores and prepared the materials by cutting 2-inch strips in the direction that best fit how they would load the material in the retrofit application. They cut both the fabric and fencing materials in this manner. When possible they cut ASTM 638 Type 1 coupons with a die to a 0.5 inch width. Note: AFRL created the curves in the following figures without using an extensometer. AFRL recommends using the materials for comparison purposes and confirming the material properties (a design best practice) using the appropriate ASTM standard that accurately measures the strain.

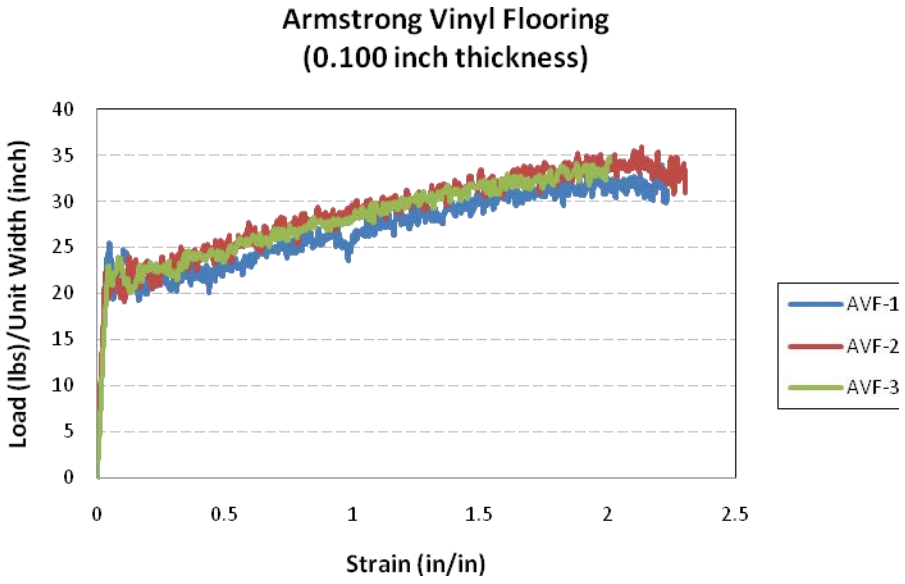

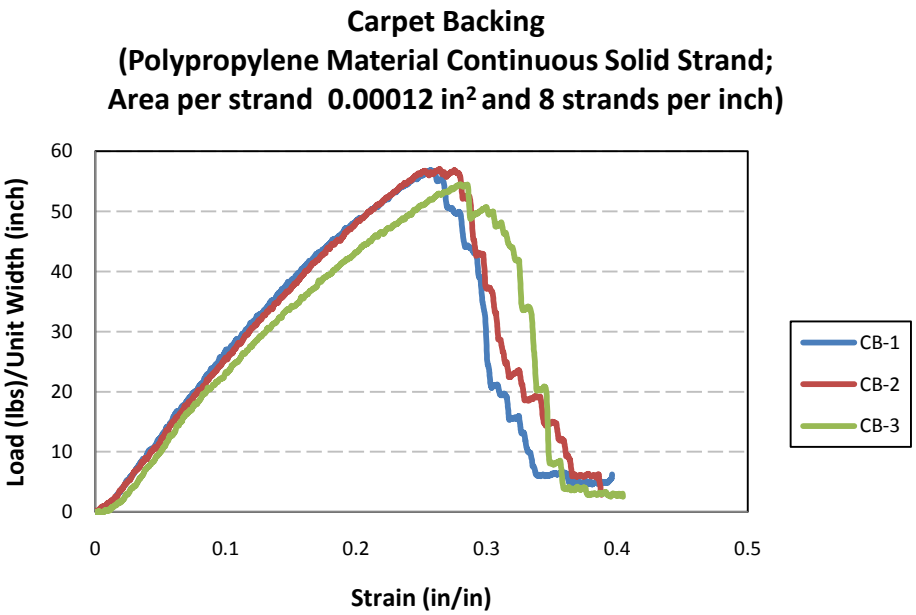

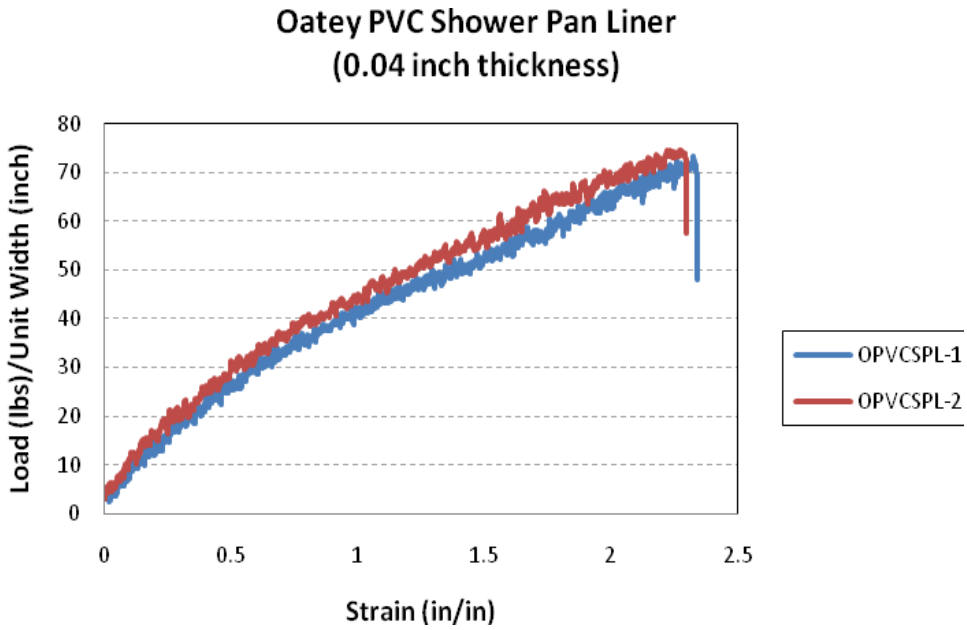
Oatey PVC Shower Pan Liner
(0.04 inch thickness)
Load (lbs)/Unit Width (inch)
80
70
60
50
40
30
20
10
0
0
0.5
1
1.5
2
2.5
Strain (in/in)
OPVCSPL-1
OPVCSPL-2

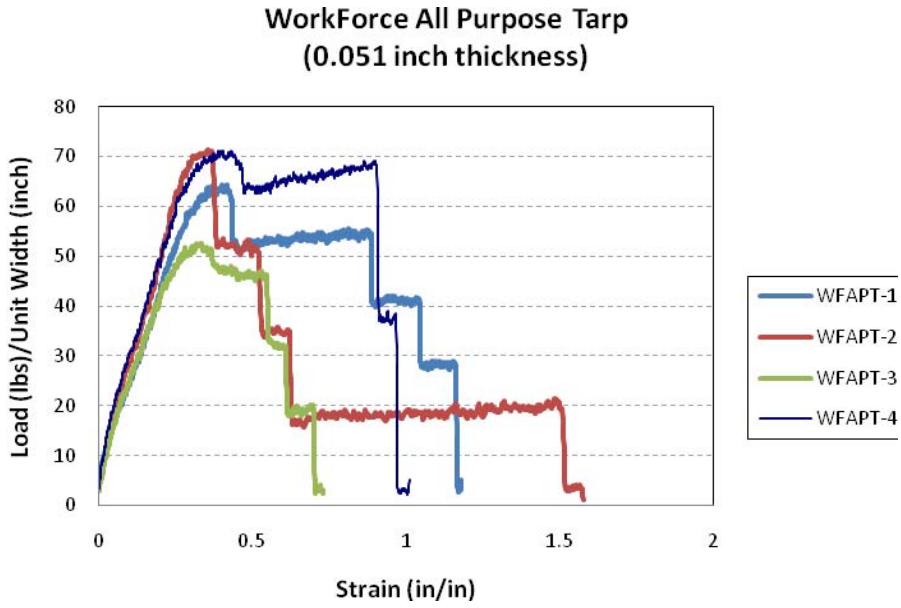
WorkForce All Purpose Tarp
(0.051 inch thickness)
Load (lbs)/Unit Width (inch)
80
70
60
50
40
30
20
10
0
0
0.5
1
1.5
2
Strain (in/in)
WFAPT-1
WFAPT-2
WFAPT-3
WFAPT-4

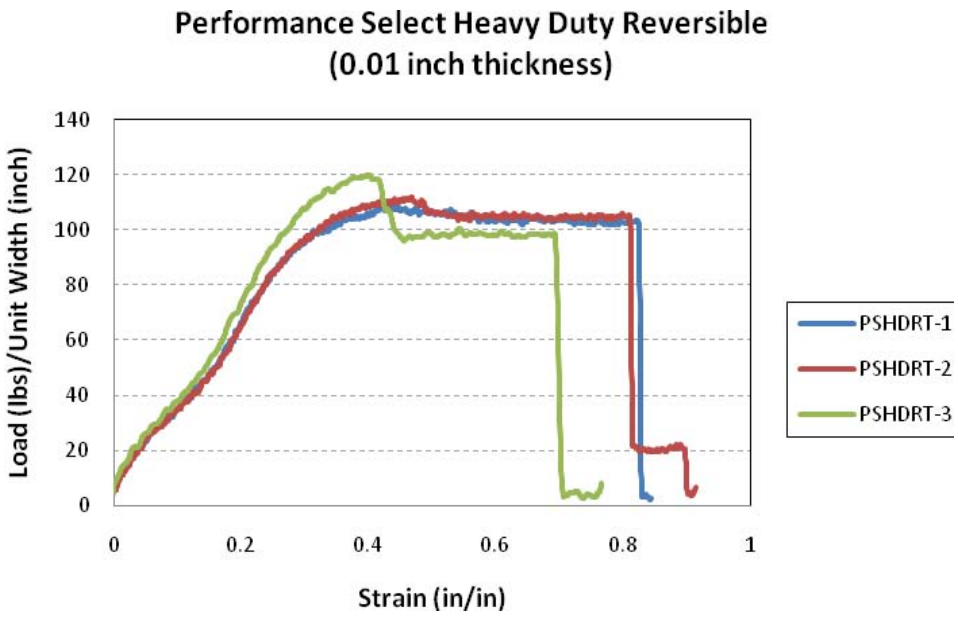
Performance Select Heavy Duty Reversible
(0.01 inch thickness)
Load (lbs)/Unit Width (inch)
140
120
100
80
60
40
20
0
0
0.2
0.4
0.6
0.8
1
Strain (in/in)
PSHDRT-1
PSHDRT-2
PSHDRT-3

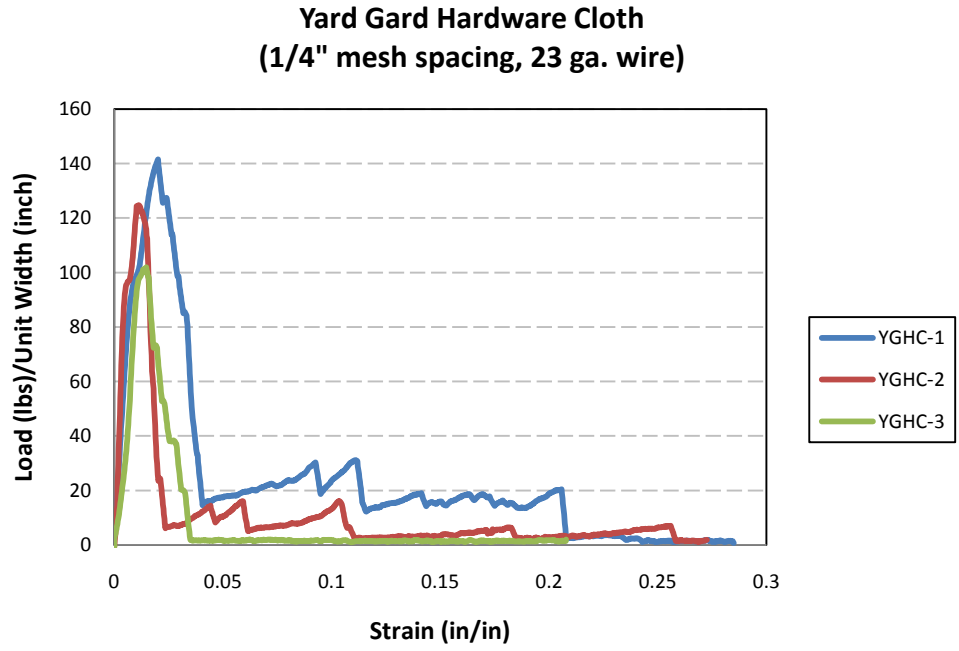
Yard Gard Hardware Cloth
(1/4" mesh spacing, 23 ga. wire)
Load (lbs)/Unit Width (inch)
160
140
120
100
80
60
40
20
0
0
0.05
0.1
0.15
0.2
0.25
0.3
Strain (in/in)
YGHC-1
YGHC-2
YGHC-3

LIST OF SYMBOLS, ABBREVIATIONS AND ACRONYMS

AFRL – Air Force Research Laboratory
PVC – polyvinyl chloride
PSI or psi – pound per square inch
ga. – gauge thickness
in – inches
lb or lbs – pound(s)
CMU – concrete masonry unit
mm – millimeter
P_s – maximum pressure
P_o – ambient pressure
t_a – arrival time
T_s – positive-phase duration
KSI or ksi – Kilo-pounds per square inch
ft^3 – foot cubed
deg. – degree
fig. – figure
% – percent sign
m - meter
ASTM = American Standard for Testing Materials
min. – minute
L – length
w – distributed load
t – material thickness
Δ – deflection
T – tension force (lb/unit width)
p – pressure equal (w/unit width)
σ – stress
σ_t – true stress
σ_e – engineering stress
A – area
b – unit width
v – passion ratio
L'– deflected length
ε – strain
$\int$ – integral symbol
$\sqrt{}$ – square root symbol